Characterizing New Photoreceptors to Expand the Optogenetic Toolbox

Doctoral thesis for a doctoral degree

in Julius-Maximilians-Universität Würzburg

Submitted by

Shiqiang Gao

From Shandong, China

Würzburg, 2015

CC BY NC ND

Submitted on: ……..……..

Office stamp

Members of the Promotionskomitee:

Chairperson:

Primary Supervisor: Prof. Dr. Georg Nagel

Secondary Supervisor: Prof. Dr. Klaus Fendler

Date of Public Defence: ……..……

Date of Receipt of Certificates: ……

Contents

Abstract 1

Zusammenfassung 3

1. Introduction 5

1.1 Channelrhodopsins 5

1.2 Optogenetics 7

1.3 The Optogenetic toolbox 9

1.3.1 Microbial rhodopsins 9

1.3.2 Photoactivated adenylyl cyclases 14

1.3.3 Artificial designed photoreceptors with different function 15

1.4 Objectives of this study 16

2. Materials and methods 17

2.1 *E. coli* manipulation 17

2.1.1 *E. coli* culture 17

2.1.2 *E. coli* storage 17

2.1.3 Chemical competent *E. coli* cells 18

2.1.4 Transformation of *E. coli* 18

2.1.5 Cracking of *E. coli* cells 19

2.1.6 Colony Polymerase Chain Reaction (PCR) 20

2.1.7 Plasmid extraction from *E. coli* 20

2.2 *C. reinhardtii* manipulation 22

2.2.1 Cultivation 22

2.2.2 RNA extraction from *C. reinhardtii* 22

2.3 *Xenopus laevis* oocytes 23

2.3.1 Oocytes preparation 23

2.3.2 RNA injection into oocytes 23

2.3.3 Oocytes maintenance 24

2.3.4 Oocyte membranes extraction 24

2.3.5 In vitro GC activity assay with oocytes membrane. 24

2.4 DNA manipulation 25
2.4.1 Polymerase Chain Reaction (PCR) 25
2.4.2 Restriction enzyme digestion 26
2.4.3 DNA agarose gel electrophoresis 26
2.4.4 DNA Gel extraction 27
2.4.5 DNA purification 27
2.4.6 DNA ligation 27
2.4.7 DNA sequencing 27
2.5 RNA manipulation 28
2.5.1 Poly-A-mRNA extraction 28
2.5.2 Reverse transcription 28
2.5.3 Rapid amplification of cDNA ends (RACE) 29
2.5.4 In vitro transcription 29
2.5.5 RNA agrose gel electrophoresis 29
2.6 cAMP and cGMP assay 31
2.7 Electrophysiology 32
2.7.1 Two electrode voltage-clamp (TEVC) 32
2.7.2 Electrodes and capillaries for TEVC 35
2.7.3 Program for TEVC and data analysis 35
2.7.4 Light sources 35
2.8 Bimolecular Fluorescence Complementation (BiFC) and LSM imaging 37
2.9 Bioinfomatics 38
3. Results 39
3.1 FR, A new proton pump rhodopsin from a sea ice diatom 39
3.1.1 Rhodopsin genes from *Fragilariopsis cylindrus* 39
3.1.2 Photocurrent of Wild type FR in *Xenopus* Oocytes 40
3.1.3 Localization of Wild type FR in *Xenopus* Oocyte 41
3.1.4 Targeting FR to the plasma membrane 42
3.1.5 FR is a light-gated proton pump 46

3.1.6 The FR action spectrum ... 48
3.1.7 FR and BR ... 48
3.1.8 Light snesitivity at different temperatures ... 50
3.1.9 FR “ch” mutant ... 52
3.2 CyclOp, new Guanylate Cyclase Opsins from Fungi ... 55
3.2.1 CyclOp sequences and predicted structure ... 55
3.2.2 Expression of CyclOps in *Xenopus* oocytes ... 58
3.2.3 In vitro assay of GC/AC activity with *Xenopus* oocytes membrane extracts ... 59
3.2.4 Comparison of various CyclOps in *Xenopus* oocytes ... 60
3.2.5 Action spectrum of BeCyclOp ... 61
3.2.6 Light sensitivity of BeCyclOp function ... 62
3.2.7 The long N-terminus of BeCyclOp ... 64
3.2.8 Activation of a CNG channel following BeCyclOp photostimulation ... 65
3.2.9 BeCyclOp is more effective than bPGC in generating cGMP ... 67
3.2.10 BeCyclOp mutant with higher sensitivity ... 67
3.3 Guanylyl Cyclase Opsins with two components system ... 71
3.3.1 Guanylyl Cyclase Opsins from *C. reinhardtii* and *Volvox carteri* ... 71
3.3.2 COP6c is a light-inhibited Guanylyl Cyclase Opsin ... 72
3.3.3 The cyclase domain of COP6c could restore the COP5 GC activity ... 72
3.4 Combination of bPAC and CNG channels ... 75
3.4.1 Membrane targeting of bPAC reduces its dark activity ... 75
3.4.2 Electrophysiological measurements of CNGA2/OLF-Y-bP in *Xenopus* oocytes ... 77
4. Discussion ... 79
4.1 FR and chFR as possible optogenetic tools ... 79
4.2 FR shed light on new energy conversion mechanism in polar diatom ... 79
4.3 BeCyclOp is a new class of microbial rhodopsins ... 81
4.4 BeCyclOp is proven to be a good optogenetic tool in *C. elegans* ... 82
4.5 In vitro assay with *Xenopus* oocyte crude membrane extracts ... 83
4.6 Guanylyl Cyclase Opsins from *Chlamydomonas* ... 83

4.7 Fusing PACs with CNG channels 84
5. References 85
6. Appendix 90
6.1 Supplement Table 90
6.2 Supplement Figure 91
6.3 Abbreviation 92
Acknowledgements 96
Declaration of independence 97
Curriculum Vitae 98

Abstract

Optogenetics is a method to control the cell activity with light by expression of a natural or engineered photoreceptor via genetic modification technology. Optogenetics early success came with the light-gated cation channel "Channelrhodopsin-2" in neurons and expanded from neuroscience to other research fields such as cardiac research and cell signaling, also due to the enrichment by new photoreceptors. In this study, I focus on searching and characterizing new photoreceptors to expand the optogenetic tool box. In this work I characterize three newly discovered microbial rhodopsins and some engineered mutants of them.

The first rhodopsin is a proton pump from the diatom *Fragilariopsis cylindrus, Fragilariopsis* Rhodopsin or abbreviated: FR. I cloned the full-length FR and proved it to be a light-activated proton pump with high efficacy in comparison to Bacteriorhodopsin (BR). During this study, I also developed a new method to improve the plasma membrane targeting of several microbial rhodopsins. I also obtained a FR mutant (channel-like FR or chFR) which behaves like a light-gated proton channel. FR can be used for optogenetic hyperpolarization or alkalization of a cell while the chFR could be used for depolarization or lowering of the cellular pH. The induction of FR expression under iron-limited conditions in the diatom indicated an alternative energy generation mechanism of *F. cylindrus* when iron-containing enzymes are scarce.

I then characterized a new microbial rhodopsin with novel light-regulated Guanylyl Cyclase (GC) activity. This rhodopsin guanylyl cyclase from the fungus *Blastocladiella emersonii* (*B.e.* CyclaseOpsin or BeCyclOp) has been proven by me to be an efficient light-gated GC with high specificity and fast kinetics. BeCyclOp also has a novel structure with eight transmembrane helices, containing a long cytosolic N-terminus which participates in the tight regulation of the GC activity. In collaboration with Prof. Alexander Gottschalk (Univ. Frankfurt/M.), BeCyclOp has been tested in muscle cells and sensory neurons of *Caenorhabditis elegans* and proven to be a powerful optogenetic tool in a living animal. I also generated a BeCyclOp mutant with enhanced light sensitivity.

Already more than ten years ago, guanylyl cyclase rhodopsins were suggested to exist in *Chlamydomonas reinhardtii* by analyzing genomic sequence data. But until now no functional proof existed. By further cloning and sequencing I discovered such a rhodopsin with light-regulated guanylyl cyclase activity. This functional Cyclaseopsin (COP6c) is quite different to BeCyclOp, as it was proven to be a light-inhibited GC. Cop6c is much larger than BeCyclOp with a His-Kinase and a response regulator domain between the rhodopsin and the cyclase domain.

I also introduced a new strategy for generating optogenetic tools by fusing the photoactivated adenylyl cyclase bPAC to two different CNG channels. These new tools function via light-gated cAMP production and subsequent CNG channel activation. These tools combined the properties of bPAC (highly sensitive to blue light) and CNG channels (high single-channel conductance and high Ca^{2+}

permeability), as demonstrated by expression in *Xenopus* oocytes. As a further benefit the fusing of bPAC to CNG channels leads to a bPAC with a more than tenfold reduced dark activity which is a valuable improvement for bPAC itself as an optogenetic tool.

Zusammenfassung

Als Optogenetik wird die Technik bezeichnet, durch genetische Veränderung Photorezeptoren in Zellen einzubringen, um die Zellaktivität mit Licht zu steuern. Frühe Erfolge der Optogenetik wurden mit dem Licht-gesteuerten Kationenkanal "Channelrhodopsin-2" in Neuronen von lebenden Tieren erzielt. Die Anwendung erweiterte sich von den Neurowissenschaften zu anderen Forschungsfeldern, wie Herzforschung und Zellbiologie, auch durch die Bereicherung mit neuen Photorezeptoren. Hier konzentriere ich mich auf die Suche und Charakterisierung neuer Photorezeptoren. In dieser Arbeit werden drei neu entdeckte, natürliche mikrobielle Rhodopsine, sowie ausgewählte Mutanten, charakterisiert.

Das erste Rhodopsin ist eine Protonenpumpe aus der Kieselalge (Diatomee) Fragilariopsis cylindrus, Fragilariopsis-Rhodopsin, abgekürzt FR. Ich klonierte FR und bewies, dass FR eine Licht-aktivierte Protonenpumpe mit hoher Wirksamkeit ist. In dieser Studie zeige ich auch eine Methode, um die Plasmamembran-Lokalisation von FR und mehreren anderen Rhodopsinen zu verbessern. Ich identifizierte eine FR-Mutante (chFR), die sich wie ein Licht-gesteuerter Protonenkanal verhält. FR kann für die Licht-gesteuerte Hyperpolarisation oder Alkalisierung der Zelle verwendet werden, während chFR möglicherweise verwendet werden könnte, um den zellulären pH Licht-gesteuert abzusenken. Die Induktion der FR-Expression unter Eisenmangel-Bedingungen legt einen neuen Energieerzeugungsmechanismus von F. cylindrus nahe, wenn Eisen-haltige Enzyme in den Chloroplasten fehlen.

Ich habe dann ein neues mikrobielles Rhodopsin mit Licht-geregelter Guanylylcyclase (GC) Aktivität untersucht. Für dieses Cyclaseopsin aus dem Pilz Blastocladiella emersonii (BeCyclOp) konnte ich zeigen, dass es sich um eine effiziente lichtgesteuerte GC mit hoher Spezifität und schneller Kinetik handelt. BeCyclOp hat eine für ein Opsin neuartige Struktur mit acht Transmembranhelices. Für den langen cytosolischen N-Terminus zeigte ich eine Beteiligung an der Regulierung der GC-Aktivität. BeCyclOp wurde im Labor von Prof. A. Gottschalk (Univ. Frankfurt/M.) in den Muskelzellen und sensorischen Neuronen von Caenorhabditis elegans getestet und erwies sich als ein leistungsfähiges Werkzeug in optogenetisch veränderten, lebenden Tieren. Ich habe dann auch eine BeCyclOp Mutante mit verbesserter Lichtempfindlichkeit hergestellt.

Bereits vor über zehn Jahren wurden anhand genomischer Daten Guanylylcyclase-Rhodopsine in Chlamydomonas reinhardtii postuliert, konnten aber funktionell bisher nicht nachgewiesen werden. Durch Klonieren von verschiedenen Chlamydomonas reinhardtii Stämmen gelang es mir, solch ein Opsin (Cop6c) zu entdecken, dessen Guanylylcyclase-Aktivität eindeutig Licht-reguliert ist. COP6c ist ganz anders als BeCyclOp, nicht nur weil die GC-Aktivität durch Licht inhibiert wird. Außerdem ist Cop6c ein viel größeres Protein mit einer zusätzlichen His-Kinase-, sowie einer Transducer-Domäne zwischen der Rhodopsin- und der Cyclase-Domäne.

Schlussendlich zeige ich auch eine neue Strategie zur Erzeugung von optogenetischen Werkzeugen durch Fusion der Licht-aktivierten Adenylyl-Cyclase (AC) bPAC mit CNG-Kanälen. Diese neuen "Werkzeuge" funktionieren über Licht-gesteuerte cAMP-Produktion und die anschließende Aktivierung eines cAMP-sensitiven Kationen-(CNG-) Kanals. Hierbei werden die positiven Eigenschaften von bPAC (sehr empfindlich auf blaues Licht) und CNG-Kanälen (hohe Leitfähigkeit bei hoher Ca2+-Durchlässigkeit) kombiniert. Darüber hinaus konnte ich demonstrieren, dass die Fusion der bPAC an den CNG-Kanal zu einer bPAC mit stark reduzierter AC-Aktivität im Dunkeln führte, was allein schon eine gute Verbesserung der bPAC als optogenetische Werkzeug ist.

1. Introduction

Simply to understand, Optogenetics[1-6] is the method used to control the cell activity by light illumination by combining different photoreceptors and genetic modification technology. The fast development of Optogenetics in neuroscience relies on the discovery of Channelrhodopsins[7,8] which allow the fast depolarization of neuron cells. Not limited to neuroscience research, Optogenetics is developing very fast in other research fields such as cardiac research[6] and cell signaling[9]. The optogenetic tool box is greatly expanded by the findings of new photoreceptors, mutations of Channelrhodopsins and artificial designation of new photoreceptors.

1.1 Channelrhodopsins

Channelrhodopsin 1 (ChR1[8]) and 2 (ChR2[7]) are light-gated ion channels in the visual system of the green alga *C. reinhardtii* (Figure 1.1). They are localized in the eyespot of *C. reinhardtii* and regulate the phototaxis of the single-celled algae.

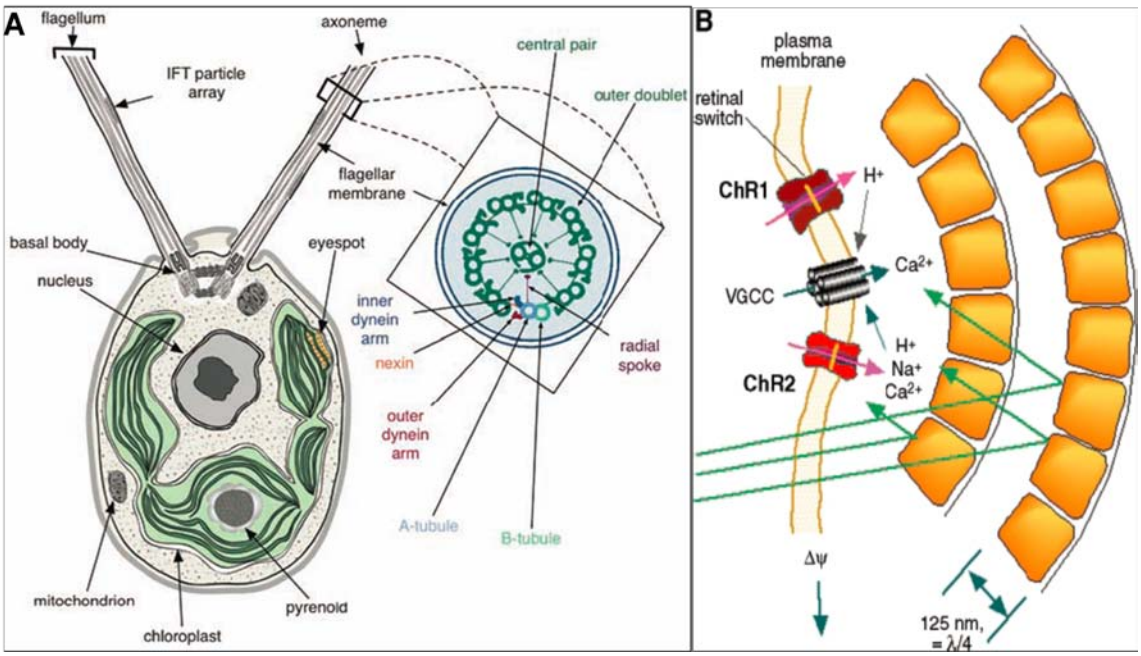

Figure 1.1 *C. reinhardtii*.

A, Scheme of *Chlamydomonas reinhardtii*, it shows the anterior flagella structure, the basal cup-shaped chloroplast, eyespot, central nucleus and other organelles. B, Stucture of eyespot with channelrhodopsin 1 (ChR1) and channelrhodopsin 2 (ChR2). Taken from[10] and [11].

Like other rhodopsins, ChR1 and ChR2 are membrane proteins with seven transmembrane helices. The N-terminal is outside of the plasmamembrane and the C-terminal is cytosolic. Both of them use all-trans-retinal (ATR) as chromophore. The chromophore is covalently binding to a lysine (K296 in ChR1, K257 in ChR2) by forming a Schiff base.

The maximum excitation wavelength of ChR2 is at around 480 nm; and 500 nm for ChR1 which is slightly red-shifted. In *C. reinhardtii*, it was found that ChR1 contributes far greater to the phototactic reactions[12,13]. But the function of ChR2 and how the coordination between different rhodopsins is are not clear yet. And for the heterologous expression in *Xenopus* oocytes, the seven transmembrane helices region (ChR1 aa 1-347, ChR2 aa 1-315) is enough for the channel activity[7,8]. The function of the long C-terminal cytosolic part is still not clear but suggested to relate to the subcellular localization in *C. reinhardtii* [14].

Heterologous expression in *Xenopus* oocytes could be used to study the properties of Channelrhodopsins very well[7,8]. It was shown that the cation-selective ion channel ChR2 is permeable to both mono and divalent cations. ChR1 was firstly described as a proton-selective channel. But in subsequent studies[13], it was detected to be conductive for other cation species. And ChR2 is found to have larger current in *Xenopus* oocytes[15] and HEK cells[16,17]. Thus ChR2 is more widely used in optogenetics (Figure 1.2).

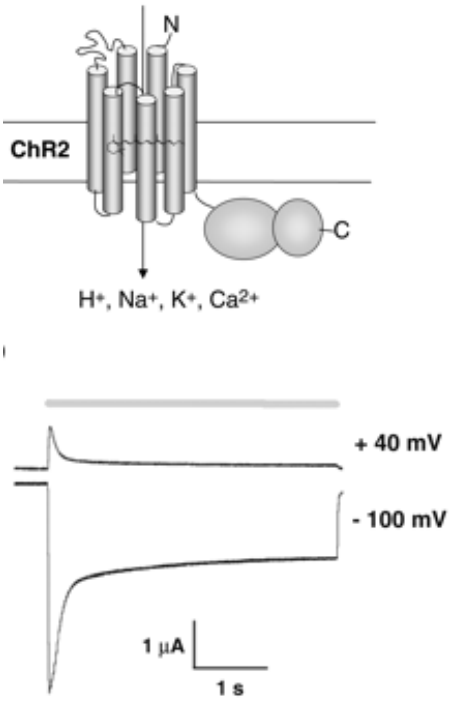

Figure 1.2 Channelrhodopsin 2 (ChR2).

A, Scheme of ChR2 transmembrane arrangement. B, Photocurrents generated by 450 nm blue light illumination of ChR2 expressing oocytes. Taken from [11] and [7].

1.2 Optogenetics

The discovery of Channelrhodopsins becomes the milestone for Optogenetics. Channelrhodopsins can be used to control specific neurons with fast speed after genetical modification of neuron cells (Figure 1.3). After illumination, the subsequent cation influx could trigger artificial action potentials (AP) in neuron cells. And this could help different researchers to address specific questions.

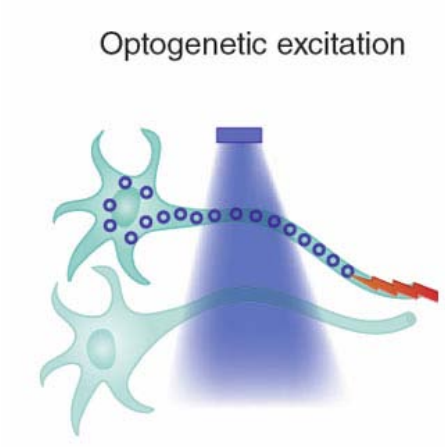

Figure 1.3 Principle of Optogenetics in neurons expressing ChR2.

Using blue light–activated channelrhodopsin for targeted excitation of neurons. Taken from [5].

About 2 to 3 years after the publication of Channelrhodopsins, several groups published their work about using ChR2 in their own research system in around 2005 and 2006. Boyden et al. delivered ChR2 into mammalian neurons by lentivirus vector. ChR2 could be expressed in mammalian neurons stably and safely. It could drive neuron depolarization with millisecond-timescale temporal resolution upon blue light illumination[18]. Nagel et al. expressed ChR2 in muscle cells and mechanosensory neurons of *C. elegans*. ChR2 could evoke strong, simultaneous contractions in muscle cells and could also evoke withdrawal behaviors that are normally elicited by mechanical stimulation in mechanosensory neurons upon illumination[19]. Li et al., Bi et al. and Ishizhuka et al. also applied ChR2 to the embryonic chick spinal cords, inner retinal neurons of blind mice and PC12 cells[20-22]. With these successes, optogenetics became popular in neuron science research area.

Not restricted to neuron science, Optogenetics is expanding fastly due to the application in different systems as well as the development of new optogenetic tools.The halorhodopsin (HR) was used to suppress neuron activity by its hyperpolarization [23]. Arrenberg et al. expressed halorhodopsin and channelrhodopsin in zebrafish cardiomyocytes and could create light-regulated pacemaker[6].

The photoactivated adenylyl cyclases (PACs) are belonging to the family of proteins with Blue-Light-Utilizing flavin adenine dinucleotide (BLUF) domains. They use flavin adenine dinucleotide (FAD) as chromophore and can be activated by blue light. They can be used for light-driven cAMP production in cells and animals[24-26].

Several optogentic systems for light-regulated gene expression are also designed. Wang et al. developed a light-switchable transgene system based on a light-oxygen-voltage[10] domain–containing protein Vivid (VVD), Gal4 and the upstream activating sequence of Gal (UASG) [27]. They have applied this system in HEK293 cells and also in living mice with convincing results. Motta-Mena et al. use a native DNA binding protein with LOV domain EL222 fused with a VP16 transcriptional activation domain (AD) and a nuclear localization signal (NLS) sequence for optogenetic control of gene expression (Figure 1.4). This system has fast kinetics with rapid activation (<10 s) and deactivation (<50 s). It is also tested in mammalian cell lines and zebrafish embryos which show low background and low toxicity[28].

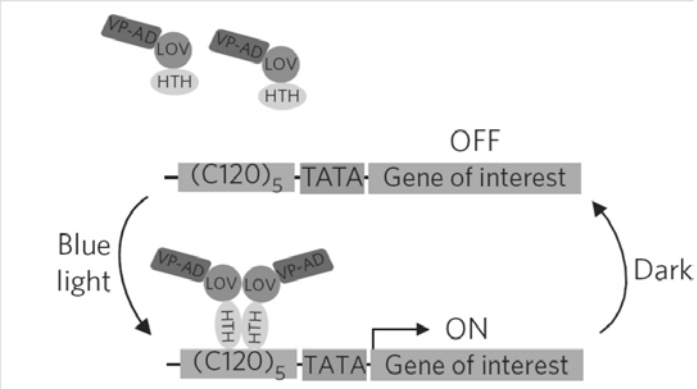

Figure 1.4 Principle of an optogenetic gene expression system.

EL222 is a protein with LOV domain and HTH DNA binding domain. It can not bind DNA in the dark. However, blue light illumination will activate the binding of HTH domain to C120 DNA motif. This binding will bring the VP16 transcriptional activation domain to the target DNA sequence and activate the gene expression. Taken from [28]

Moreover, there are some recent reviews about optogenetics in other areas. Zhang et al. reviewed recent progress in intracellular signaling pathways research with optogenetics[29]. Weitzman et al. introduced optogenetics in area related to cell migration and beyond[30]. Wojtovich et al. summarized the experimental use of RGPs to study ROS signaling[31]. Karunarathne et al. reviewed subcellular optogenetics concerning single cell behavior and signaling pathways related to G-protein-coupled receptors (GPCRs) and receptor tyrosine kinases[32].

1.3 The Optogenetic toolbox

ChR2 and its mutants, also new channelrhodopsins from other organisms are now the most popular tools in optogentics. Other photoreceptors like new rhodopsins with different function, photo-activated nuleotide cyclases and some artificial designed photoreceptors are also potential powerful tools for optogenetics.

1.3.1 Microbial rhodopsins

Becoming popular with ChR2, optogenetics never stop in expanding its toolbox from microbial rhodopsin family. New channelrhodopsins from different organisms, new channelrhodopsin mutants and new microbial rhodopsins with different functions are still the mainforce of optogenetics.

1.3.1.1 Light-regulated proton pump

The first microbial rhodopsin was discovered from the purple membrane of *Halobacterium halobium* by Oesterhelt et al. in 1971[33]. This Bacteriorhodopsin (BR) is a light-gated proton pump.

The BR structure was very well studied at around end of 20th century[34-40]. The BR structure also provided useful guidances for channelrhodopsin study.

BR has seven transmembrane helices with the extracellular N-terminal and cytosolic C-terminal. They form homotrimer of 26 kDa subunits. Interactions of the subunits were thought to stabilize the conformation of the monomers (Figure 1.5).

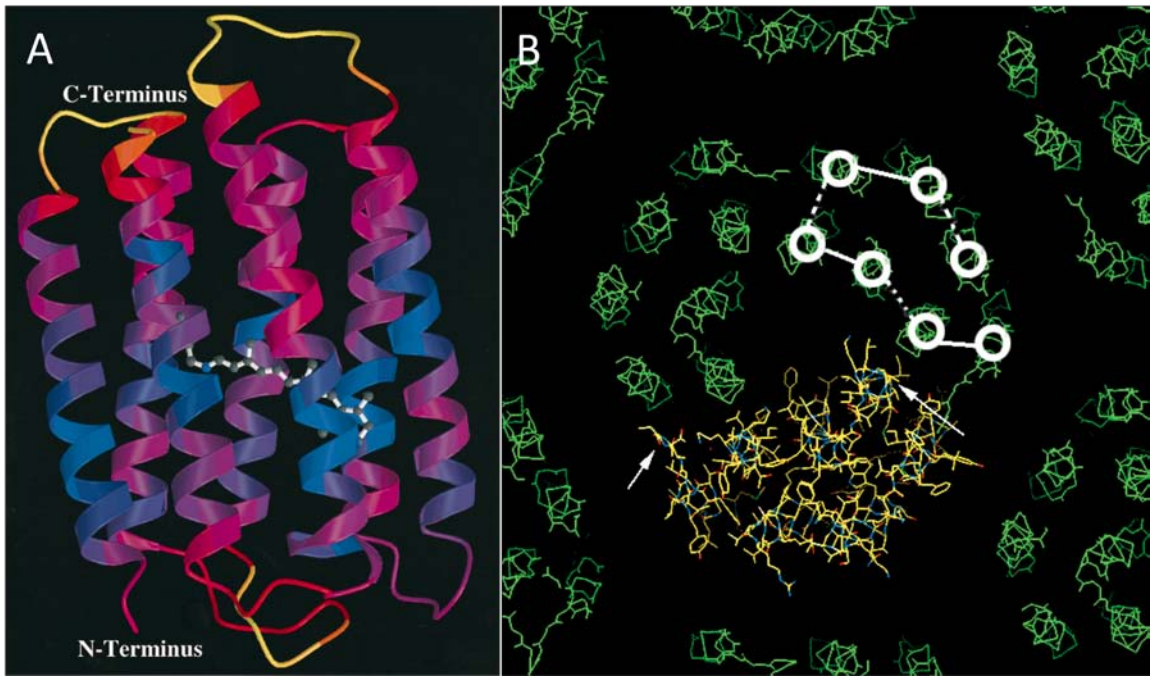

Figure 1.5 Bacteriorhodopsin structure.

A, Scheme of BR transmembrane arrangement with a retinal binds to the Lysine in the 7th helix. B, The schematic of BR trimers. It is viewed along the c axis from the cytoplasmic toward the extracellular space.

Modified from[35,39].

Although BR seems not to be an ideal tool for optogenetics because of its small current compared to the popular optogenetic tools at the moment. But it is a surprisingly membrane protein with new function in 1970s. And the studies with BR established new techniques such as electrical measurement which bring convenience for studying new photoreceptors used for optogenetics now. And some newly discovered more powerful light-regulated proton pumps are being applied in optogenetics with good outcome.

Chow et al. showed that some microbial rhodopsins with proton pump function can be used for efficient silencing of neurons[41].They expressed archaerhodopsin-3 (Arch) from *Halorubrum sodomense* in the mouse cortex and could achieve near-100% silencing of neurons in the awake brain when illuminated with yellow light. And with a blue–green light sensitive proton pump from the fungus *Leptosphaeria maculan* [42], they can silence neurons with blue light. Combining the Mac and a light-regulated chloride pump halorhodopsin from *Natronomonas pharaonis* (NpHR), they could achieve multicolour silencing of two neural populations with blue and red light.

1.3.1.2 Channelrhodopsin mutants

A crystal structure of wild type (WT) channelrhodopsins was difficult to obtain. All previous work was based on structural models by homology modeling. The first real crystal structure of a chimeric channelrhodopsin consisting of the transmembrane helices 1-5 from ChR1 and 6-7 from ChR2 was published by Kato et al.[14] in 2012. Based on the structure modeling information, many Channelrhodopsin mutants are made and lots of them showed to be more superior optogenetic tools than the WT ChR2.

Briefly, there are 3 goals of the mutation:

- Increase the conductance or change the permeability for certain ion.
- Change the speed of the photocycle.
- Tune the action spectrum (red shift is preferred for deep in tissue application).

Based on ChR2, there are several key positions for mutation.

E90. This position was thought to be important for the cation flux through the channel[43]. The ChR2 E90R became a chloride-conducting channel with only negligible cation conductance[44].

E123. Mutations in this postion from E to A or T lead to channelrhodopsins with faster deactivation kinetics. The action spectrum of ChR2 E123T mutant is also about 20 nm red shifted. This could sustain spike trains up to 200 Hz[45].

C128. C128 mutants are often slower with closing time up to seconds or even minutes. This also reduced the light requirement and is ideal for experiments which require long excitation[19,46].

H134. The ChR2 H134R mutant has reduced level of inactivation and generates larger photocurrents than ChR2 wild-type with slower kinetics[17].

D156. Smilar to C128, mutations in this position usually slow down the channel and will enhance the light sensitivity. A ChR2 D156C mutant (ChR2-XXL) gives the largest current than other published channelrhodopsins and increases light sensitivity more than 10,000-fold over wild-type ChR2 when tested in *Drosophila* larvae[47] (Figure 1.6).

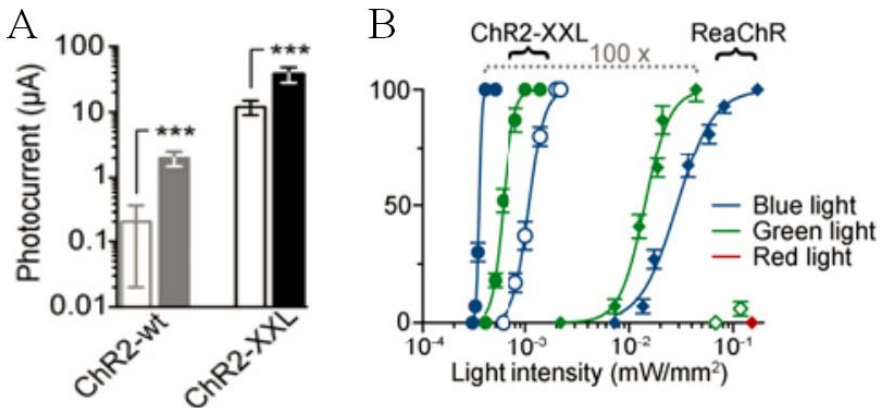

Figure 1.6 ChR2-XXL, a D156C mutant.

A, Steady state photocurrent of ChR2-Wt and ChR2-XXL with and without additional all-trans-retinal in *Xenopus* oocytes. B, Lightinduced immobilization of adult flies expressing ChR2-XXL (circles) or ReaChR (diamonds) in motor neurons with different light illumination. Modified from[47].

T159. The T159C mutant showed increased photocurrents[48], which can be used to induce action potentials at low light intensities. Combining with E123T mutation, the ET/TC double mutant has large photocurrent and fast kinetics with about ~ 35 nm red shift[48].

Besides the point mutation, some interesting channelrhodopsin mutants are also made by chimerization. A red-shifted variant of channelrhodopsin, ReaChR, is a chimera with transmembrane helices 1-5 and 7 of VChR1, transmembrane helix 6 of VChR2, N-terminal of the ChEF/ChIEF variant and a L171I point mutation[49]. ReachR has an action spectrum peaking around 530 nm and can be excited with orange to red light above 600 nm. Red-shifted ChRs would improve the efficiency of stimulation deep through the animal tissue.

1.3.1.3 New channelrhodopsins

After the successful application of ChR2 in neuron science, many new channelrhodopsins are discovered from different organisms. Some of them showed new characters for versatile optogenetic applications.

Volvox carteri is the multicellular relative of *C. reinhardtii*.They share high homology in the genome sequences. It is not amazing to find 2 channelrhopsins from *V. carteri*, vChR1 and vChR2, which are similar to *C. reinhardtii*. Compared to ChR2, vChR1 has an action spectrum peaking around 535 nm.

It could induce spiking with 589 nm illumination in hippocampal neuron[50]. The ReachR was made by partly chimerization of *Volvox* channelrhodopsins[49].

Recently 2 new channelrhodopsins were reported by Klapoetke et al.[51]. Chronos, the ShChR from *Stigeoclonium helveticum*, has the fastest kinetics with a turn-on of 2.3 ± 0.3 ms (n = 8 cells) and a turn-off of 3.6 ± 0.2 ms (n = 7 cells). Usually faster kinetics leads to lower light sensitivity. However, Chronos is the fastest channelrhodopsin with still relative high light sensitivity at the moment. It can drive spiking between 5 and 60 Hz (Figure 1.7).

Chrimson, CnChR1 from *Chlamydomonas noctigama*, is a yellow-peaked channelrhodopsin. Chrimson is the most red-shifted channelrhodopsin with a spectral peak at around 590 nm at the moment. Chrimson would benefit specific experiments which require red light such as deep in tissue targeting.

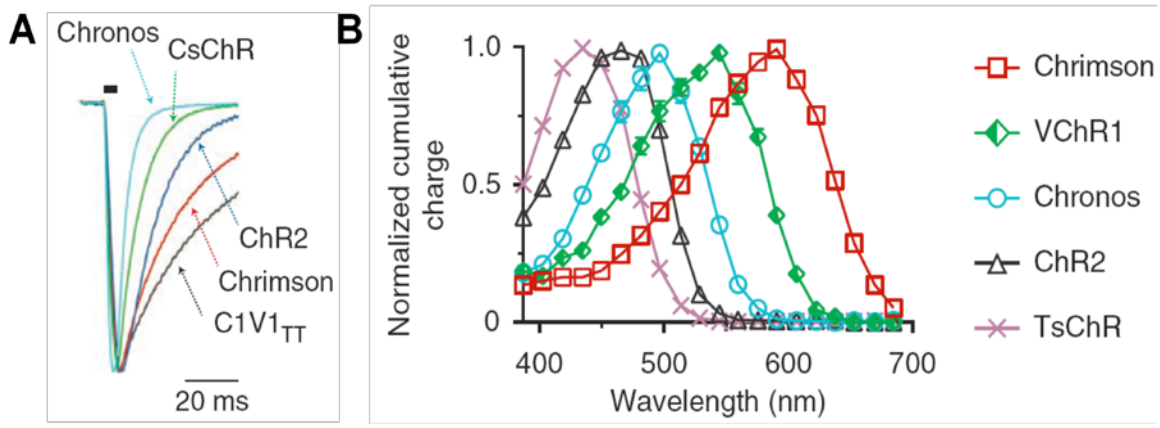

Figure 1.7 Kinetics and action spectra of channelrhodopsins.

A, Turn-on and turn-off kinetics of different channelrhodopsins. B, Turn-on and turn-off kinetics of different channelrhodopsins. Modified from[51].

The new properties of Chronos and Chrimson related to kinetics and spectra provided new possibilities for optogenetics. Combination of Chronos and Chrimson can also be used for two-color experiment[51].

1.3.1.4 Other microbial rhodopsins

The halorhodopsin (HR) is a light-activated chloride pump found in halobacteria. It pumps Cl^- into the cell to cause hyperpolarization under illumination. The most popular light-activated chloride pump now is the halorhodopsin from *N. pharaonis* (NpHR). Zhang et al. used it to suppress neuron activity[23]. Due to the spectral and functional difference between NpHR and ChR2, they can be combined for multimodal controlling of neural circuits.

Gradinaru et al. improved the performance of NpHR in hippocampal neurons by improving molecular trafficking[2]. They fused to it the membrane trafficking signal and ER export motifs from a potassium channel Kir2.1. This can dramatically improve the membrane trafficking of NpHR and also for BR.

Thus this enhances the rhodopsin performance and efficacy in neuron cells by dramatically improved photocurrents (Figure 1.8).

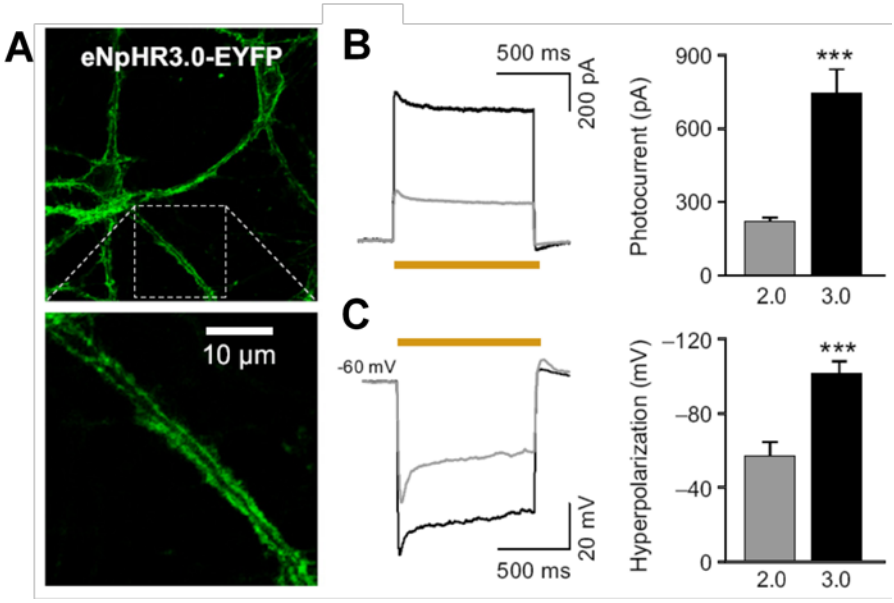

Figure 1.8 Improved NpHR membrane trafficking in Hippocampal neurons.

A, EYFP fluorescence signal showing the improved NpHR membrane targeting after modified with membrane trafficking signal and ER export motif. B, Enhanced NpHR photocurrent in neuron cells after modification. C, Enhanced hyperpolarization ability of NpHR in neuron cells after modification. Modified from [2].

Kleinlogel et al. also fused NpHR or BR with ChRs by using a transmembrane helix from the β subunit of the rat gastric H^+, K^+-ATPase to achieve co-localized expression and equal-copy-number of two membrane proteins[52]. This allows the synchronized excitation and suppression of neuron cells at defined location.

Jaws is engineered from a recently discovered most red-shifted cruxhalorhodopsin Halo57 from *Haloarcula salinarum* (strain Shark)[53]. Halo57 is proven to be a light-driven chloride pump with red-shifted spectra. Using this as backbone, Chuong et al. introduced 2 point mutations, K200R and W214F, to Halo57 and added the trafficking sequences from the potassium channel Kir2.1 to generate Jaws. The final molecule Jaws showed dramatically increased photocurrent without changing the red-shifted action spectrum of Halo57. Jaws also showed enhanced peak spike frequency distribution, 189.5 ± 15.9 Hz versus 67.8 ± 7.0 Hz with eNpHR, when expressed in mouse retinal cones.

There are also other microbial rhodopsins predicted from the sequence to be related to Guanylyl cyclase activity, such as Cop5 and Cop6 from *Chlamydomonas*[11]. Avelar et al. recently discovered a new microbial rhodopsin fused with a Guanylyl cyclase domain[42]. Although not being functionally proven yet by others, these new microbial rhodopsins would definitely enrich the optogenetic toolbox and improve optogenetics in versatile research areas. In my thesis, we will also introduce the progress in characterizing this new class of microbial rhodopsins and possible applications in optogenetics.

1.3.2 Photoactivated adenylyl cyclases

Proteins with BLUF domains are photoreceptors that can be activated by blue light. They are mostly from plants or bacteria and they use FAD, which exists in most cell types, as chromophore. The Photoactivated adenylyl cyclases (PACs) are belonging to this family and they can be used as optogenetic tools for light-driven cAMP production in cells and animals[24-26]. The second messenger cAMP could then affect the behavior by activating protein kinase A, or CNG channels.

EuPACα was the first photoactivated adenylyl cyclase discovered by Iseki et al. from *Euglena gracilis*[54]. It catalyses cAMP synthesis upon blue light illumination and mediates the photophobic response in *Euglena*. Schroder-Lang et al. expressed EuPACα and EuPACβ in *Xenopus* oocytes, HEK293 cells and *D. melanogaster* for optogenetic control of cAMP production[25]. EuPACα is efficient for light-driven cAMP increase, but the EuPACα also has relatively high basal activity in these systems. The L/D ratio for PACα/β is ~80[54].

Ryu et al. and Stierl et al. expressed another PAC from *Beggiatoa* (bPAC or BlaC) in *Escherichia coli*, *Xenopus* oocytes and pyramidal neurons for light-gated cAMP production[24,26] (Figure 1.9). bPAC is a even smaller molecule than EuPAC, and it has lower dark activity while the illumination could induce up to 300-fold increase of adenylyl cyclase activity. The bPAC seems to be a perfect tool for optogenetic control of cellular cAMP level; however the bPAC still has obvious dark activity in different systems. Ryu et al. also engineered bPAC into a photoactivated guanylyl cyclase (bPGC or BlgC) by triple mutations (K197E/D265K/T267G) of bPAC. But the bPGC has not been applied in animal cells so far, possibly due to its low efficiency of the light-regulated guanylyl cyclase activity. Thus another optogenetic tool for controlling the second messager cGMP is needed and this could be addressed by my results here with a new microbial rhodopsin for light-gated cGMP production.

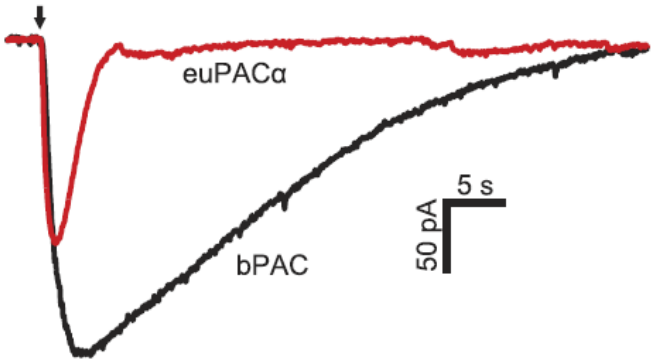

Figure 1.9 bPAC and EuPACα induced currents in neurons.

bPAC and EuPACα are expressed in CA1 pyramidal cells together with CNG-A2 channel.cAMP elevation of bPAC was longer than EuPACα after 100 ms blue light pulse (140 µW/mm^2). Taken from[24].

1.3.3 Artificial designed photoreceptors with different function

Scientists also try to design artificial photoreceptors to expand the optogenetic toolkit. LOV (Light, Oxygen, or Voltage sensing) or some photoreceptors can be designed into light-regulated gene expression system due to their character of regulating dimerization such as the EL222[28] we have mentioned before.

Gasser et al. recombined the photosensor module of *Deinococcus radiodurans* bacterial-phytochrome with the effector module of *Homo sapiens* phosphodiesterase 2A according to the structure homology. The engineered light-activated phosphodiesterase (LAPD) can be used for up-regulating hydrolysis of cAMP and cGMP by red light[55].

Ryu et al. use a bacteriophytochrome c-di-GMP synthase (diguanylate cyclase, DGC) BphG1[56] from *Rhodobacter sphaeroides* together with a constitutive c-di-GMP-specific phosphodiesterase (PDE), YhjH [57], for optogenetic control of c-di-GMP in *E. Coli*[58].

AzimiHashemi et al. modified the chromophore molecule by using synthetic retinal analogues Dimethylamino-retinal (DMAR), trimethoxyretinal[59], thiophene-retinal and naphthyl-retinal etc. The modified retinal can then modify in colour tuning and altering photocycle characteristics of existing optogenetic tools[60].

1.4 Objectives of this study

In this study, I focus on characterizing new photoreceptors or generating new optogenetic tools by generally 3 methods.

The first is to search new genome data for possible new microbial rhodopsin genes or other photoreceptors. This method is to study new natural tools and could possibly lead to new photoreceptors with novel functions. In this study I also mainly focus on this method in collaboration with other groups. We have characterized several different new photoreceptors from a diatom (*F. cylindrus*), a fungus (*B. emersonii*) and an alga (*C. reinhardtii*) in this work.

The second method is to make mutations or chimera of existing optogenetic tools similar to the work with ChR2 XXL[47] or ReaChR[49]. This would help to optimize the existing tools and also for a better understanding of the mechanism.

The third method is to combine different proteins or different functional domains. In this study, I have tried to fuse bPAC with different CNG channels to make new tools. The combination of bPAC with CNG channels will lead to new tools with combined properties from bPAC and different CNG channels.

Besides the focus on optogenetic tools, we also try to study the regulation mechanism of different photoreceptors for better understanding of the photo activation mechanism, which in turn might also facilitate artificial design of new tools in the long run.

2. Materials and methods

All the chemicals mentioned in this part are from Sigma (Deisenhofen), Fluka (Neu-Ulm), Applichem and Roth unless otherwise specified.

2.1 *E. coli* manipulation

2.1.1 *E. coli* culture

Pre-made liquid mediums and agar plates containing antibiotics were stored at 4 ℃ for not very long (< 1 month). *Escherichia coli* strain MRF was inoculated in LB liquid medium or spread on LB agar plates (Table 2.1) with appropriate antibiotics (Table 2.2). For small scale liquid culture, colonies from agar plates or stocks from −80 ℃ were transferred to 15 ml centrifuge tubes (SARSTEDT, Nuembrecht, Germany) with 5 mL LB medium with antibiotics. For larger scale culture, 250 mL erlenmeyer flasks with 100 mL LB liquid medium were used. The cultures were incubated in 37 ℃ and 150 rpm in a rotary shaker (G25 Incubator, New Brunswick Scientific).

Table 2.1 LB medium recipe

10 g tryptone
5 g yeast extract
10 g NaCl;
15 g agar (only for plate)
add water to 1 L

The mediums used are autoclaved for 15–20 min at 121℃.

Table 2.2 Antibiotic concentrations used,

Antibiotic	Stock Solution	Final concentration
Ampicillin	50 mg/mL in water	50 μg/mL
Kanamycin	50 mg/mL in water	50 μg/mL

2.1.2 *E. coli* storage

E. coli liquid culture with LB medium was mixed with glycerol (50% (v/v) stock solution, autoclaved) to a final glycerol concentration of 15% (v/v). The mixture was quick-frozen with liquid nitrogen and stored at −80 ℃.

2.1.3 Chemical competent *E. coli* cells

E. coli MRF overnight cultures were inoculated to 100 mL SOB medium (Table 2.5) and cultivated at 37 ℃, 220 rpm in a rotary shaker. The bacterial culture is harvested into 50 mL centrifuge tubes when the OD_{600} reaches 0.4–0.5. The tubes were put on ice for 15 min to cool down, and then centrifuged down at 2500 rcf, 4 ℃ for 15 min. The pellet was re-suspended in 15 mL sterile and pre-cooled (on ice) TFB1 (Table 2.3) buffer and then put on ice again for 30 min. The re-suspended culture was centrifuged down again at 2500 rcf, 4 ℃ for 10 min. Followed by second re-suspension of the pellets in 2 mL pre-cooled TFB2 (Table 2.4) buffer. Aliquots with 50 µL chemical competent *E. coli* cells in 1.5 mL eppi tubes were frozen in liquid nitrogen and stored at −80 ℃ for future use.

Table 2.3 TFB1 buffer

30 mM KAc
100 mM RbCl
10 mM $CaCl_2$
12% Glycerol
50 mM $MnCl_2 \cdot 4H_2O$
Adjust pH to 5.8 with acetic acid

Both of TFB1 and TFB2 buffer were sterilized with a 0.2 µm filter.

Table 2.4 TFB2 buffer

10 mM Na-MOPS
10 mM RbCl
75 mM $CaCl_2$
12% Glycerol
Adjust pH to 6.8 with NaOH

2.1.4 Transformation of *E. coli*

A heat shock method was used to transform the plasmids into chemical competent *E. coli* MRF cells. Thaw the chemical competent *E. coli* MRF cells on ice before the transformation. The ligated plasmids were pre-cooled on ice and added into competent *E. coli* cells and mixed gently. The mixture was put on ice for 15–20 min and then transfered to a 42 ℃ heat block for 50 s. The mixture was immediately put on ice for 2 min to cool down. For plasmids with ampiciline resistance, the mixture

can be spreaded directly to the agar plates with ampiciline and incubated at 37 ℃ for overnight. For plasmids with kanamycin resistance, 400 µL SOC medium (Table 2.5) was added to the mixture and incubated at 37 ℃ for 30 min, then 200 µL mixture can be spreaded directly to the agar plates with kanamycin and incubated at 37 ℃ for overnight.

Table 2.5 SOC and SOB medium recipe

20 g tryptone
5 g yeast extract
0.5 g NaCl;
5 g $MgSO_4 \cdot 7H_2O$
add water to 1 L
SOB was made similar with SOC buffer plus additional 20 mM glucose.

The mediums are autoclaved for 15–20 min at 121℃.

2.1.5 Cracking of *E. coli* cells

The transformed *E. coli* colonies can be lysed by cracking buffer (Table 2.6). The lysate can be run in a DNA gel to pre-screen the transformants with correct plasmid size. This is a fast and convenient way to improve the efficiency before the plasmid extraction.

Add 5-10 µL of H_2O into a tube (PCR tubes or strips, 1.5 mL Eppi tubes etc.). Then pick up the colony into the tube by pipette tips and mix by pipetting up and down. (One colony to one tube, and mark the colonies picked. The agar plate should be put back to the incubator and let the picked colony grow bigger for later inoculation and plasmid extraction the next day.) Add equal volume of cracking buffer into the tube and vortex to mix, let it stand for 10 min. Then add the loading dye, run the DNA gel and check the size of the super-coiled plasmid. 3 colonies with right plasmid size were inoculated to 5 mL LB liquid medium and incubated at 37 ℃ overnight for the plasmid extraction next day.

Table 2.6 2 × Cracking buffer,

0.2N NaOH
0.5% SDS
20% Sucrose

2.1.6 Colony Polymerase Chain Reaction (PCR)

Colony PCR is another convenient way to pre-screen right *E. coli* colonies. Colonies were picked up by white pipette tips and transferred into tubes (PCR tubes or strips, 1.5 mL Eppi tubes etc.) containing 10 µL sterile water and mix by pipetting up and down (one colony to one tube, and mark the colonies picked, and put the agar plate back to the incubator and let the picked colony grow bigger for later inoculation and plasmid extraction the next day.). The 10 µL mixture was then incubated at 98 ℃ for 10 min in a thermo cycler or a heat block. The mixture was then centrifuged down at 14000 rpm for 10 min. The supernatant was then used as PCR template. The primer pair binding to target DNA can then be used for PCR with these templates (Table 2.7).

Table 2.7 Colony PCR reaction mix (20 µL total volume):

Template	1 µL
5 × HF Buffer	4 µL
Forward primer (10 µM)	0.8 µL
Reverse primer (10 µM)	0.8 µL
dNTP mix (10 mM each)	0.8 µL
Phusion DNA Polymerase	0.2 µL
Add H_2O to 20 µL	

The PCR program was optimized to individual primer pair according to standard PCR program requirements.

The PCR products were analyzed by DNA agarose gel electrophoresis to screen out the colonies with right bands. 3 colonies with right plasmid size were inoculated to 5 mL LB liquid medium and incubated at 37 ℃ overnight for the plasmid extraction next day.

Cracking and colony PCR are two convenient ways for high throughput screening of positive colonies. These 2 methods can be choosen depending on the real situation.

2.1.7 Plasmid extraction from *E. coli*

Plasmid extraction was performed by Qiaprep spin miniprep kit (Qiagen, Hilden, Germany). 5 mL overnight culture in the 15 mL tube was centrifuged down at 5000 rpm for 10 min. The plasmid extraction was then continued according to the protocol. Larger scale plasmid preparation was done by QIAGEN Plasmid Midi Kit (Qiagen, Hilden, Germany). The plasmids were eluted with H_2O and the concentration was measured by absorbtion at 260 nm with a nano photometer (NanoPhotometer™, Implen, Munic, Germany). The quality of the plasmid was checked by the absorption ratio

between 260 nm and 280 nm. The extracted plasmids can be stored at -20 ℃ freezer for further use.

2.2 *C. reinhardtii* manipulation

2.2.1 Cultivation

C. reinhardtii strains were ordered from *Chlamydomonas* Resource Center, University of Minnesota. The cultivation was with TAP medium with recipe from Gorman et al.[61]. The *C. reinhardtii* agar plates with TAP medium were grown at 23 ℃. The liquid culture was grown at 23 ℃ in a rotary shaker. The cell density was measured by absorbtion at OD600.

2.2.2 RNA extraction from *C. reinhardtii*

The RNA extraction from *C. reinhardtii* was made by a combination of Trizol (Invitrogen, Carlsbad, USA) and RNeasy Mini Kit (Qiagen, Hilden, Germany).

45 mL *C. reinhardtii* cells were transferred to 50 mL Falcon tubes and centrifuged down at 4500 rpm for 6 min. The supernatant was discarded and 1 mL Trizol was added to the pellet and vortexed to mix completely and let it stand for 5 min. The mixture was centrifuged down at 14000 rpm, 4 ℃ for 5 min. The supernatant was transferred to a new 1.5 mL Eppi tube and 200 µL chloroform was added and invert to mix, let it stand for 15 min. Centrifuge the mixture again at 14000 rpm, 4 ℃ for 15 min. 400 µL supernatant was transferred to a new Eppi tube and mixed with 400 µL Isopropanol. The mixture was frozen at -20 ℃ for 10 min and then centrifuged at 14000 rpm, 4 ℃ for 10 min. The pellet was washed with 70% ethanol and dried in the fuming hood for 3 min.100µL RNase-free H_2O was used to solublize the pellet and mixed with 350 µL RLT buffer and then mixed with 250 µL ethanol. 700 µL mixture was loaded to the RNeasy Mini Spin column and centrifuge at 10000 rpm for 30 s. 500 µL RPE was used to wash the RNeasy Mini Spin column twice followed by centrifugation. The column was centrifuged down another time at 14000 rpm for 1 min. 50 µL RNase-free water was used to elute the total RNA by centrifugation at 10000 rpm for 1 min. The eluted RNA can be stored at -20 ℃ for shorter time and -80 ℃ for longer for future use.

2.3 *Xenopus laevis* oocytes

The oocytes of the South African clawed frog *X. laevis* were used for the electrophysiological measurement in this study. The frogs can be operated once every ~6 months to obtain the oocytes for electrophysiological study.

2.3.1 Oocytes preparation

The frog to be operated was taken out to an empty barrel with 1.5 L tap water containing 1 g/L Tricain to be anesthetized for about 30 min. A handful ice was added to the barrel in the middle during this process. The frog (abdomen upwards) was then transferred to a tray filled with ice and bedded with tissue paper soaked with Tricain solution. A ~10 mm long incision was done with a sterilized scalpel in the abdominal skin and then a shorter incision was done to the underlying muscle. The oocytes in the ovary was dragged out with forceps, cut with surgical scissors and put into 50 mL Falcon tubes with Ca^{2+}-free ND96 buffer (Table 2.8) containing gentamycin. The incision was then sewed with sterile nonabsorbable monofilament polyester thread. The frog was put back to the barrel with fresh water to wake up in about 2 hours.

Table 2.8 ND96

NaCl	96 mM
KCl	2 mM
$MgCl_2$	1 mM
$CaCl_2$	1 mM
HEPES	10 mM
Gentamycin	50 μg/mL
Adjust pH to 7.4	

The ovary was broken into 2-3 mm^2 pieces, washed twice with a calcium free ND96 solution and digested with 5 mg/mL collagenase. After digestion, the Oocytes were washed three times with a calcium-containing ND96. The ready for use oocytes can be stored at 16 ℃ before RNA injection.

2.3.2 RNA injection into oocytes

The RNA made from in vitro transcription was injected to the oocytes by the nano injection machine (Nanoject, Drummond Scientific Company). The injection capillary (3.511 Drummond #3-000-203-G/X; Drummond Scientific Company) was made by a vertical Puller (PP-83; Narishige).

2.3.3 Oocytes maintenance

The injected oocytes were kept in ND96 buffer, 16 ℃ with or without additional all-trans-retinal (ATR). The oocytes should be checked everyday if possible and fresh buffer can be changed depending on the condition.

2.3.4 Oocyte membranes extraction

The crude membrane extraction from *Xenopus* oocytes can be simply performed by 2-step centrifugation for in vitro assay or other purposes.

20 oocytes were washed three times with solution A and then homogenized in 1 ml of solution A (Table 2. 9) on ice. The yolk and cellular debris were sedimented at 800 × g at 4 ℃ for 20 min, and the supernatant was discarded. The membrane fraction was then sedimented at 20,000 × g at 4 ℃ for 20 min. The membrane pellets were gently washed twice with 800 µL solution A and resuspended in 80 µL solution A.

Table 2.9 Solution A for membrane extraction

NaCl	83 mM
$MgCl_2$	2 mM
HEPES	10 mM
Protease Inhibitor Cocktails	1 ×
Adjust pH to 7.5	

2.3.5 In vitro GC activity assay with oocytes membrane.

2 µL of the membrane extract was mixed with 18 µL Guanylate Cyclase reaction buffer mix (Table 2. 10) for 1 reaction. The temperature was controlled in a water bath. The reaction can be stopped by adding 180 µL sample diluents containing 0.1 N HCl to every 20 µL reaction.

Table 2.10 Guanylate Cyclase reaction buffer mix

Tris - Cl	75 mM
$MgCl_2$	10 mM
DTT	5 mM
ATP	1 mM
GTP	2 mM

Adjust pH to 7.5

2.4 DNA manipulation

2.4.1 Polymerase Chain Reaction (PCR)

PCR was used to amplify the target DNA for molecular cloning or other purposes. The PCR reaction was normally prepared on ice in 8-tube strips (0.2 mL each). Phusion High-Fidelity DNA Polymerase (F530-L, Life Technologies) was used for the PCR. The normal recipe was shown as Table 2. 11. Some additives such as BSA, glycerol or DMSO can be added depending on the real situation. PCR master mixes were made when large scale needed. The reaction was performed in a fast thermal cycler (PIKO thermal cycler, Thermo Scientific).

Table 2.11 PCR reaction mix

Template	10–100 ng
5 × HF Buffer	10 µL
Forward primer (10 µM)	2 µL
Reverse primer (10 µM)	2 µL
dNTP (10 mM)	2 µL
Phusion DNA Polymerase	0.5 µL
Add water to 50µL	

A standard touch down PCR program optimized for Phusion DNA polymerase was set as following:

Step 1 : 98 ℃ 45 s

Step 2 : 98 ℃ 15 s

Step 3 : 72 ℃ 15 s per kb

Step 4 : repeat step 2 - 3 for 6 cycles

Step 5 : 98 ℃ 15 s

Step 6 : 66 ℃ 15 s

Step 7 : 72 ℃ 15 s per kb

Step 8 : repeat step 5 - 7 for 6 cycles

Step 9 : 98 ℃ 15 s

Step 10: 60 ℃ 15 s

Step 11: 72 ℃ 15 s per kb

Step 12: repeat step 9 - 11 for 25 cycles

Step 13: 72 ℃ 2 min

Step 14: 4 ℃ Store

The PCR products can be checked on DNA agarose gel or stored under -20 ℃ for future use.

2.4.2 Restriction enzyme digestion

The restriction enzymes digestion was used to generate fragments for DNA ligation or to check the plasmids. The restriction enzymes used in this study are from Fermentas (Fermentas, Thermo, Waltham, USA) unless otherwise specified. The reactions were performed following the specification for different enzymes.

2.4.3 DNA agarose gel electrophoresis

DNA samples were mixed with 5 × DNA loading dye (Table 2.12) for the DNA agarose gel electrophoresis. 2% agarose gel was used for DNA fragments shorter than 500 bp. 1% agarose gel was used for DNA fragments larger than 500 bp. The Lambda PstI (Gibco/Invitrogen, Carlsbad, USA) was used as a size standard.

Table 2.12 5 × DNA loading dye

Bromophenol blue	0.05%
Xylen cyanol	0.05%
EDTA (pH = 8)	20 mM
Glycerol	10%

The electrophoresis buffer used was 1× TAE (Table 2. 13). The electric field applied is ~10–12 V/cm. 0.005% GelGreen (Biotium, Hayward, USA) was mixed in the DNA Agarose gel to stain the DNA for imaging check with an Image Master (VDS, Pharmacia, Uppsala, Sweden).

Table 2.13 1 × TAE for DNA Agarose gel

Tris-base	40 mM
acetic acid	20 mM

EDTA	1 mM

2.4.4 DNA Gel extraction

The bands containing target DNA can be cut from the gel by a scalpel under UV light and further purified by QIAquick Gel Extraction Kit (Qiagen, Hilden, Germany). The extracted DNA was eluted with H_2O and can be stored at −20 ℃ for further use.

2.4.5 DNA purification

DNA from PCR reaction or restriction enzyme digest can be purified by QIAquick PCR Purification Kit (Qiagen, Hilden, Germany) according to the protocol. The purified DNA was eluted with H_2O and can be stored at −20 ℃ for further use.

2.4.6 DNA ligation

The DNA insert was ligated to the vector by T4 DNA ligase (Fermentas, Thermo, Waltham, USA) at room temperature for 1 h. The molar ratio of DNA fragment to vector ranges from 5∶1 to 10∶1. The ligate was transformed to *E. Coli* for future work.

2.4.7 DNA sequencing

The sequences of DNAs from PCR or recombinant plasmids were checked by DNA sequencing. The samples were sent to GATC Biotech (GATC Biotech, Constance, Germany) and sequencing reactions performed.

2.5 RNA manipulation

2.5.1 Poly-A-mRNA extraction

The messenger RNA (mRNA) with poly-A tail was isolated with Dynabeads mRNA purification kit (Invitrogen, Carlsbad, USA). The mRNA was eluted with RNase-free water and can be stored at −80 ℃ for future use. The mRNA can then be used for reverse transcription or rapid amplification of cDNA ends (RACE).

2.5.2 Reverse transcription

The total RNA or mRNA was used as template for reverse transcription. The reverse transcription was done by SuperScript III First-Strand Synthesis System for RT-PCR (Cat No. 18080-051, Invitrogen, Carlsbad, USA).

The following protocol is modified according to the standard protocol.

Thaw all the reagents on ice and prepare the reaction as following in a fresh 0.5 mL RNase-free PCR tube. ~1 μg RNA was mixed with 1 μL 100 μM Oligo-dT, 2.5 μL 10 mM dNTPs and add RNase-free H_2O to 25 μL. The tube with mixture was then put into the Thermal Cycler. The program for this step is as following,

65 ℃ 5 min

55 ℃ 1 h (Add 2 μL RNase OUT and reaction mixture when it come to 55^{o}C)

85 ℃ 5 min

4 ℃ forever

Prepare the following mixture while the reaction is going on,

DEPC-H_2O	3 μL
10 × RT buffer	5 μL
25 mM $MgCl_2$	10 μL
0.1 M DTT	5 μL
SS Rtase	1.2 μL

Open the thermal cycler, and add the above mixture to the reaction tube when it reaches 55 ℃. Pipette the mixture to mix and continue with the program. After finishing the program the cDNA can be stored at −20 ℃ for further PCR.

2.5.3 Rapid amplification of cDNA ends (RACE)

Rapid amplification of cDNA ends was used to get complete gene sequence. Both toatal RNA and mRNA can be used as template for Rapid amplification of cDNA ends. But using mRNA is much better. The RACE is performed by SMARTer™ RACE cDNA Amplification Kit (Clontech, Otsu, Japan) according to the protocol. The target gene was then amplified using nest PCR.

2.5.4 In vitro transcription

In vitro transcription was used to generate RNA for injection into *Xenopus* oocytes. The DNA fragements generated from PCR or the linerized plasmids containing the target gene were used as template. The reaction starts from the T7 promoter using T7 RNA polymerase.

The in vitro transcription was done by AmpliCap-MaxT7 High Yield Message Maker Kit (Epicentre Biotechnologies). The reaction was prepared as in Table 2.14.

Table 2.14 In vitro transcription mix

10 × Transcription Buffer	2 μL
DNA template	~1 μg
Cap/NTP PreMix	8 μL
DTT (100 mM)	2 μL
T7 Enzyme Mix	2 μL
Add DEPC-H_2O to 20 μL	

The reaction mix was put on a 37 ℃ heat block for 1-2 h. Then equal volume of 3 M Ammonium acetate was added to the reaction. Mix thoroughly and store at −20 ℃ for at least 20 min (can be stored for longer time). The mixture was then centrifuged down at 14000 rpm, 4 ℃ for about 1 h. The pellet was washed with 70% ethanol twice and dried in a fuming hood for 5 min. The RNA was solubilized with RNase-free water and can be stored at −20 ℃ for later injection. For longer time storage, the RNA should be stored at −80 ℃.

2.5.5 RNA agrose gel electrophoresis

To avoid degradation by RNase, the RNA samples and gels are prepared in a special way. 1 × MEN buffer was diluted from 10 × MEN stock solution (Table 2.15) for making the RNA agrose gel and agrose gel electrophoresis.

Table 2.15 10 × MEN stock solution

MOPS	0.1%
Na-Acetate	50 mM
EDTA	5 mM
Adjust pH to 7.0	

The stock solution should be stored away from light.

To make the RNA agrose gel, 0.75 g Agarose was added to 41 mL 1 × MEN and boil to melt the agarose. 5 μL Gel red for dying the RNA molecular and 9 μL Formaldehyde to stabilize the RNA were added to the boiled agarose solution. Pour the gel to the proper chamber with proper comb for later use.

The method to prepare the RNA samples is modified from Thrston et al. [62]. 1 μL RNA sample was mixed with 2 μL Glyoxal buffer (10 % DMSO und 8 % Glyoxal). The mixture was put on a 55 ℃ heat block for 20 min followed by putting on ice for 2 min. 2 μL RNA loading (Table 2.16) dye was then added to the RNA mixture to load the sample to the gel and start the gel electrophoresis. The following protocol was similar to DNA agrose gel electrophoresis in 2.4.3.

Table 2.16 RNA loading dye

Formamid	47.5%
SDS	0.0125%
Bromophenol blue	0.0125%
Xylen cyanol	0.0125%
EDTA pH=8	0.25 mM
Glycerol	10%

2.6 cAMP and cGMP assay

The cGMP assay was performed with DetectX Direct Cyclic AMP Enzyme Immunoassay Kit (Cat. No. K020-H5, Arbor assays). The cAMP assay was performed with DetectX Direct Cyclic AMP Enzyme Immunoassay Kit (Cat. No. K019-H5, Arbor assays).

The principle of both kits is based on a competetive immuno-binding method. A standard curve (Figure 2.1) needs to be measured for the calculation of the exact cAMP or cGMP concentration. The standard curve is variable depending on the batches of kit and also the condition of the kit. So the standard curve needs to be measured relatively often.

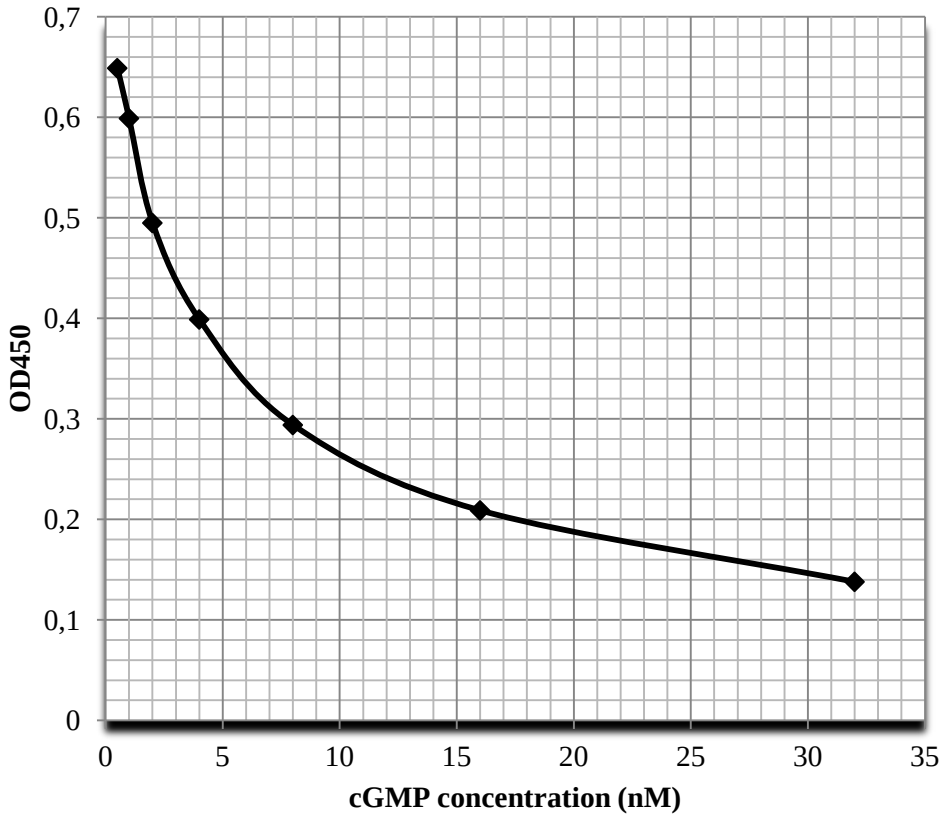

Figure 2.1 A normal standard curve for the cGMP assay

The optical density at 450 nm of the reaction in each well was read out to calculate the final concentration.

2.7 Electrophysiology

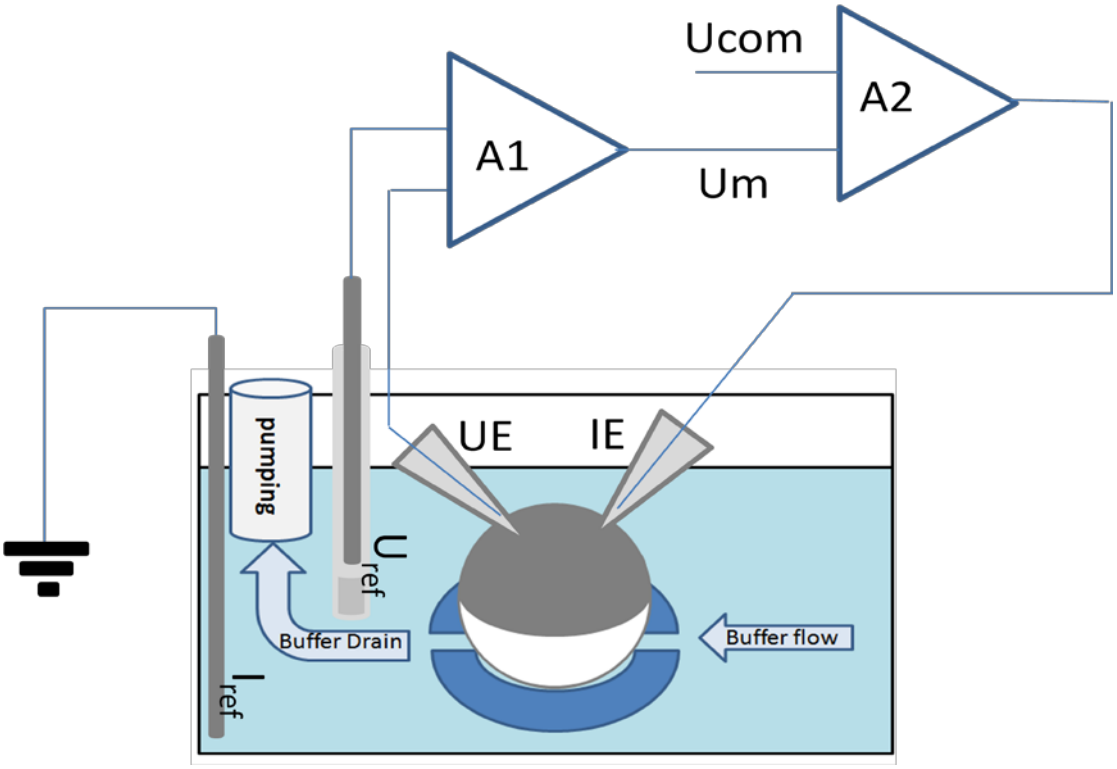

Figure 2.2 Schematic diagram of two electrode voltage-clamp (TEVC) with *Xenopus* Oocyte.

Here shows an oocyte sitting in the chamber with flowing buffer. The potential electrode (UE) and current electrode (IE) were injected into the oocyte. Two reference electrodes for potential (U_{ref}) and current (I_{ref}) were connected to the buffer solution surrounding the oocyte. Um refers to the membrane potential of the oocyte. Ucom refers to the command potential that can be inputed by the computer program. A1 and A2 refer to the potential amplifier and feedback amplifier.

2.7.1 Two electrode voltage-clamp (TEVC)

The injected oocytes were measured with two electrode voltage-clamp (TEVC, see Figure 2.2) for photocurrent. The TEVC technique dates back to 1939 by Cole and Curtis[63]. This technique was further developed by Neher and Sakmann to patch-clamp technique, for wich they are awarded the Nobel Prize in Physiology or Medicine 1991 "for their discoveries concerning the function of single ion channels in cells"[64,65]. TEVC make it possible to measure the current from the intact cell such as *Xenopus* oocyte. *Xenopus* oocyte is ideal for TEVC due to its big size and also high efficiency and stability in expressiong heterologous proteins.

The oocyte was put in a small chamber with flowing buffer in the bath as shown in Figure 2.2. Two reference electrodes for potential (U_{ref}) and current (I_{ref}) were connected to the bath solution surrounding the oocyte. The buffer is kept refreshing by pumping. The potential electrode (UE) and current electrode (IE) were injected into the oocyte. The *Xenopus* oocyte membrane potential Um was

recorded by the difference between UE and U_{ref}. The current injected to the oocyte by the setup to maintain the command potential corresponds to the current across the oocyte membrane.

The two electrode clamp system in this study was TURBO TEC-03X from npi (npi electronic GmbH, Tamm, Germany). Two electrode voltage-clamp recordings of photocurrents were made in standrad Ringer's solution (Table 2.17) or modified with variable components and pH according to real condition.

Table 2.17 Ringer's solutions

Standard ORi pH 7.6	
KCl	5 mM
NaCl	110 mM
$CaCl_2$	2 mM
$MgCl_2$	1 mM
Hepes	5 mM
Adjust pH to 7.6 with NaOH	

ORi $BaCl_2$ pH 7.6	
KCl	5 mM
NaCl	110 mM
$BaCl_2$	2 mM
$MgCl_2$	1 mM
Hepes	5 mM
Adjust pH to 7.6 with NaOH	

ORi $BaCl_2$ pH 5.6	
KCl	5 mM
NaCl	110 mM
$BaCl_2$	2 mM
$MgCl_2$	1 mM

MES	5 mM
Adjust pH to 5.6 with NaOH	

ORi $BaCl_2$ pH 9	
KCl	5 mM
NaCl	110 mM
$BaCl_2$	2 mM
$MgCl_2$	1 mM
Tris	5 mM
Adjust pH to 9 with HCl	

ORi-NMG pH 7.6	
NMG	115 mM
$BaCl_2$	2 mM
$MgCl_2$	1 mM
Hepes	5 mM
Adjust pH to 7.6 with HCl	

ORi-NMG pH 9	
NMG	115 mM
$BaCl_2$	2 mM
$MgCl_2$	1 mM
Tris	5 mM
Adjust pH to 7.6 with HCl	

ORi-NMG pH 7.6	
NMG	115 mM

$BaCl_2$	2 mM
$MgCl_2$	1 mM
MES	5 mM
Adjust pH to 7.6 with HCl	

NMG-Aspartat pH 7.6	
NMG	115 mM
$BaCl_2$	2 mM
$MgCl_2$	1 mM
Hepes	5 mM
Adjust pH to 7.6 with DL-Aspartate	

2.7.2 Electrodes and capillaries for TEVC

The silver electrodes used for TEVC should be chlorinated to generate a layer of AgCl in their surfaces for stability. UE and IE (Figure 2.2) are inserted into capillaries (Φ=1.5 mm, Wall thickness 0.178 mm, Hilgenberg). The capillaries are made by a vertical puller (PC-10, Narishige) and filled with 3 M KCl containing 0.1% agarose. The resistances of UE and IE should be between 0.4 MΩ to 1MΩ.

Reference electrode I_{ref} can be put directly to the bath solution. Reference electrode U_{ref} should be protected by an agarose bridge (1% agarose gel with 3 M KCl) in a plastic tube filled with 3 M KCl containing 0.1% agarose.

2.7.3 Program for TEVC and data analysis

The softwares used for TEVC were WinWCP (University of Strathclyde) and WinEDR (University of Strathclyde). Data analysis was performed by Clampfit 9.0 (Axon Instruments).

2.7.4 Light sources

For normal TEVC, a 532 nm laser and a 473 nm laser were used as light sources. For the action spectrum measurement, we need light of different wavelengths. Light with different wavelengths was obtained by narrow bandwidth interference filters of different wavelengths (Edmund Optics) together with a white light generator PhotoFluor II light source (89North). LEDs with different wavelengths can also be used. But LEDs tend to have broader spectra. The wavelength was further confirmed with

a spectrometer (Ocean Optics). The light intensities at different wavelengths were measured with a Laser Check photometer (Coherent Technologies).

2.8 Bimolecular Fluorescence Complementation (BiFC) and LSM imaging

BiFC[66] was used to determine the interaction between proteins. For the BiFC assay, YFP are split into two non-fluorescent fragments, YN and YC. They are fused to two putative interaction partners separately. The interaction of A and B will bring YN and YC together to restore the fluorescence of intact YFP (Figure 2.3).

Here we use the The N-terminal 155 aa of YFP (aa 1-155; YN) and the C-terminal 85 aa of YFP (aa 155-239; YC) as two parts to fuse to different protein terminus for BiFC test.

The fluorescence imaging was checked by confocal laser scanning microscope (LSM 5 Pascal, Carl Zeiss) equipped with a Zeiss Plan-Neofluar 10×/0.5 objective. The fluorescence images were processed using LSM 5 Image Browser and the pictures were exported for insertion into figures.

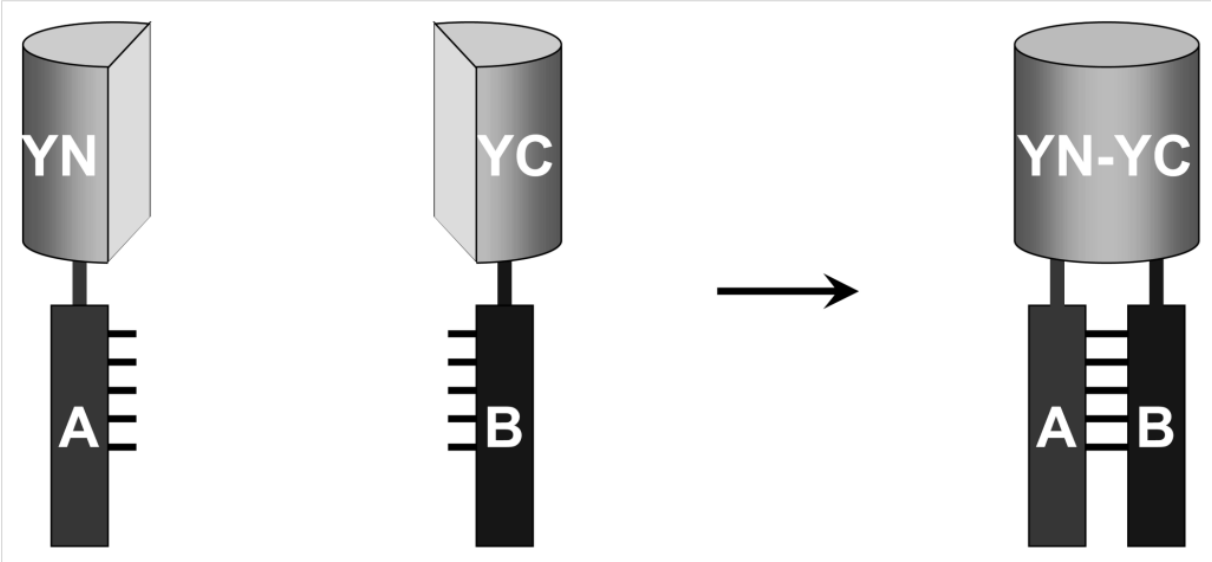

Figure 2.3 Schematic diagram of BiFC principle.

Two non-fluorescent fragments, YN and YC are two N- and C- terminals from YFP. They are fused to two separated putative interaction partners. The interaction of A and B will bring YN and YC together. The approach of YN and YC could restore the fluorescence of intact YFP. Picture from[67]

2.9 Bioinfomatics

BioEdit (Ibis biosciences) and Vector NTI (Life technologies) are used for DNA and Protein sequences editing and normal alignments.

Sequence alignments were done by online portal of ClustalX 2.1[68].

BoxShade (http://www.ch.embnet.org/software/BOX_form.html) was used to color different sequence boxes.

A web-based tool Weblogo (http://weblogo.berkeley.edu/)[69] was used to generate sequence logo based on conservative.

Transmembran helix prediction was done by the TMHMM 2.0 web based tool (http://www.cbs.dtu.dk/services/TMHMM/)[70].

The snake plot of transmembrane protein was done using Protter (http://wlab.ethz.ch/protter/start/)[71], utilizing the Phobius algorithm[72].

3. Results

In this part, we have briefly 4 parts of work with different photoreceptors.

3.1 FR, A new proton pump rhodopsin from a sea ice diatom

3.1.1 Rhodopsin genes from *Fragilariopsis cylindrus*

F. cylindrus is a diatom which is very abundant in sea ice and at the ice-edge zone in polar area (Figure 3.1). It plays important roles in the food chain of the polar area. *F. cylindrus* has been recently sequenced (http://genome.jgi-psf.org/Fracy1/Fracy1.home.html). A rhodopsin gene was found from the *F. cylindrus* genome by Strauss et al. from University of East Anglia. This is the first microbial rhodopsin gene from diatoms, as no rhodopsin gene homolog was identified from the other sequenced diatoms *Thalassiosira pseudonana* and *Phaeodactylum tricornutum.*

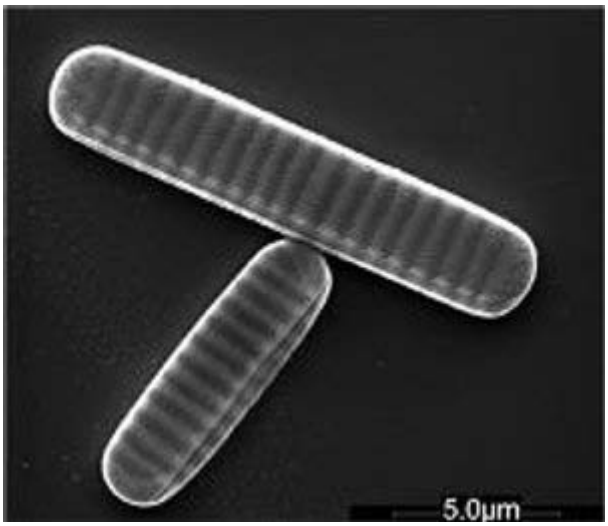

Figure 3.1 the sea ice diatom *Fragilariopsis cylindrus.*

Image courtesy of Henrik Lange and Gerhard Dieckmann (Alfred-Wegener Institute for Polar and Marine Research, Germany).

There are 2 rhodopsin sequences found in the sea ice diatom *F. cylindrus* (Figure 3.2). The only difference of these 2 rhodopsin proteins is in the N terminal. One is 30 amino acids longer in the N terminal than the other. The shorter rhodopsin could be easily cloned from *F. cylindrus* cDNA but no function could be detected for the shorter one when expressed in *Xenopus* oocytes for electrophysiological measurement.

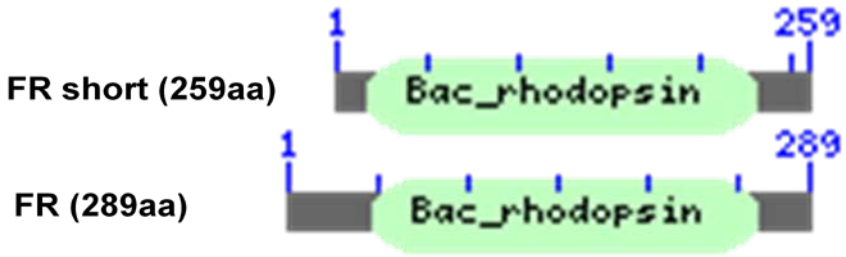

Figure 3.2 Microbial rhodopsins from *F. cylindrus.*

2 rhodopsin sequences from *F. cylindrus* which are different only in the length of the N-terminus.

The longer rhodopsin could only be cloned from *F. cylindrus* cDNA under iron limited condition (Figure 3.3) which is identical with the qPCR analysis in *F. cylindrus* (Personal communications with Jan Strauss). Then the longer rhodopsin is cloned into pGEM-HE vector for generating cRNA by in vitro transcription and follow-up expression in *Xenopus* oocytes for electrophysiological measurement.

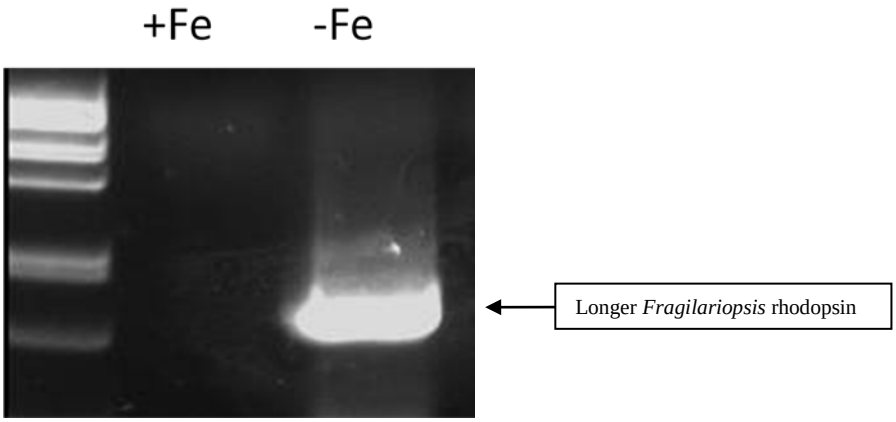

Figure 3.3 Molecular cloning of *F. cylindrus* rhodopsin.

The longer rhodopsin could only be cloned from *F. cylindrus* cDNA under iron limited condition. +Fe, *F. cylindrus* cDNA under condition with iron, -Fe, *F. cylindrus* cDNA under iron limited condition.

3.1.2 Photocurrent of Wild type FR in *Xenopus* Oocytes

The longer FR was expressed in *Xenopus* oocytes and a small outward current could be detected together with 532nm green laser illumination by two elctrode voltage clamp (TEVC) measurement (Figure 3.4). And when a yellow fluorescence protein (YFP) was attached to the C-terminal of the rhodopsin, the current completely disappeared. However, the function of the longer *Fragilariopsis* rhodopsin could be somehow seen and we focus on the longer *Fragilariopsis* rhodopsin for further characterization. For convenience, the longer *Fragilariopsis* rhodopsin is called FR in short.

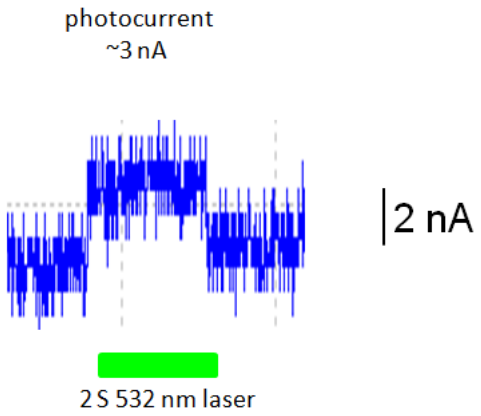

Figure 3.4 Photocurrent of FR measured from *Xenopus* oocytes.

Green bar indicates the green light illumination. Blue traces indicate the current.

Under some rare condition, we could see big outward current of FR (Figure 3.5). Under this condition, the oocyte seems bad and cannot last for longer measurement. After several measurements the oocyte became very leaky and totally dead. But we can roughly characterize the FR to be a proton pump rhodopsin with these measurements. The hypothesis for this was that: the FR was mostly expressed in some inner membrane of the cell and could not be targeted to the plasma membrane very well, only under some rare conditions such as in the process of cell apoptosis some of the inner membranes could fuse to the plasma membrane, and we can get some measurements of FR with big current.

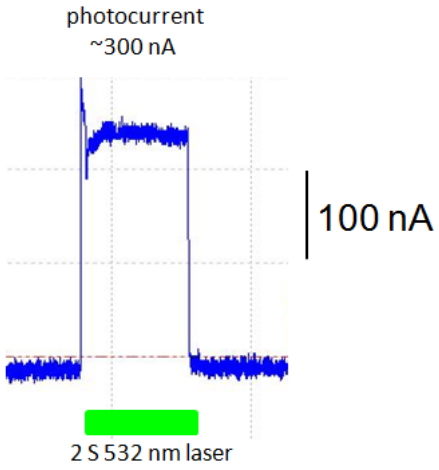

Figure 3.5 Photocurrent of FR measured from *Xenopus* oocytes.

Green bar indicates the green light illumination. Blue traces indicate the current.

3.1.3 Localization of Wild type FR in *Xenopus* Oocyte

So we check the expression of FR with a C-terminal YFP tag in comparison with a cytosolic protein bPAC and a membrane targeting protein Channelopsin-2 (Chop2) (Figure 3.6). We could see some difference of the fluorescence pattern of three different YFP-tagged proteins. For the FR-YFP expressing oocyte, we could see fluorescent vesicles from the intact oocyte and also the broken ooycte.

For the bPAC-YFP expressing oocyte, we see no obvious spotted fluorescence but more evenly fluorescenece, and in the broken oocyte, the fluorescence seems to be everywhere but much weaker possibly due to the dilution effect of incubation buffer to the broken oocyte ingredients. For the Chop2-YFP expressing oocyte, we see sharper "ring like" fluorescence for the intact oocyte, and in the broken oocyte, we see some membrane like structure with fluorescence, and this structure with fluorescence might be plasma membrane cluster of broken oocyte.

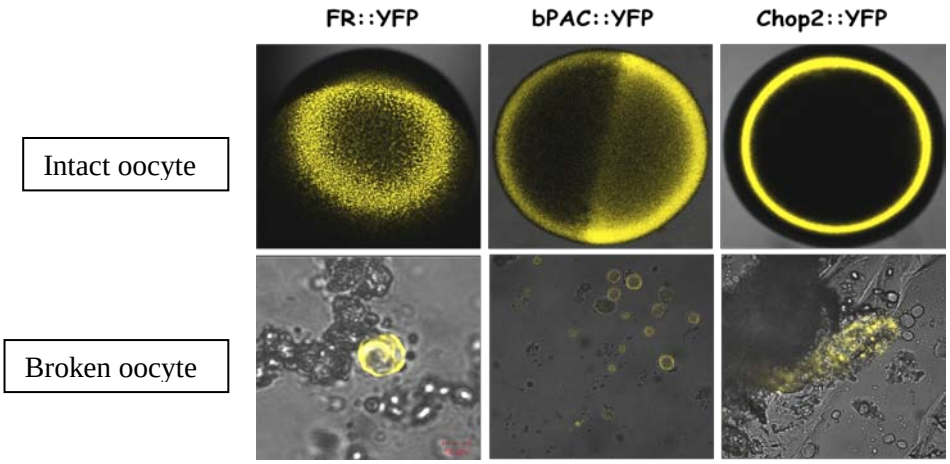

Figure 3.6 YFP fluorescences from *Xenopus* oocytes expressing different photoreceptors.

The expression of FR with a C-terminal YFP tag in comparison with a cytosolic protein bPAC and a membrane targeting protein Chop2. Top row shows the LSM image from intact oocyte. Lower row shows the LSM image from broken oocyte in ND96 buffer.

To have a more detailed look at the fluorescence spots of FR-YFP expressing oocyte, the fluorescence seem to localize in some small particles which we could not recognize yet. Possibly the expressed FR-YFP was forming kind of inclusion body in the form of membrane aggregate or vesicles (Figure 3.7).

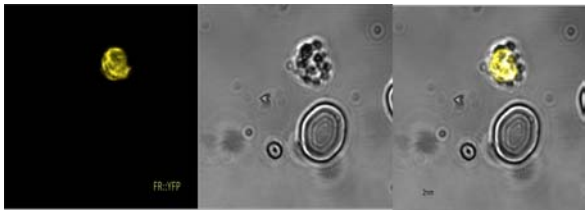

Figure 3.7 YFP fluorescences from *Xenopus* oocytes expressing FR.

Here shows the LSM image from a broken oocyte expressing FR with a C-terminal YFP in ND96 buffer.

So we think that the major problem that we can usually detect very small photo-currents for FR expressing oocytes is due to the bad plasma membrane targeting.

3.1.4 Targeting FR to the plasma membrane

A β linker (Amino acid sequences 1-105 of the rat gastric H+,K+-ATPase β –subunit[52]) was put to the N-terminal of FR to enhance the plasma membrane targeting with good effects (Figure 3.8A). The β

linker was previously used by Kleinlogel et al. as a linker to fuse ChR2 and BR. With this modification, we can get obvious photocurrents of FR expressing oocytes 3 days post injection (dpi) under -20 mV holding potential (Figure 3.8B). With green light illumination, we can get > 1 µA photocurrent.

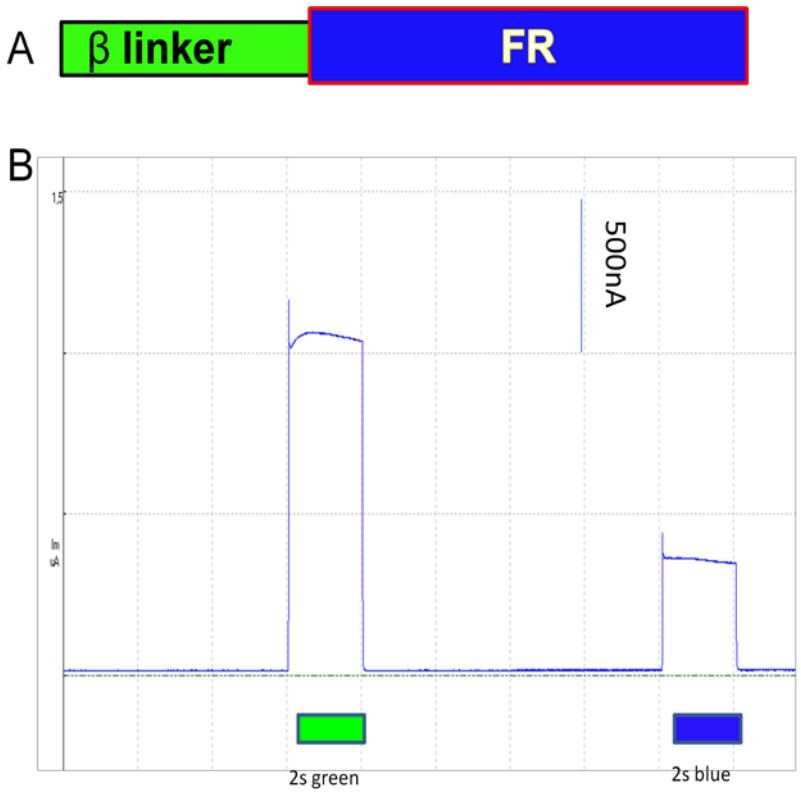

Figure 3.8 Fuse β linker to FR to enhance the plasma membrane targeting.

A, A schematic of β-FR construct. B, Photo current of β-FR with green and blue illumination. Oocytes are measured 3 dpi under -20 mV holding potential.

The β linker could target the FR to the plasma membrane efficiently which facilitates the TEVC measurements (Figure 3.9). But when the YFP was fused to β -FR, no photocurrent could be detected and the fluoreacence was similar to FR wild type with YFP (data not shown). The N-terminal fusion of YFP to β -FR leads to no expression of the fusion protein and no photocurrent could be detected. The YFP fusion to the C-terminal seems to inhibit the plasma membrane targeting of FR. A PAS linker between the YFP and FR could not help to improve this (data not shown). The smaller tag, myc, has similar effect like YFP. But a cc linker, which is the last 72 aa of CvRh (*Chlorella vulgaris* rhodopsin) [1], could improve this to make the photocurrent measurable but with dramatical current decrease (Figure 3.9).

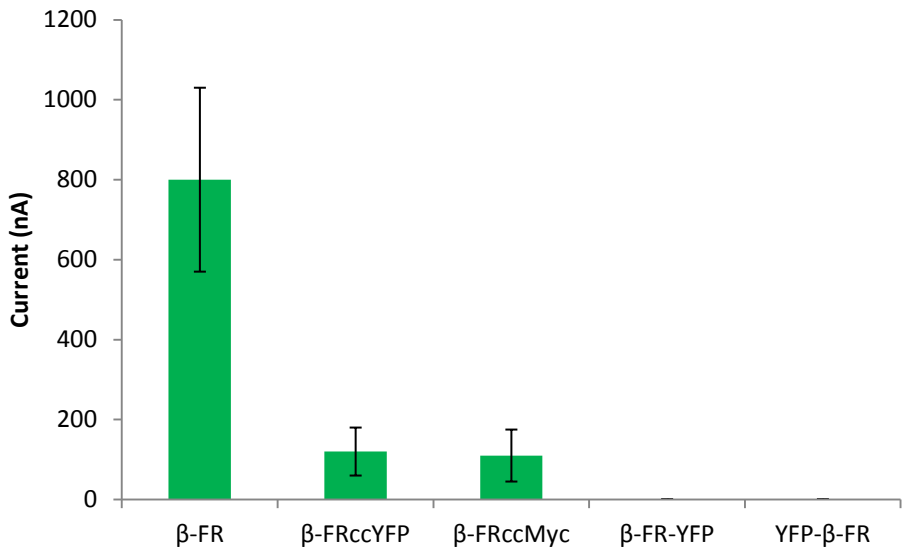

Figure 3.9 Photocurrents of β-FR with and without YFP fusion.

Photo currents of β-FR constructs with or without YFP fusion under 532 nm green laser illumination. Oocytes are measured 3dpi under -20 mV holding potential. cc, the C-terminal 72 aa of CvRh .

Later a plasma membrane trafficking signal and a ER export signal from Kir2.1[2] were used to flank the YFP, which was all together abbreviated as TYE for plasma membrane Trafficking signal, YFP and ER export signal. Then the TYE was fused to the β -FR C-terminus (Figure 3.10A). A combination of N-terminal β linker with C-terminal TYE could efficiently enhance the FR plasma membrane targeting together with YFP tag. And the fluorescence pattern seems like plasma membrane targeting proteins (Figure 3.10C). The new construct β -FR-TYE showed even higher photocurrent than β -FR (Figure 3.10D) with similar amount of cRNA injection.

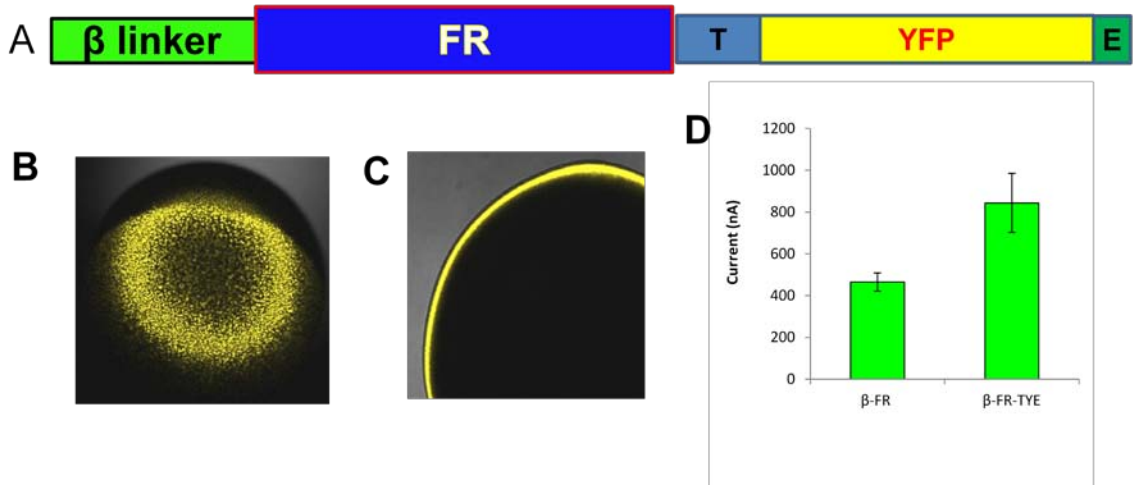

Figure 3.10 A β-FR-TYE construct with enhanced plasma membrane trafficking and photocurrents.

A. A schematic of β-FR-TYE construct. B. LSM image of FR-YFP. C. LSM image of β-FR-TYE. D. Photo current of β-FR and β-FR-TYE with 532 nm green laser illumination. Oocytes are measured 3 dpi under -20 mV holding potential. 28 ng cRNA injection for β-FR-TYE and 18 ng for β-FR.

Such a β-TYE system was also tested for enhancing the plasma membrane targeting effects of other microbial rhodopsins. The TYE tag could already enhance the expression and the photocurrents of Bacteriorhodopsin (BR). The additional β linker could further increase the expression and the photocurrents. (Figure 3.11).

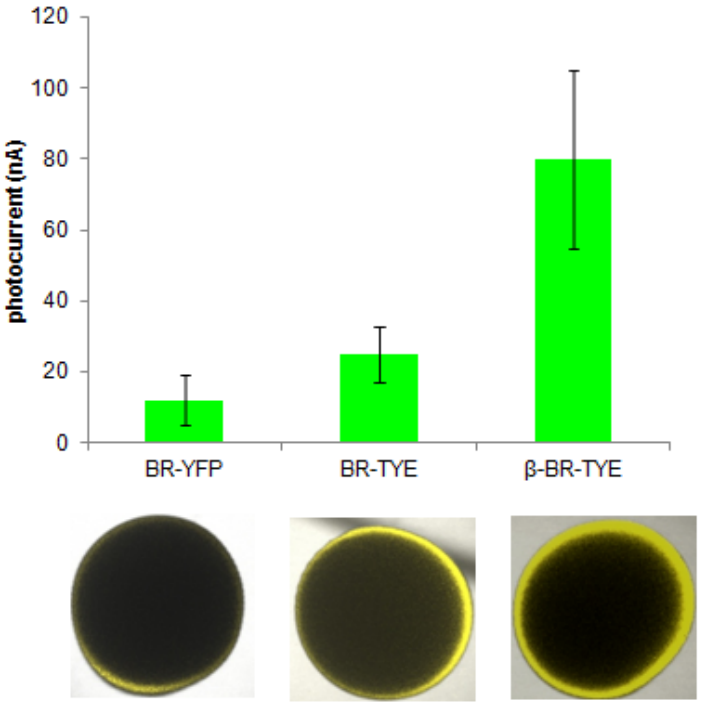

Figure 3.11 Using β-TYE to enhance the plasma membrane targeting of BR.

The upper diagram shows the photocurrent of BR with YFP, TYE and β-TYE with 532 nm green laser illumination. Oocytes are measured 3dpi under -20 mV holding potential, 28 ng RNA were injected for all constructs. The lower fluorescence picture shows the expression of BR constructs with YFP, TYE and β-TYE from left to right.

EeChR1 is a new channelrhodopsin from *Eudorina elegans* cloned by Reza Ramezannejad Ghadi from Armin Hallmann Group in University Bielefeld. Here we tested a D151C mutant of EeChR1 for which the plasma membrane targeting could also be enhanced by the TYE and β linker (Figure 3.12).

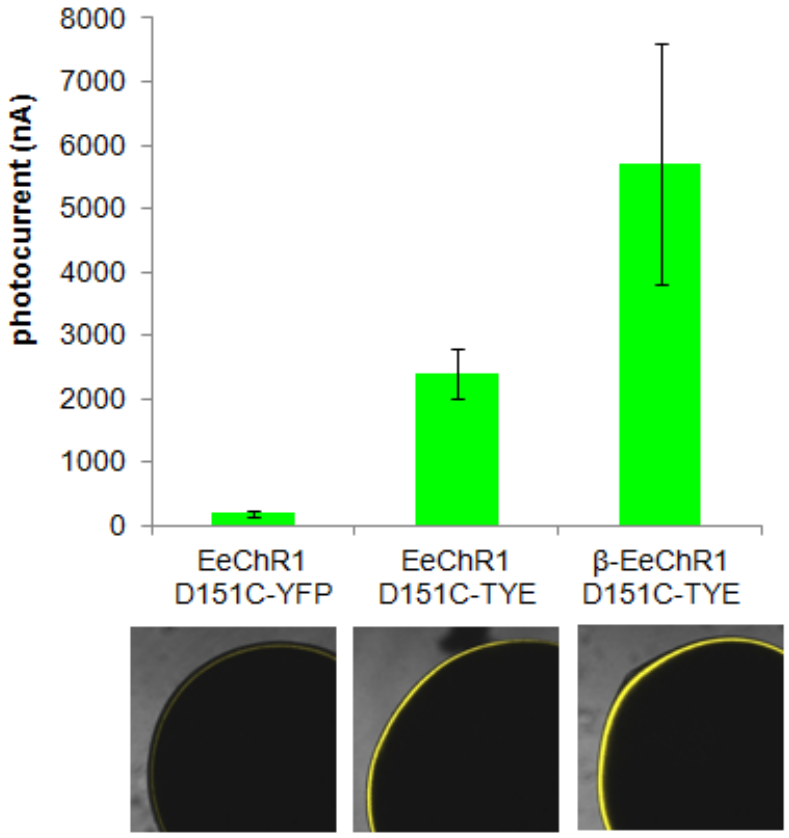

Figure 3.12 Using β-TYE to enhance the membrane targeting of EeChR1 D151C.

The upper diagram shows the photocurrents of EeChR1 D151C with YFP, TYE and β-TYE with 532 nm green laser illumination. Oocytes are measured 3 dpi under -80 mV holding potential, 28 ng RNA were injected for all constructs. The lower fluorescence picture shows the expression of EeChR1 D151C constructs with YFP, TYE and β-TYE from left to right.

3.1.5 FR is a light-gated proton pump

To further confirm the character of FR, we performed TEVC measurement for FR expressing *Xenopus* Oocytes with different buffers. The Ori buffer contains mostly Na^+ and K^+ as cation besides H^+. The NMG buffer contains NMG which is permeable to plasma membrane as major cation besides H^+. The NMG Asp buffer contains aspartate instead of Cl^-. The photocurrents were measured under different potentials from -120 mV to +30 mV. And we see no obvious differences of FR photocurrents in these 3 buffers, which show that the FR photocurrents were probably due to the proton in the cytosol. The slight higher photocurrent in NMG Asp was due to the slight higher pH (0.05) of this solution. (Figure 3.13).

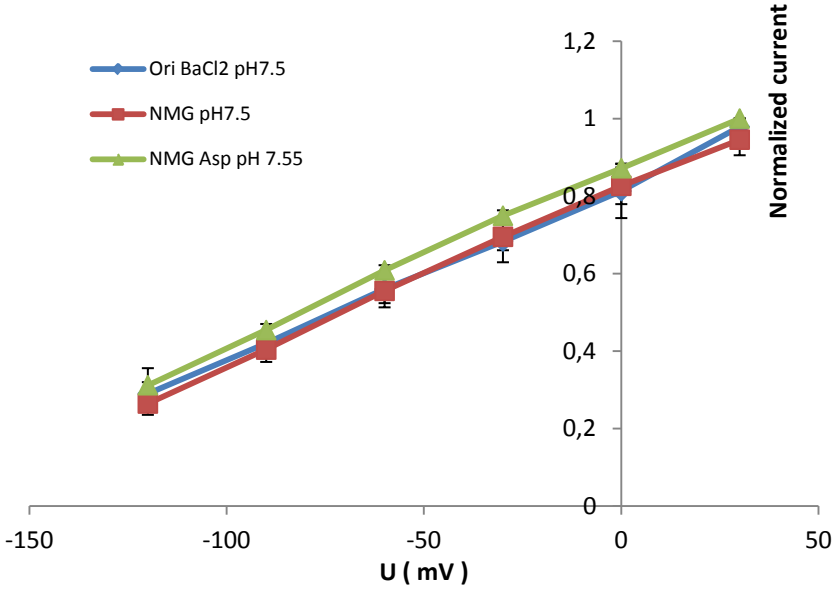

Figure 3.13 FR photocurrents in different buffers and under different potentials.

28 ng RNA were injected for oocytes expression. FR photocurrent was measured in Ori $BaCl_2$ pH 7.5, NMG pH 7.5 and NMG Asp pH 7.55 buffers and under 6 different potentials from -120 mV to +30 mV. The photocurrents were normalized to the FR photocurrent in NMG Asp pH 7.55 buffer under +30 mV. A 532 nm laser was used for illumination.

We also checked the FR photocurrents with NMG buffer of different pH (pH5.6, pH7.6 and pH 8.8). The FR photocurrent increases with the increase of extracellular pH, which is in accordance with proton pumping (Figure 3.14).

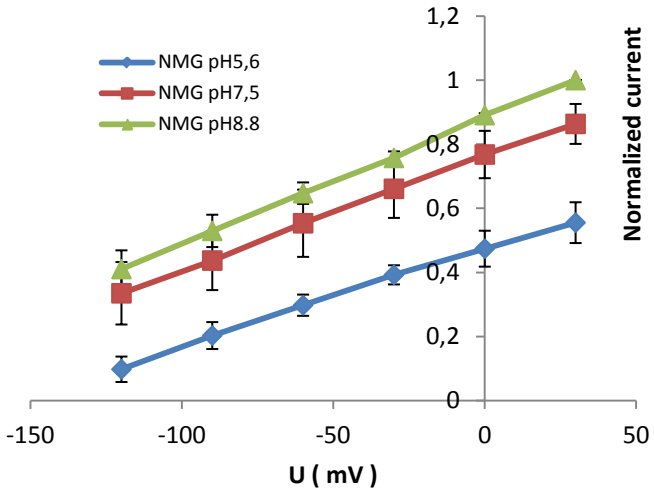

Figure 3.14 FR photocurrents in NMG buffers of different pH and under different potentials.

28 ng RNA were injected into oocytes for expression. FR photocurrents were measured in NMG buffer with pH 5.6, 7.5 and 8.8 under 6 different potentials from -120 mV to +30 mV. The photocurrents were normalized to the FR photocurrent in NMG pH 8.8 buffer under +30 mV. A 532 nm laser was used for illumination.

With the above results, we confirm the new rhodopsin FR is a light-regulated proton pump similar to BR.

3.1.6 The FR action spectrum

The action spectrum of FR was measured in NMG pH7.6 buffer with a white light source and glass filters of different wavelength (from 420 nm to 620 nm). The intensities of light with different wavelengths are all adjusted to around 0.55 mW/mm^2. The FR action spectrum has a peak at around 515 nm and is blue-shifted compared to BR, red-shifted compared to ChR2. (Figure 3.15).

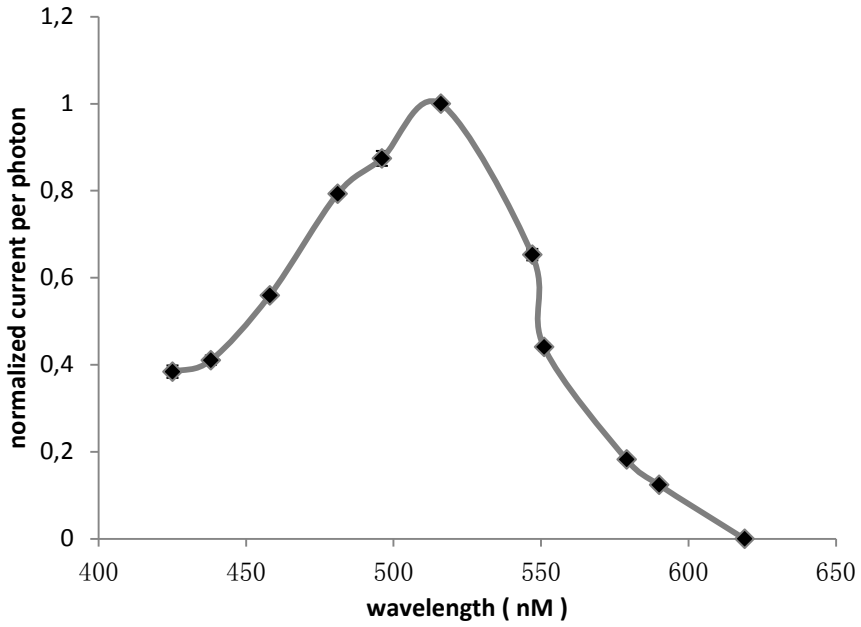

Figure 3.15 The FR action spectrum.

28 ng RNA were injected for oocytes expression. FR photocurrents were measured in NMG buffer with pH7.5 under -20 mV. The photocurrents were normalized to the FR photocurrent with 516 nm light illumination.

3.1.7 FR and BR

Microbial rhodopsins can usually bind retinal as chromophore to function. The *Xenopus* Oocyte contains endogenous retinal but not very abundant. We incubated FR expressing oocytes in ND96 with additional 1 μM all-trans-retinal (ATR) from the beginning (+ATR), no addtional retinal (-ATR) and additional 1 μM all-trans-retinal 1 dpi (+1 dpi ATR). The fluorescences were checked 2 dpi for oocytes with different retinal conditions. The FR expressing oocytes in ND96 with additional 1 μM ATR from the beginning seems to have a little bit stronger expression by the fluorescence (Figure 3.16).

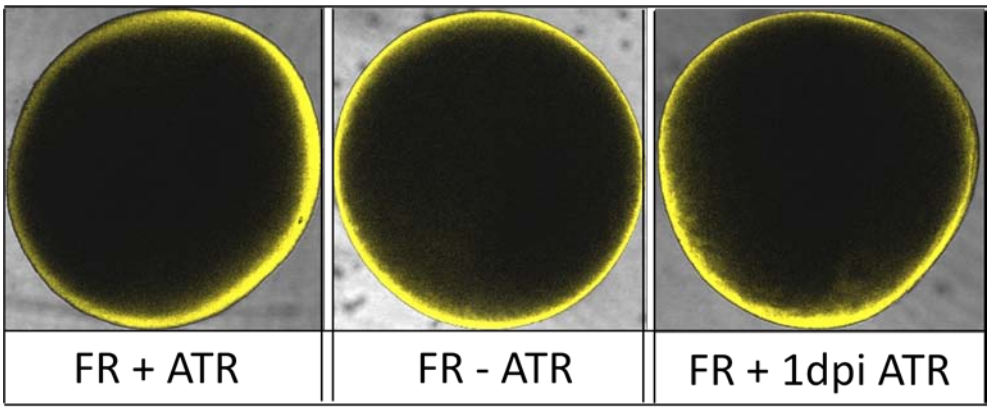

Figure 3.16 FR expressions with and without additional ATR.

25 ng RNA were injected for oocytes expression. +ATR, with addtional 1 µM ATR in ND96 buffer. –ATR, no additional ATR in ND96. +1dpi ATR, 1 µM addtional ATR was added to ND96 1 dpi. Fluorescences were checked 2 dpi.

The FR photocurrents were also checked 2 dpi for FR expressing oocytes with additional retinal, no additional ATR and with 1 dpi ATR. The FR photocurrents were bigger for +ATR than –ATR, but the difference is not big. The differeneces for +ATR and +1 dpi ATR, +1 dpi ATR and –ATR are not statistically obvious (Figure 3.17). Compared to ChR2, FR seems not require much additional ATR which is corresponding to the fluorescence check.

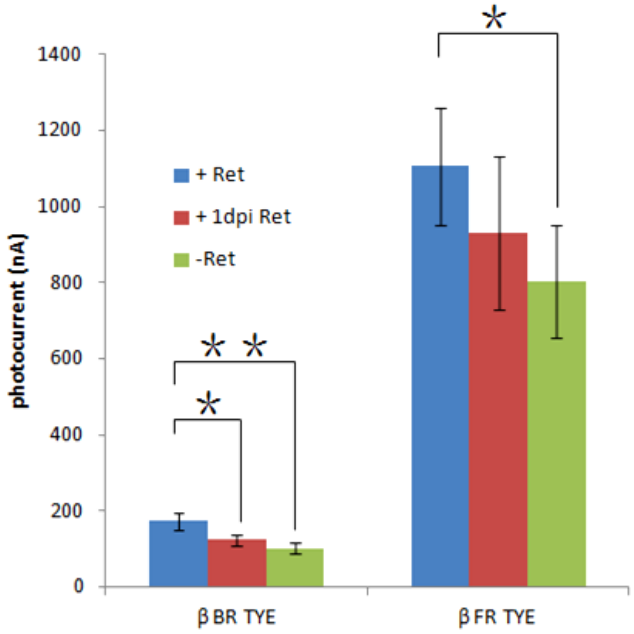

Figure 3.17 FR and BR photocurrents with and without additional ATR

25 ng RNA were injected for oocytes expression. +ATR, with addtional 1 µM ATR in ND96 buffer. –ATR, no additional ATR in ND96. +1 dpi ATR, 1 µM addtional ATR was added to ND96 1 dpi. Photocurrents were measured under -30 mV holding potential in Ori NMG pH 7.5 buffer. A 532 nm green laser was used for illumination. Significance of difference: $*$, $P < 0.05$; $* *$, $P < 0.01$ (done by OneWay ANOVA test, OiginPro 9). +Ret and +1 dpi Ret of FR, +1 dpi Ret and –Ret of FR, +1 dpi Ret and –Ret of BR are not significantly

different at the 0.05 level. n=4, error bars=SD.

BR shows similar ATR dependence to FR. The BR photocurrents were also larger with +ATR, then with +1 dpi ATR and the last is –ATR (Figure 3.17). In comparison with the well studied BR, the new rhodopsin FR has much stronger activity (Figure 3.17). We have also measured the membrane potential changes with green light illumination for oocytes expressing BR and FR. The hyperpolarization ability of FR upon illumination in *Xenopus* oocytes is stronger than BR. FR could increase the *Xenopus* oocytes membrane potential from about -25 mV to about -140 mV while BR could increase the membrane potential from about -25 mV to about -70 mV (Figure 3.18).

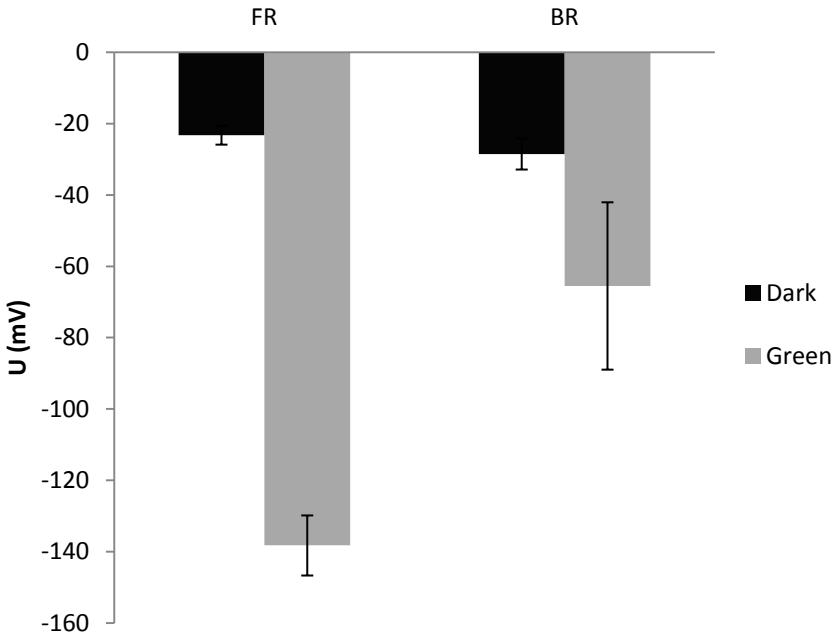

Figure 3.18 Hyperpolarization abilities of FR and BR in *Xenopus* oocytes.

Membrane potentials were measured in Ori NMG pH 7.5 buffer. 25 ng RNA were injected for oocytes expression. All are with addtional 1 µM ATR in ND96 buffer and a 532 nm laser was used for illumination. n=4, error bars=SD.

3.1.8 Light snesitivity at different temperatures

As the *F. cylindrus* is living in the cold polar area. FR is hypothesized to be more active at low temperature than BR. A preliminary test showed that the FR photocurrent at 4 ℃ was only reduced to about half of the photocurrent at 20 ℃ (Figure 3.19). This indicates FR to have good activity at low temperature.

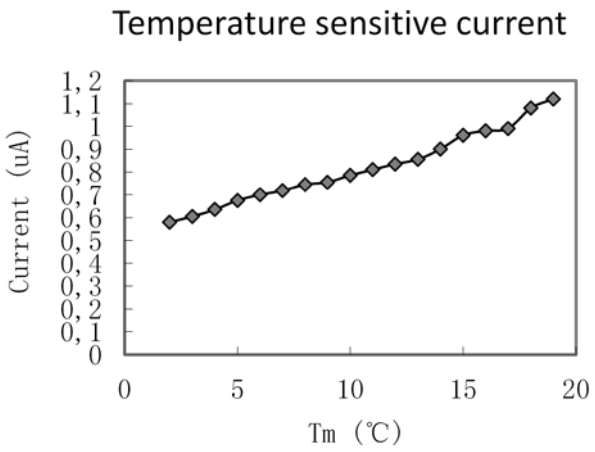

Figure 3.19 FR photocurrents at different temperatures.

25 ng RNA were injected for oocytes expression. All are with addtional 1 μM ATR in ND96 buffer and a 532 nm laser was used for illumination.

We also tested the photocurrents of FR at different temperatures with different light intensities in comparison with BR. The BR proton pump activity requires relative high light intensity and it is more sensitive to the temperature. The BR photocurrent was reduced to about 40% from 30 ℃ to 10 ℃ with 532 nm light intensity around 10 mW/mm^2. The half-maximal activation ($K_{0.5}$) were observed at 15 mW/mm^2, 12.5 mW/mm^2 and 10 mW/mm^2 for 30 ℃, 20 ℃ and 10 ℃ respectively, which indicates that the BR photocycle is getting slower with the decrease of temperature. The FR proton pump activity also requires relative high light intensity but it is less sensitive to the temperature. From 30 ℃ to 10 ℃, the FR photocurrent was only reduced to about 65% with 532 nm light intensity around 10 mW/mm^2. The $K_{0.5}$ for FR were all observed at around 11-12 mW/mm^2 for 30 ℃, 20 ℃ and 10 ℃ without dramatical differences (Figure 3.20).

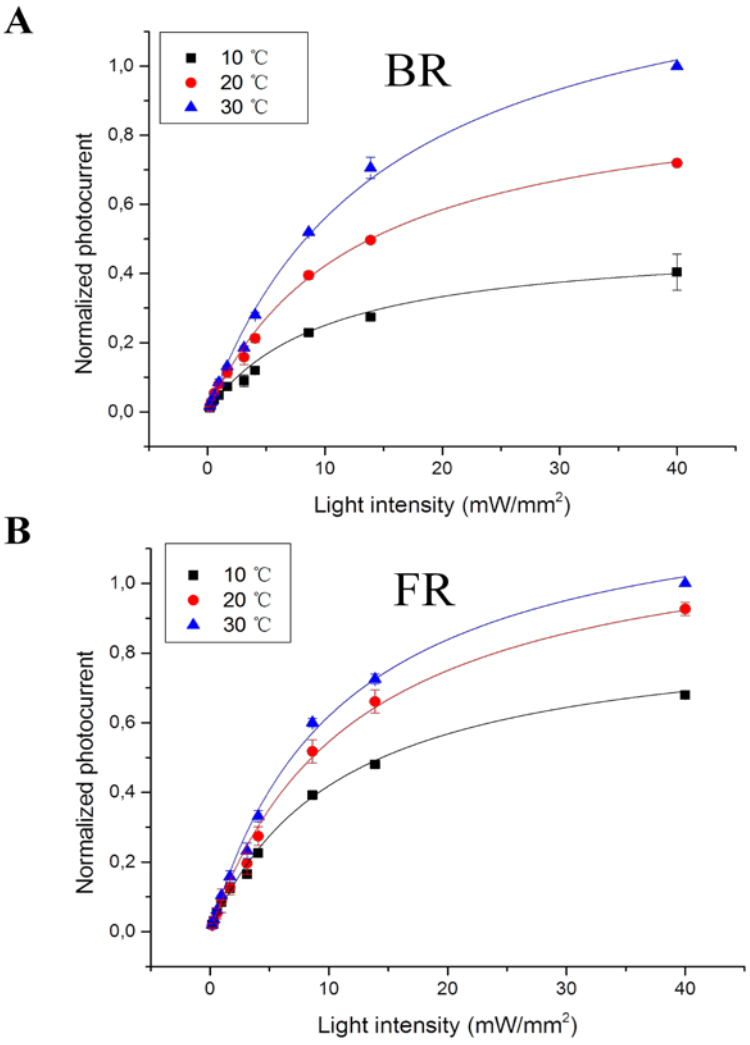

Figure 3.20 FR and BR photocurrents at different temperatures and different light intensities.

FR and BR photocurrents were tested at 10 ℃, 20 ℃ and 30 ℃ with different light intensities. 25 ng RNA were injected for oocytes expression. All are with addtional 1 µM ATR in ND96 buffer and a 532 nm laser was used for illumination. Michaelis-Menten curves were fitted. n=3, error bars=SD.

3.1.9 FR "ch" mutant

An unexpected point mutation was obtained during the screening of FR colonies. Surprisingly, this point mutation dramaticaly altered the proton pump activity of FR and make FR behave like a proton channel (Figure 3.21A). This mutant was named chFR for its bi-directional transport activity of proton. In NMG pH 7.5 buffer, an inward proton flux can be detected under more negative potential for chFR while for FR wt we can only see the outward proton flux upon illumination (Figure 3.22). The reversal potential for chFR is about -20 mV in NMG pH 7.6 buffer (Figure 3.22).

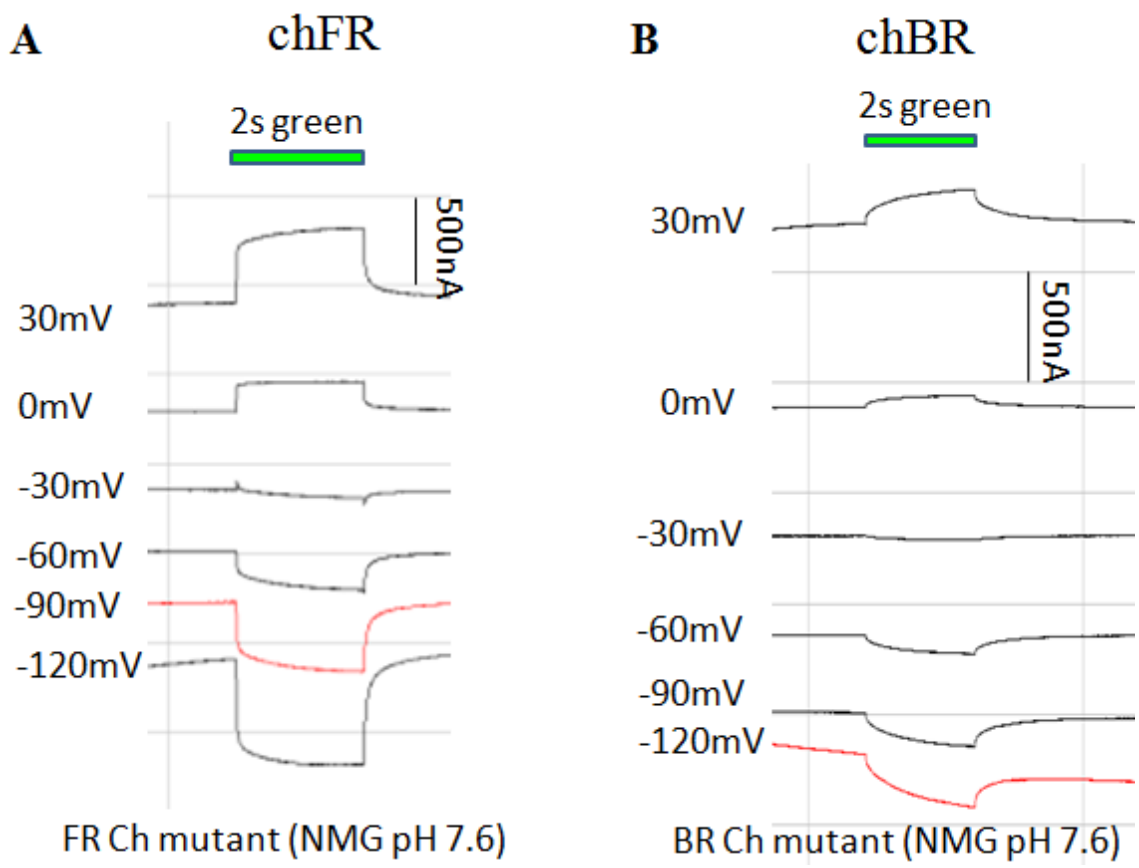

Figure 3.21 FR and BR "ch" mutants photocurrents under different potentials.

FR and BR "ch" mutants were both tested in NMG pH 7.6 buffer under different holding potentials. 2 s 532 nm green light was used for illumination.

A similar point mutation was made with BR to generate chBR. We can also detect the inward proton flux (Figure 3.21B). This suggests the mutation point is important for regulating the direction of proton movement.

I also tested FR and chFR photocurrents in different buffers. For the FR wt I see a little bit lower photocurrent in NMG pH 7.6 buffer than in NMG Asp pH 7.7 due to the pH difference. But for the chFR we see a little bit higher current in NMG pH 7.6 than in NMG Asp pH 7.7. This might be because of the effect of Cl^- in the buffer. Further experiments will have to clarify the exact permeabilities for cations and anions.

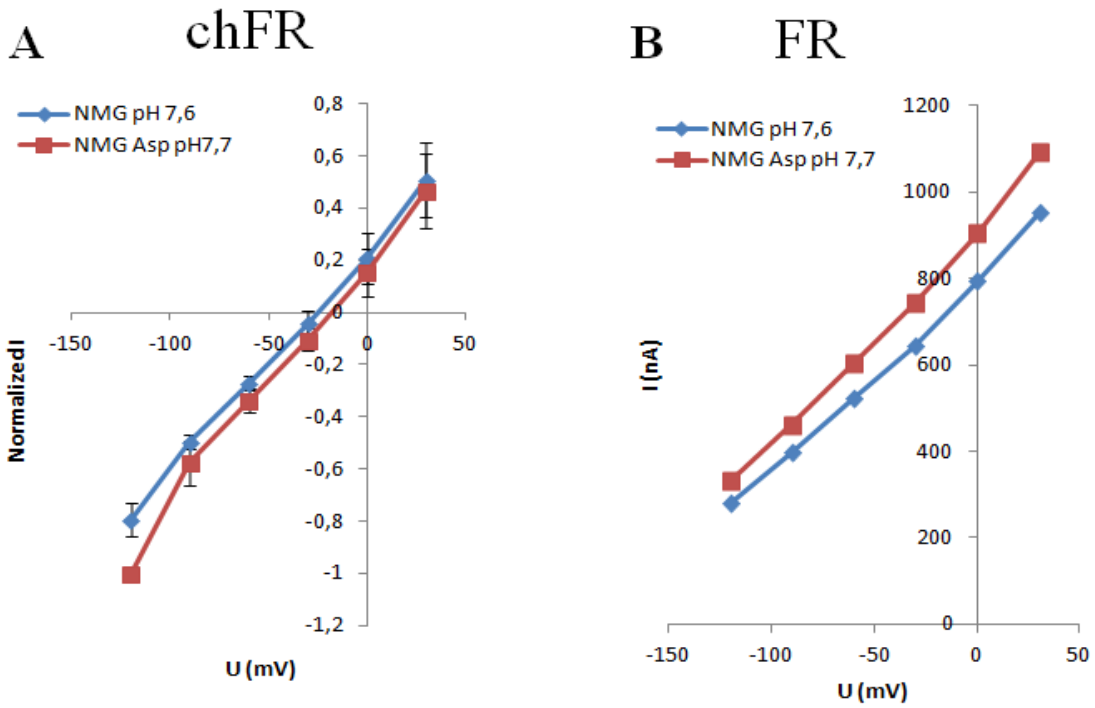

Figure 3.22 FR and chFR photocurrents under different potentials and in different buffers.

FR and chFR were both tested in NMG pH 7.6 and NMG Asp pH7.7 buffer under different holding potentials. 2 s 532 nm green light was used for illumination.

3.2 CyclOp, new Guanylate Cyclase Opsins from Fungi

Recently, Avelar *et al.* found in the genome of the fungus *B. emersonii* a new type I rhodopsin, fused with a Guanylyl Cyclase [42]. This rhodopsin guanylyl cyclase, BeGC1, was convincingly proven to be essential for phototaxis in *B. emersonii* through green light-regulated cGMP production. Yet the light-regulated guanylyl cyclase activity of BeGC1 was not directly demonstrated. Here I report the direct proof of the light-regulated guanylyl cyclase activity of BeGC1, which we name BeCyclOp, and 4 other guanylyl cyclase opsins from *Allomyces macrogynus* (AmCyclOp1, AmCyclOp2 and AmCyclOp3) and *Catenaria anguillulae* (CaCyclOp) by in vitro and in vivo assay with a *X. laevis* oocyte expression system. Furthermore the detailed characterization of BeGC1 suggests it to be a powerful optogenetic tool for light-gated cGMP production with high specificity and fast kinetics.

3.2.1 CyclOp sequences and predicted structure

The full length cDNA of BeCyclOp has been confirmed in *B. emersonii* by Avelar *et al.*[42]. The BeCyclOp protein has 626 residues with calculated 68 kDa molecular weight. It comprises a microbial (type I) opsin domain near the N-teminal and then a GC domain in the C-terminal part connected by a short coiled-coil domain in the middle. Compared to other microbial opsins, BeCyclOp has a very long N-terminus. Transmembrane helix prediction by TMHMM indicates that BeCyclOp might have 8 TM helices, while all other opsins known so far are 7 TM proteins with extracellular N- and cytoplasmic C-termini, respectively. The N-terminus of BeCyclOp appears to contain no signal sequence, and should thus be cytosolic, like the predicted C-terminus. The 1st TM is predicted to span amino acids (aa) 147 to 169. The 4th helix (aa 249-270) in BeCyclOp shows high conservation with TM 3 in other type I opsins. The conserved lysine for binding retinal is in the last, the predicted 8th helix. To retain consistency with other microbial rhodopsins, we number the additional predicted transmembrane helix in the N terminus as “T0”. (Figure 3.23)

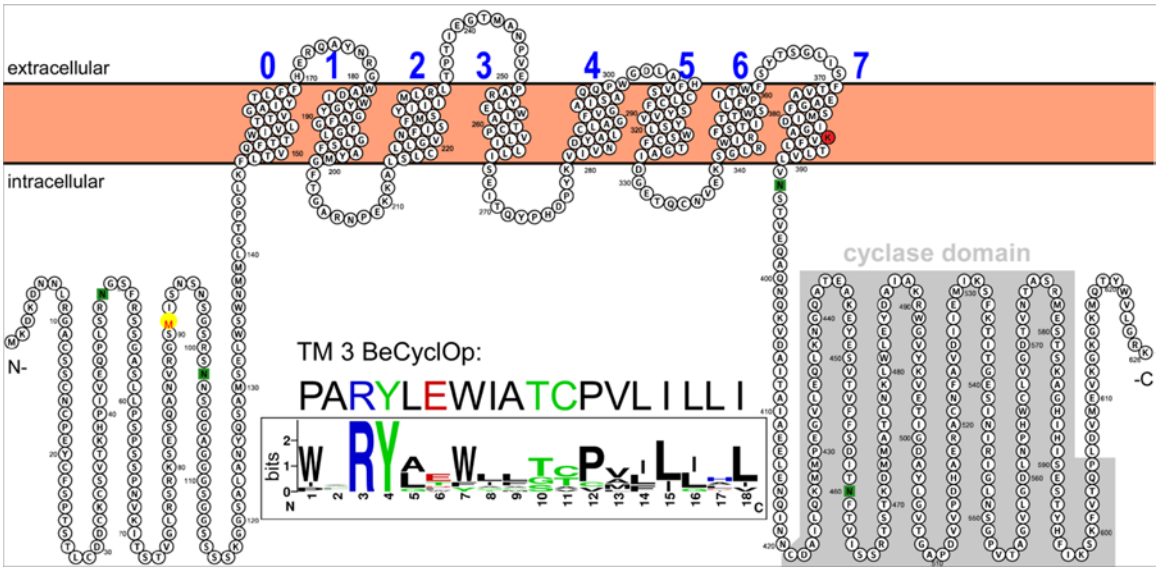

Figure 3.23 The predicted BeCyclOp structure.

The predicted BeCyclOp structure with sequence labelling. Transmembrane helices are decided by TMHMM[70] prediction and sequences alignment with other microbial rhodopsins. The lysine (K) residue in TM 7 for retinal binding to form Schiff base is labeled red. The putative cyclase domain predicted by alignments with other type III guanylyl cyclases is shaded in grey. Inset: The BeCyclOp 4th TM helix (TM 3) sequence and sequence logo of the highly conserved 3rd helix of microbial rhodopsins, based on the alignment of BeCyclOp, *H. salinarum* bacteriorhodopsin and halorhodopsin (HsBR and HsHR), *Natronomonas* halorhodopsin (NpHR), *Anabaena* sensory rhodopsin (ASR), *Natronomonas* sensory rhodopsin II (NpSRII), *Chlamydomonas* channelrhodopsins 1 and 2 (ChR1 and ChR2), and *Volvox* ChR1, was generated by Weblogo 2.8.2 [69]. Picture is drawn by Protter[71].

Avelar et al. [42] also identified four other CyclOps from other fungal genome sequences: Three predicted CyclOps (AmCyclOp1, 2 and 3) from *A. macrogynus* and CaCyclOp from *C. anguillulae* (Fig. 3.24). All of them have similar predicted structure with 8 TM helices, including the T0 as a specific addition to CyclOps.

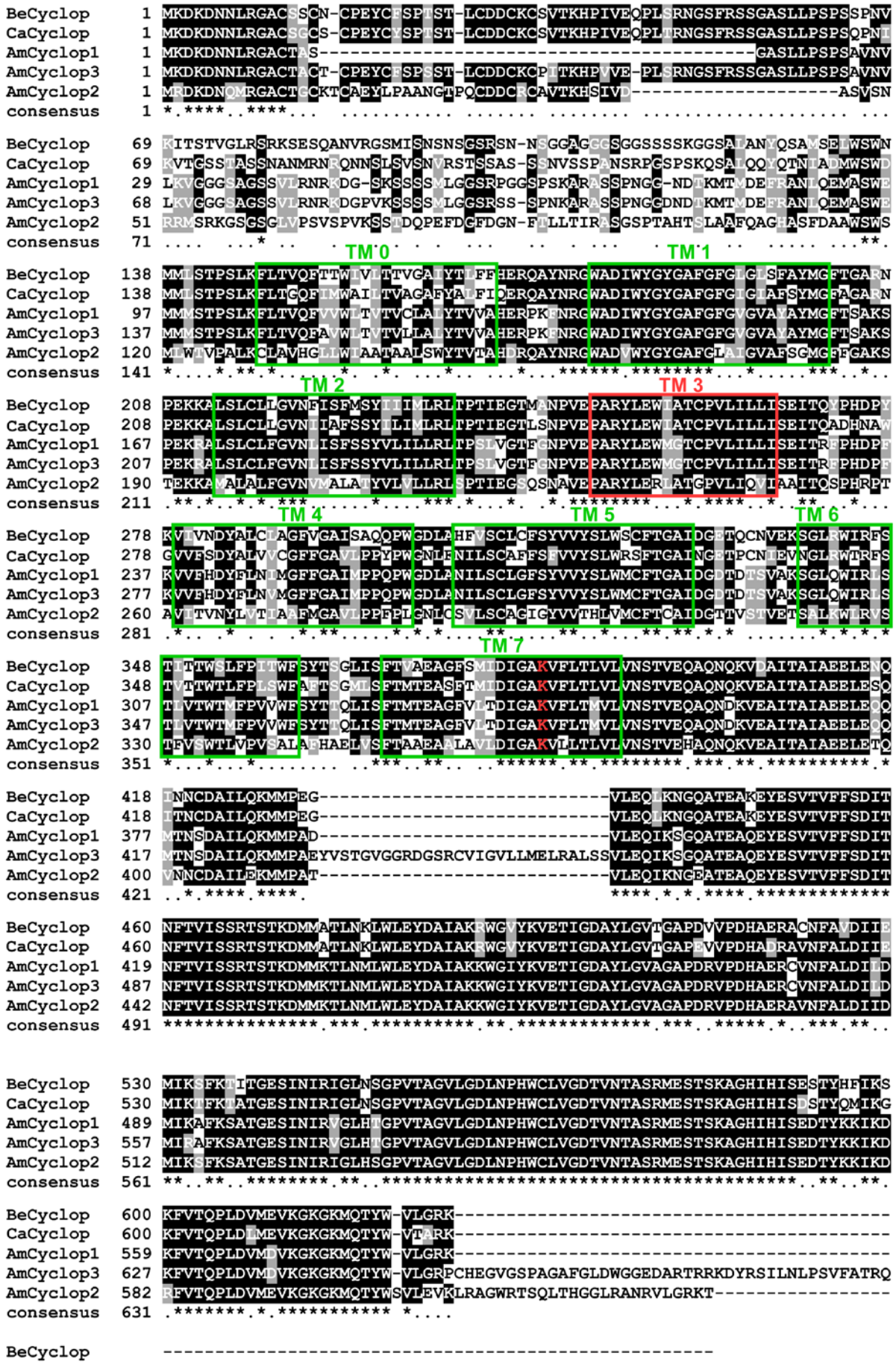
TM 0
TM 1
TM 2
TM 3
TM 4
TM 5
TM 6
TM 7

Figure 3.24 Sequence alignments of the BeCyclOp, AmCyclOp1-3 and CaCyclOp.

The predicted TM helices are marked with green boxes while the conserved TM 3 with a red box. The conserved lysine (K) in TM 7 for retinal binding is printed in red. Black shading indicates identity and grey shading homology in >50% of the sequences. Alignment is performed by ClustalW and Boxshade was used for shading conserved sequences.

3.2.2 Expression of CyclOps in *Xenopus* oocytes

We let all five CyclOps synthesized with codon usage optimized to *Mus musculus*, cloned to pGEMHE vector, which is optimized for generating RNA for *Xenopus* oocytes. cRNA was made by T7 in vitro transcription kit and injected into *Xenopus* oocytes for expression. YFP tag was fused to the C-terminus. All five CyclOps showed good expression in oocytes 3 days post injection (dpi) judged by the YFP fluorescence (Figure 3.25a). For BeCyclOp expressing oocytes without additional retinal seems little weaker than oocytes with additional retinal (Figure 3.25a).

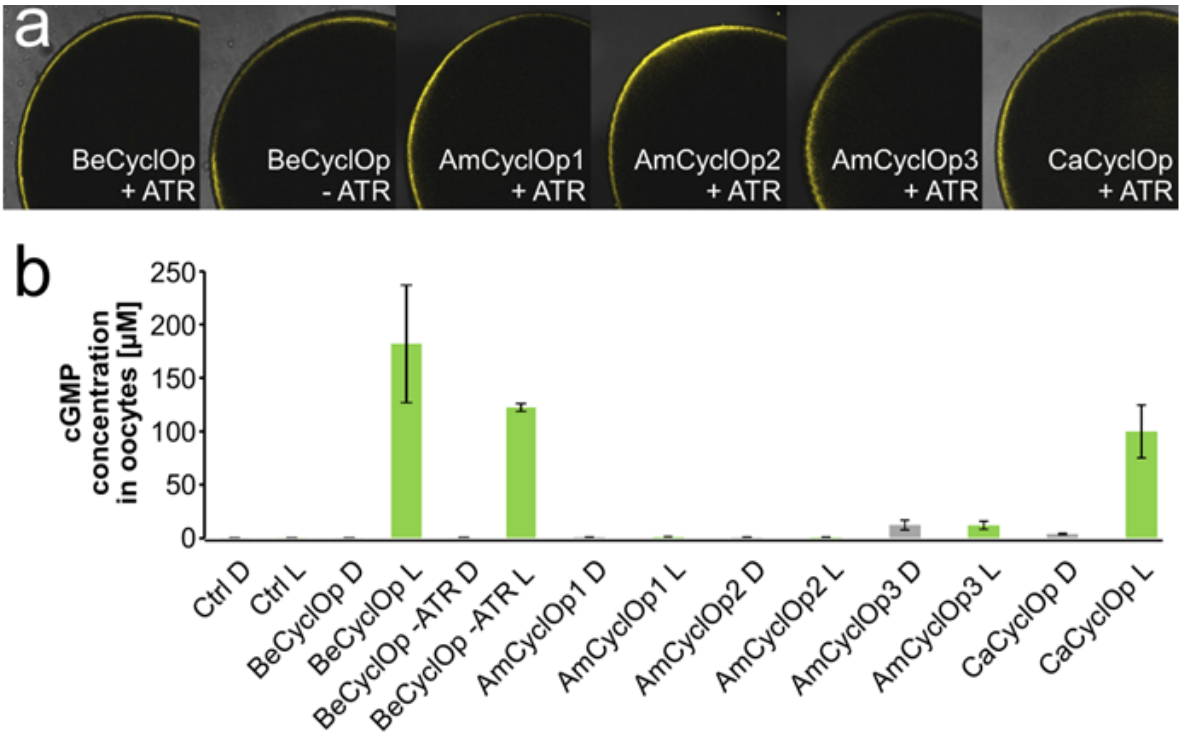

Figure 3.25 Expression of different CyclOps in *Xenopus* oocytes and GC activity test.

a, LSM imaging of YFP tagged CyclOps. + ATR, with additional 1 µM all-trans-retinal in the ND96 buffer. – ATR, no additional retinal. b, GC activity test in dark and 2 min green light illumination for oocytes expressing different CyclOps. D, samples in dark. L, samples with 2 min 532 nm green light illumination. Light intensity, 0.15 mW/mm^2 for BeCyclOp or 0.5 mW/mm^2 for all other CyclOps. N=2 experiments, mean of 5-6 oocytes each, error bars = SD

The GC activity was tested then by cGMP immuno assay of homogenized oocytes. The injected oocytes were homogenized by pipetting in dark or after 2 min illumination with green light (532 nm; 0.15 mW/mm^2 for BeCyclOp or 0.5 mW/mm^2 for all other CyclOps), followed by a colorimetric assay

for cGMP content. The BeCyclOp expressing oocytes have similar cGMP content as the contol oocytes without injection in dark and light conditions. 2 min light-treatment of BeCyclOp expressing oocytes led to a ~180 fold increased level of cGMP concentration, compared to extract prepared from control oocytes kept in the dark (Figure 3.25b). Addition of 1 μM ATR to the oocyte medium ND96 buffer led to slightly increased BeCyclOp YFP fluorescence (Fig. 3.25a). The binding of ATR possibly also stabilizes the BeCyclOp protein in the oocyte plasma membrane, as previously observed for ChR2[73]. With correspondence to the expression level, the cGMP production upon illumination was also slightly higher with additional ATR, which is ~1.5 fold compared to oocytes without additional ATR (Fig. 3.25b). The in vivo assay of cGMP production with 4 other CyclOps in *Xenopus* oocytes was also performed. The CaCyclOp have higher light induced GC activity compared to AmCyclOps, but it also shows higher dark activity (Fig. 3.25b). For the 3 AmCyclOps, AmCyclOp 1 showed weak light induced GC activity, AmCyclOp 2 showed no obvious GC activity and AmCyclOp3 showed GC activity both in dark and after illumination without obvious difference (Fig. 3.25b).

3.2.3 In vitro assay of GC/AC activity with *Xenopus* oocytes membrane extracts

With the in vivo assay, we could demonstrate the GC activity of 5 CyclOps in dark after light illumination. However, the relative big variations of the individual oocytes make accurate quantification difficult. And the living oocytes contain phosphodiesterases (PDEs) which may degrade the newly generated cGMP. Also it is difficult to compare the exact ratio between light and dark conditions (L/D) due to long time culture of oocytes in dark for expression. We thus designed an in vitro assay based on isolated oocyte membranes simply by 2 step centrifugation. The crude membrane extract was then added to the prepared GC reaction buffer to start ther reaction in different conditions. In vitro assay with membrane extract of BeCyclOp expressing *Xenopus* oocytes shows linerizaed cGMP increase in dark (D) and light (L) (Figure 3.26). Measurements after a light flash showed a fast increase of cGMP level and then a stable cGMP concentration as we measured for up to 20 min (data not shown). This demonstrated the absence of PDE activity in our in vitro assay. With the in vitro assay we could make accurate quantification with uniformity.

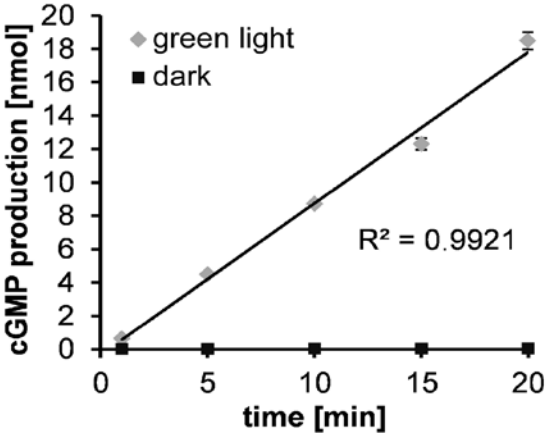

Figure 3.26 In vitro assay of BeCyclOp GC activity with oocytes membrane extracts.

Light-induced cGMP production with membrane preparations from oocytes expressing BeCyclOp. Membranes were kept in dark or illuminated (L, green bars, 532 nm, 0.5 mW/mm²). The final cGMP production was normalized to the membnrane extract of 1 oocyte. n=3, error bars = SD.

Then the in vitro assay was firstly used to determine GC activities in light (L) and in the dark (D) to calculate the L/D ratio of GC activity (Figure 3.27). The L/D ratio of BeCyclOp without YFP tag was highest at 5000±15, which is suggested the strongest light activation of any light-activated nucleotide cyclase. The BeCyclOp with C terminal YFP tag showed similar high activity in the light, but a four-fold increased activity in the dark (Figure 3.27). This is possibly because the dimerization of YFP pulls the GC domain closer to function in dark.

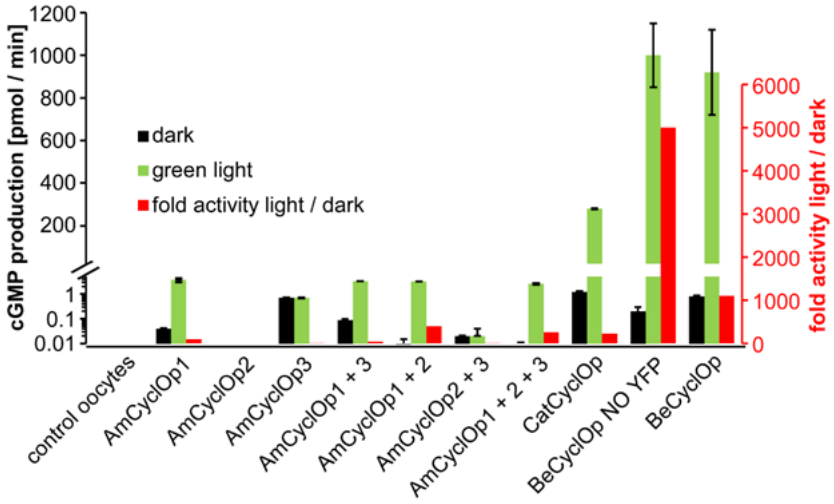

Figure 3.27 In vitro assay of different fungal CyclOps.

Light-induced cGMP production with membrane preparations from oocytes expressing 5 various CyclOps and also different combinations of AmCyclOp 1, 2 and 3. Membranes were kept in dark (D, black bars) or illuminated (L, green bars, 532 nm, 0.5 mW/mm²). The final cGMP production was normalized to the membnrane extract of 1 oocyte. n=3, error bars = SD. (see Tab. 3.1 for amounts of cRNAs injected)

3.2.4 Comparison of various CyclOps in *Xenopus* oocytes

CaCyclOp has the highest homology to BeCyclOp among the 4 other CyclOps. It shows a strong light-activated GC activity with about 230 L/D ratio. However, its dark activity was higher than that of BeCyclOp (Figure 3.27). The AC activity was also tested for these CyclOps (Table 3.1). CaCyclOp is the only CyclOp with a detectable AC activity; however it was very weak in light and was less than 1% of GC activity.

For the 3 AmCyclOps, AmCyclOp1 showed very weak, and AmCyclOp2 showed virtually no photo-activated GC activity, in both the in vitro (Figure 3.27) and in vivo (Figure 3.25b) assay. AmCyclOp3 showed ~11 fold higher GC activity than controls in both light and dark conditions with no obvious light regulation. These proteins belong to class III cyclases, which form homo- or heterodimers[74,75]. Therefore, we performed co-injections with different combinations of cRNA for the three AmCyclOps.

AmCyclOp1 and 2 were mixed 1:1. For AmCyclOp3, only 1/10th was used to increase the probability of AmCyclOp3 to form a heterodimer with AmCyclOp1 or 2 due to high dark activity and no light activation of AmCyclOp3 itself. Nearly all different combinations showed some light-gated GC activity in oocytes, however, at much lower levels than BeCyclOp (generally less than 1%). The in vitro assay indicated that AmCyclOp1 and AmCyclOp2 could possibly form a heterodimer and function with higher (light) and lower (dark) activity (L/D = 400) than the AmCyclOp1 homomer (L/D = 93). AmCyclOp1 could also possibly dimerize with AmCyclOp3, but this dimerization leads to higher dark activity. But to exactly determine how these 3 AmCyclOps function in one organism, further analysis, involving the fungus, is required to show how these 3 CyclOps function in vivo.

Membranes from oocytes expressing (ng cRNA injected)		cGMP [pmol / min]			cAMP [pmol / min]	
		Dark	Green	L/D	Dark	Green
Control oocytes	(0)	NA	NA		NA	NA
AmCyclOp1	(28)	0.04 ± 0.003	3.7 ± 0.7	93	NA	NA
AmCyclOp2	(28)	NA	NA		NA	NA
AmCyclOp3	(28)	0.7 ± 0.03	0.7 ± 0.03	1	NA	NA
AmCyclOp1 + 3	(14 + 1.4)	0.09 ± 0.006	3.3 ± 0.04	37	NA	NA
AmCyclOp1 + 2	(14 + 14)	0.008 ± 0.007	3.2 ± 0.01	400	NA	NA
AmCyclOp2 + 3	(14 + 1.4)	0.02 ± 0.001	0.02 ± 0.02	1	NA	NA
AmCyclOp1 + 2 + 3	(7 + 7 + 1.4)	0.01 ± 0.001	2.6 ± 0.2	260	NA	NA
CaCyclOp	(28)	1.2 ± 0.1	280 ± 2	230	NA	0.2 ± 0.04
---------- different oocyte batch ----------		----------	----------		----------	----------
BeCyclOp no YFP	(28)	0.2 ± 0.1	1,000 ± 150	5,000	NA	NA
BeCyclOp	(28)	0.8 ± 0.08	920 ± 200	1,100	NA	NA

Table 3.1 In vitro assay of cGMP and cAMP generation by different fungal CyclOps.

BeCyclOp, AmCyclOps, and CaCyclOp membrane extract GC/AC activity under dark (D) and 0.5 mW/mm^2 532 nm green laser was used for illumination (L). cRNA injection amounts as indicated in the table. Final activity refers to the activity of membrane extract from 1 oocyte. All constructs are with C-terminal YFP tag. (n=3 experiments, NA, no obvious activity detectable, errors = SD).

Among the five CyclOps tested by both in vitro and in vivo assay in *Xenopus* oocytes, BeCyclOp seems the best to be used as an optogenetic tool with high L/D ratio and good specificity. We thus focus on BeCyclOp for further characterization.

3.2.5 Action spectrum of BeCyclOp

The in vitro assay was also used for obtaining the action spectrum of BeCyclOp. Aliquots of the BeCyclOp expressing oocytes membrane preparation were illuminated with light of different wavelengths generated by a combination of filters for certain wavelength and a white light source. The intensities of light at different wavelengths were adjusted to around ~0.02 mW/mm^2 for reliability. cGMP production per photon amount was calculated to generate the action spectrum.

The action spectral peak of BeCyclOp was around 530 nm (green light), which is red-shifted to the one of ChR2 and blue-shifted compared to BR (Figure 3.28). The spectrum is relatively broad, similar

to other microbial rhodopsins while 660 nm (red) and 385 nm (UV) light could still activate BeCyclOp, albeit much less efficiently. This is in good agreement with previous analyses of the effect of different light wavelengths in promoting phototaxis of *B. emersonii* zoospores.

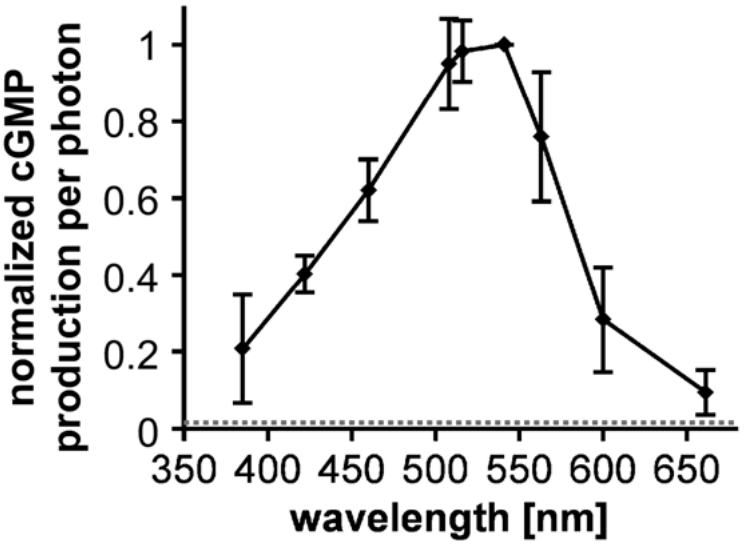

Figure 3.28 BeCyclOp action spectrum.

Light intensities at different wavelengths were adjusted to ~0.02 mW/mm^2. cGMP production of oocyte membranes per photon amount was calculated, normalized to the action spectrum peak. The dotted grey line indicates the relative dark activity, Mean of n=3 experiments, error bars: SD.

3.2.6 Light sensitivity of BeCyclOp function

The light sensitivity of new rhodopsins can be a indication for possible function and also a good index for using as a optogenetic tool. So the BeCyclOp expressing oocyte membranes are illuminated with 532 nm, which is near the action spectra peak of BeCyclOp, with green light of different intensities. In vitro cGMP assays are performed then to check the BeCyclOp light sensitivity. This showed a half-maximal activation ($K_{0.5}$) at about 0.055 mW/mm^2 (Figure 3.29) which is already sensitive as an optogenetic tool. The bPAC from Beggiatoa is even more sensitive to light than BeCyclOp with a half-maximal activation ($K_{0.5}$) at about 4 µW/mm^2 [24]. But usually an enhanced light sensitivity is related with a slower photocycle. For bPAC, the cyclase activity will continue in the dark after a light flash because of the slow photocycle. The bPAC cAMP production in the dark levels off with a time constant τ = 23±2 s at pH 7.4 after a 4 s light flash, which is in accordance with the higher light sensitivity. Similarly, mPAC from *Microcoleus* has a $K_{0.5}$ = 6 µW/mm^2 and also a slow photocycle with a time constant τ = ~14 s [76]. The bigger $K_{0.5}$ value for BeCyclOp indicates a faster photocycle.

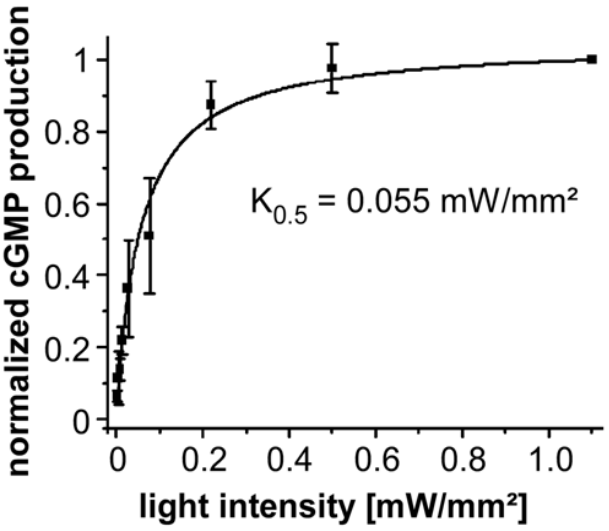

Figure 3.29 BeCyclOp light sensitivity.

A. Light (532 nm green laser) intensity dependence of mean normalized cGMP production of BeCyclOp-expressing oocyte membranes; pH 7.35. A Michaelis-Menten curve with $K_{0.5}$ = 0.055 mW/mm^2 was fitted. n=3 experiments, error bars=SD. Experiment performed in 20 ℃ water bath.

We firstly tried to measure the time constant of BeCyclOp in the time range of seconds (Figure 3.30). But we see no obvious further cGMP production after 1 s light illumination, which indicates a faster photocycle of BeCyclOp and this can not be manipulated by hand pipetting. Figure 3.30 also shows stable cGMP concentration, indicating the absence of PDE activity in extracted oocyte membranes.

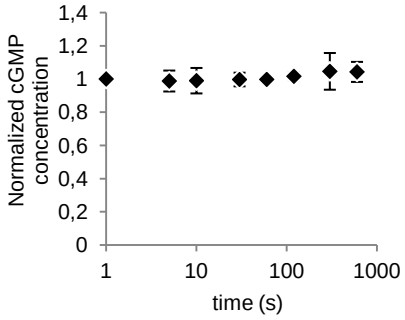

Figure 3.30 BeCyclOp activity after 1 s illumination.

1 s light illumination (532 nm, 0.2 mW/mm^2) was performed in the beginning. The cGMP production was measured then for the samples in the dark at different time from 1 s to 15 min. n=3 experiments, error bars=SD

Previous studies showed that the BeCyclOp closing kinetics might be in ms level. To measure this, we built a computer-controlled system where cyclase activity was initiated by a 20 ms laser flash (532 nm, 0.5 mW/mm^2), and stopped after different time intervals (from 20 ms to 2.6 s) by quenching with buffer containing 0.1 M HCl. The results show that the cGMP concentration keeps increasing in the dark after the 20 ms 532 nm light flash with τ = 320±20 ms at 21℃, reaching saturation after ~1.5 s

(Figure 3.31). This indicated that BeCyclOp has a fast photocycle, which makes BeCyclOp a well-controllable tool for optogenetics.

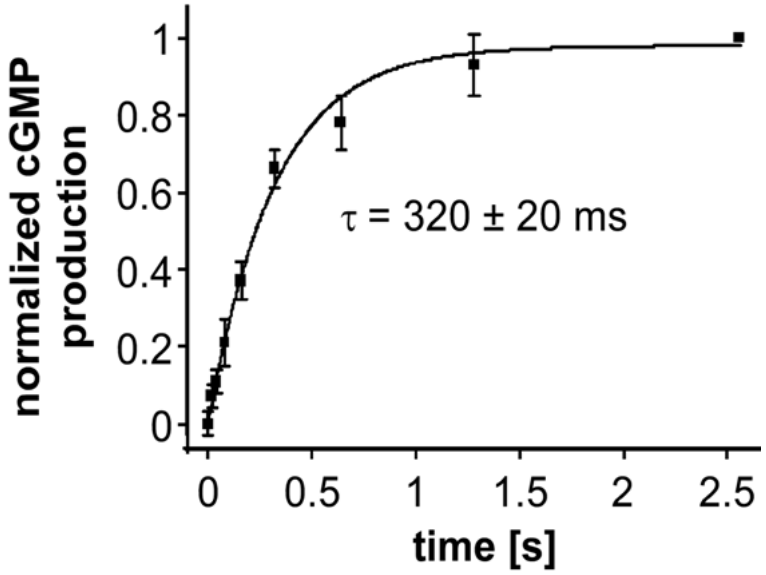

Figure 3.31 BeCyclOp closing kinetics.

Closing kinetics measured by cGMP production of BeCyclOp--expressing oocytes membranes, measured at indicated times after 20 ms illumination (532 nm, 0.5 mW/mm^2). A mono-exponential fitting curve with τ = 320±20 ms. Experiment performed in 21 ℃. n=3 experiments, error bars=SD

3.2.7 The long N-terminus of BeCyclOp

Based on the analysis of BeCyclOp primary sequence, we built a BeCyclOp model with 8 transmembrane helices and a rather long cytosolic N-terminus. This structure model is quite different with other 7 TM rhodopsins studied to date.

We try to test the function of the cytosolic N-terminus part by generating a terminally truncated version of BeCyclOp by cutting the first 90 aa, using the 2nd methionine (M91) as translational start. The shorter version (BeCyclOpS) could also express well in *Xenopus* oocytes (Fig. 3.32b) judging by the fluorescence of the C-terminal YFP tag and the GC activity could also be enhanced by light (Fig. 3.32c). However, compared to full length BeCyclOp, BeCyclOpS shows higher dark activity and lower light-induced GC activity. This suggested that the BeCyclOp N-terminus is required for tight light-regulation of GC activity possibly by interaction with the GC domain.

Then we used Bimolecular Fluorescence Complementation (BiFC)[77] to test the N-terminus cytoplasmic localization and its possible interaction with GC domain. We designed a BeCyclOp construct (BeCyclOp::BIFC; Figure. 3.32a) to this end by fusing the C-terminal 84aa of YFP (YC) to the N-terminus of BeCyclOp and the N-terminal 154aa of YFP [28] to its C-terminus. Strong fluorescence was observed (Figure. 3.32b) for BeCyclOp::BIFC, indicating YC and YN interaction

and reconstitution of YFP. This further proved the cytoplasmic localization of both N- and C- termini of BeCyclOp and also possible interaction of the N and C-termini. The BeCyclOp::BIFC GC activity in the dark was not increased and was only slightly weaker than that of BeCyclOp::YFP during illumination (Figure. 3.32c), which is different to BeCyclOpS.

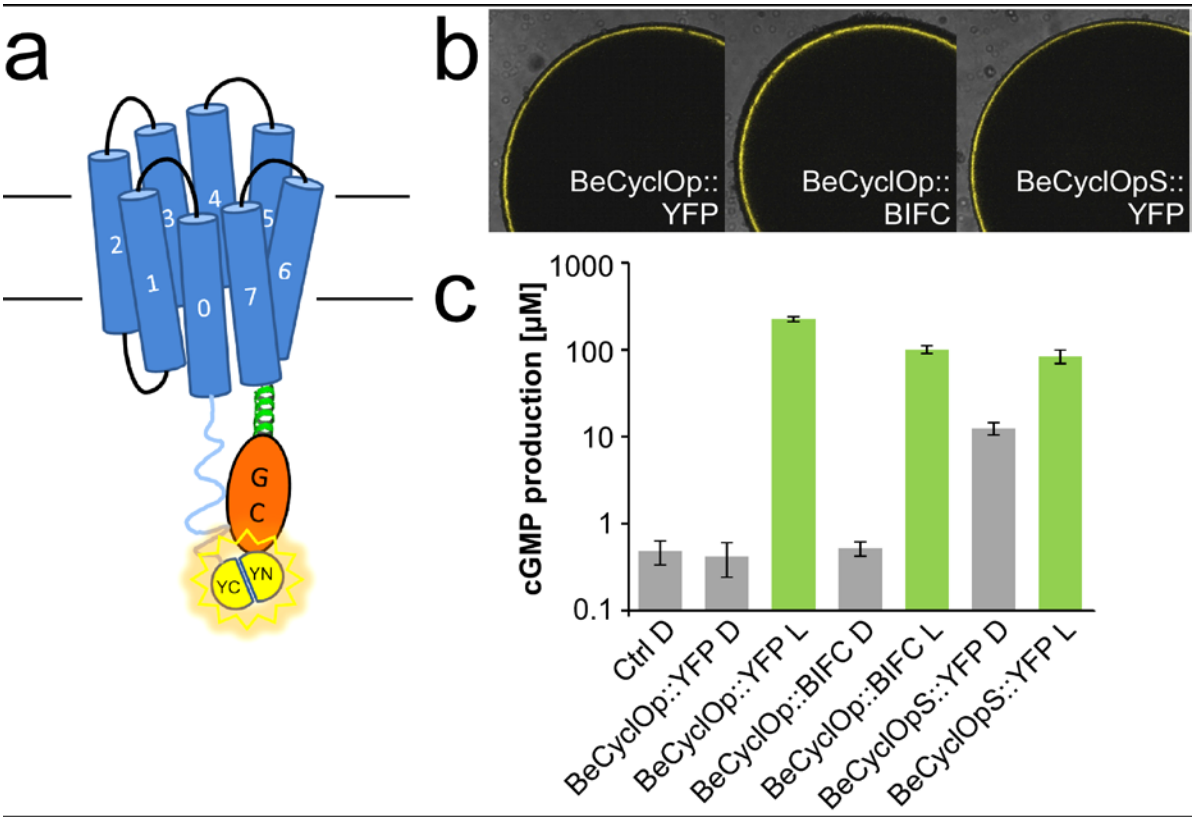

Figure 3.32. Cytosolic localization and regulation of cyclase activity by the BeCyclOp N-terminus.

A. BeCyclOp BIFC construct: YN (aa 1-154 of YFP) fused to C-, and YC (aa 155-238 of YFP) fused to the N-terminal ends of BeCyclOp. **B**. Fluorescence images of oocytes expressing different BeCyclOp constructs. BeCyclOpS refers to deletion of aa 1-90 in the N terminus from BeCyclOp. **C**. cGMP production in *Xenopus* oocyte expressing different BeCyclOp constructs in dark (D) and after illumination (L; 532 nm, 0.2 mW/mm^2, 2 min). n=2 experiments, mean value of 6 oocytes each, error bar = SD.

3.2.8 Activation of a CNG channel following BeCyclOp photostimulation

Nagel and coworkers previously measured activity of light-activated cyclases (EuPAC, bPAC and mPAC) indirectly by activation of CNG channels[24,25,76] after co-expression in *Xenopus* oocytes. OLF/T537S is a bovine CNG channel [78] mutant which is very sensitive to cAMP ($K_{0.5}$ = ~ 14 µM) and even more to cGMP ($K_{0.5}$ = ~ 0.7 µM). We use the two-electrode voltage-clamp technique to monitor light-induced cGMP production *via* cGMP-activated currents (Figure 3.33a) after co-expression of BeCyclOp and the OLF channel in *Xenopus* oocytes by RNA injection. 3 dpi of 0.6 ng BeCyclOp and OLF cRNA each, a short green laser flash (100 ms, 532 nm) induced ~ 5 µA of inward current in oocytes (Figure 3.33b). A zoomed view showed that the light-induced currents became obvious already 100 ms after illumination. And the photocurrent starts decreasing ~ 1 s after activation, which

is much faster than the PAC measurement together with OLF, presumably due to a combined effect of cGMP diffusion and PDE activity (Figure 3.33c). The fast kinetics here is corresponding to our previous in *vitro* assay, the photocycle of BeCyclOp is relatively fast with a rise time of τ = 320 ms for the light-activated GC activity.

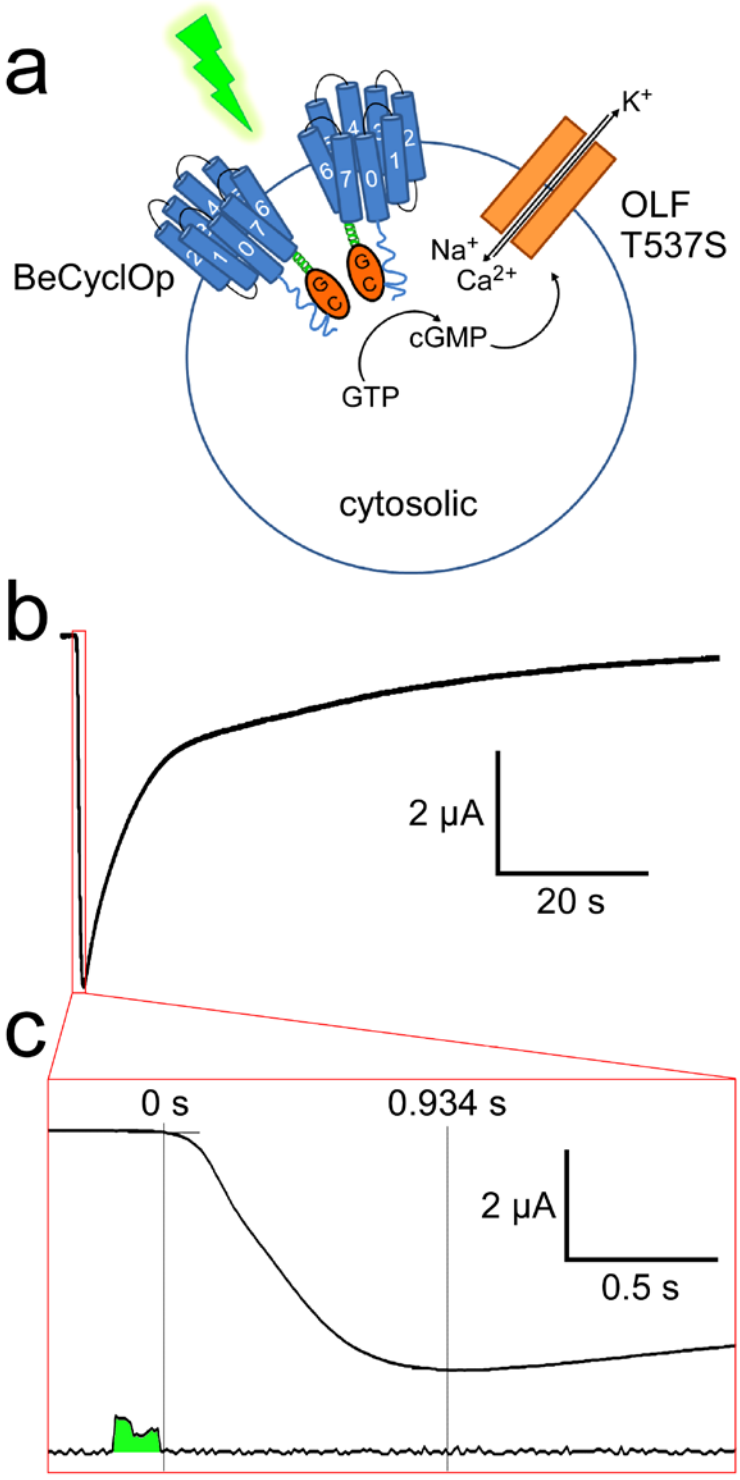

Figure 3.33. Light activation of cGMP-sensitive cation channel OLF/T537S *via* BeCyclOp.

A. Principle for electrophysiological measurement of BeCyclOp cGMP production by currents of the co-

expressed cyclic nucleotide gated (CNG) channel mutant OLF/T537S. **B**. Photocurrent induced by a 100 ms green laser flash (9 mW/mm^2, 532 nm) in *Xenopus* oocyte, 3 dpi of 0.6 ng BeCyclop cRNA and 6 ng OLF/T537S cRNA. **C**) Enlarged current trace, indicating the on- and off-kinetics of the BeCyclOp/OLF system. The upper trace indicates the photocurrent; the lower trace is a record of the 100ms green laser signal.

3.2.9 BeCyclOp is more effective than bPGC in generating cGMP

The soluble bPGC (BlgC) is a light-regulated GC generated from *Beggiatoa* PAC (bPAC) by three point mutations[26]. But the bPGC was not yet applied in animal cells possibly due to its low efficacy upon illumination. To compare BeCyclOp::YFP and bPGC::YFP (BlgC-YFP), we expressed them in oocytes (**Figure 3.34a**), and measured the cGMP/cAMP concentrations obtained 2 dpi, in the dark, or with 2 min of illumination with blue light (464 nm, 10 µW/mm²; **Figure 3.34b**). These illumination conditions favored bPGC with its action spectrum maximum in the blue and also its higher light sensitivity. However, blue light still yielded ~ 40 times more cGMP in BeCyclOp-expressing oocytes than in bPGC-expressing oocytes. Further, when illuminating for longer as 20 min, bPGC-expressing oocytes contained significantly more cAMP than controls, while BeCyclOp-expressing oocytes did not exceed the cAMP level of controls (**Figure 3.34c**). BeCyclOp is a more specific and effective light-regulated GC than bPGC.

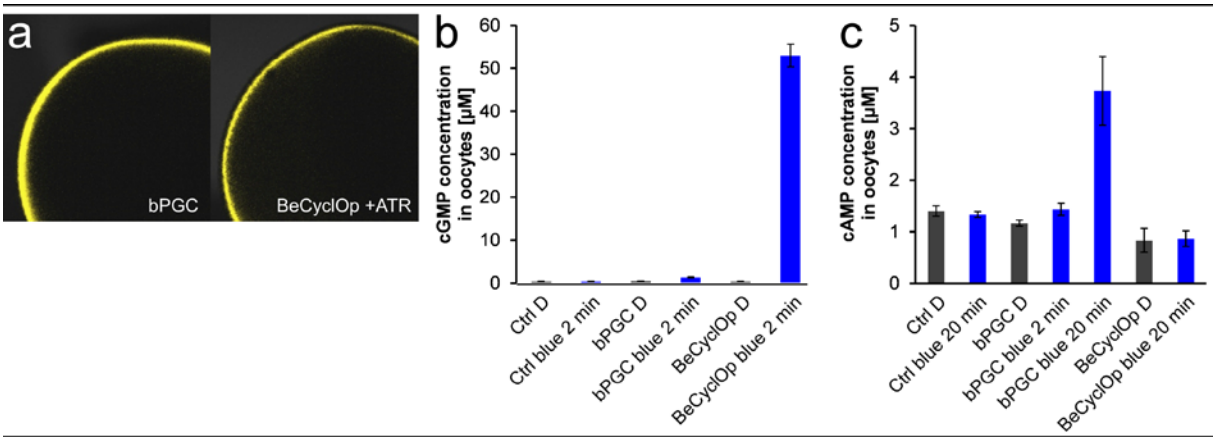

Figure 3.34. BeCyclOp is more efficient in cGMP generation than bPGC.

a. Fluorescence image of *Xenopus* oocytes expressing BeCyclOp (with 1 µM ATR) and bPGC, both constructs with C-terminus YFP tag. **b.** cGMP production of BeCyclOp and bPGC in *Xenopus* oocytes under dark (D) and 2 min blue light (464 nm, 10 µW/mm^2) illumination (L) **c.** cAMP production of BeCyclOp and bPGC. Samples are made 3 days post injection, ~ 25 fmol cRNA injected for each gene. n=3 experiments, each with 4 oocytes; error bars = SD.

3.2.10 BeCyclOp mutant with higher sensitivity

Principly a slower opsin will be more sensitive to light. From better studied ChR2, mutations at positions C128[46,79] and D156[47]could lead to a slow channelrhodopsin. Similar mutations were performed on BeCyclOp. Two more sensitive mutants, BeCyclOp C259T and BeCyclOp D283C, were obtained as expected. Both of them have similar activity as wild type BeCyclOp under saturating

green light illumination as indicated from the measurements of oocytes in vivo assay (Figure 3.35). Both mutants are very sensitive and they can even be activated by the far red lamp light which we are working with, while the far red light can not activate the wild type BeCyclOp (Figure 3.35). This is inconvenient for the sample handling. The reaction should be carried out in black eppi tubes with caution. The BeCyclOp C259T seems more sensitive than BeCyclOp D283C and makes it more difficult to measure. So we focus on BeCyclOp D283C first to measure its light sensitivity and closing kinetics in dark after a short light flash.

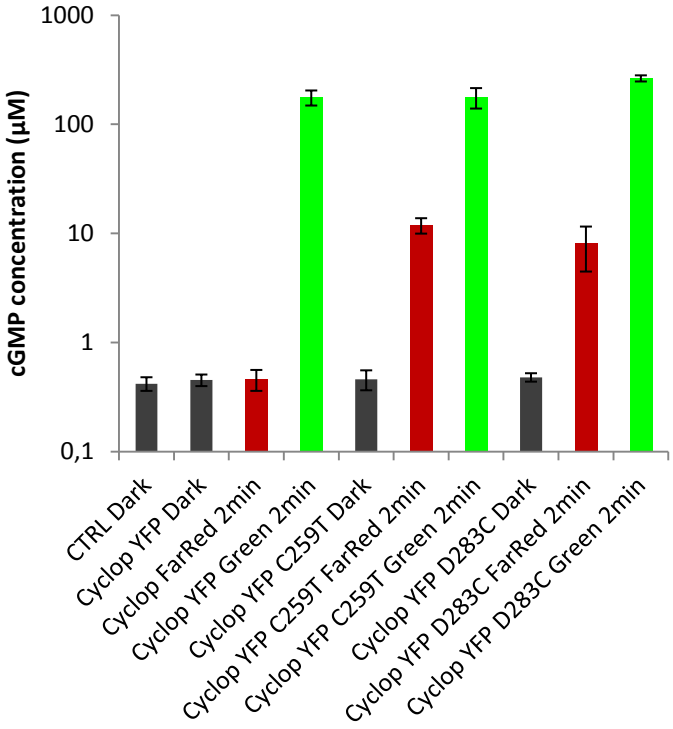

Figure 3.35. Two more sensitive mutants of BeCyclOp.

Samples are made directly from black tubes or illuminated with green or far-red light for 2min, 3dpi. ~ 25 fmol cRNA injected for each gene. n=3 experiments, each with 4 oocytes; error bars = SD.

The BeCyclOp D283C expressing oocytes membranes were used for the in vitro assay to calculate the time constant of BeCyclOp D283C GC activity decrease with time in dark. The position D283 in BeCyclOp showed similar effect on the photocycle as D156 in ChR2. A 80 ms 0.5 mW/mm^2 532 nm green laser flash was performed in the beginning and the cGMP production was measured at different time points in dark. As shown in Figure 3.36, BeCyclOp D283C is much slower than wild type BeCyclOp with a time constant τ = ~ 18 s, the time constant for wild type BeCyclOp is τ = ~ 0.3 s in comparison.

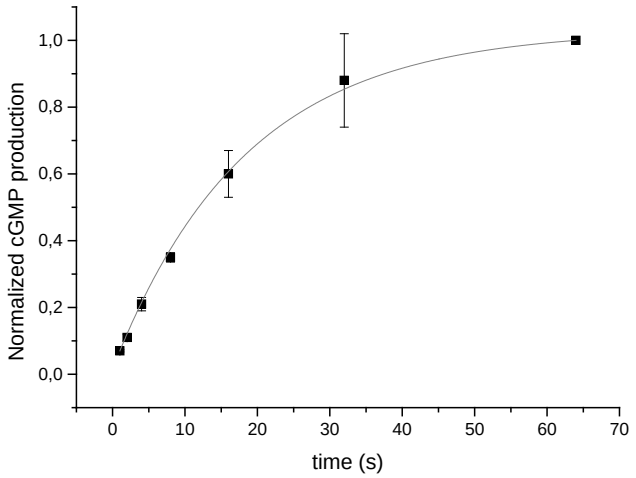

Figure 3.36. Closing time of BeCyclOp D283C.

The cGMP production were measured at different time point in dark after a 80 ms 0.5 mW/mm^2 532 nm green laser flash. For each set of data, the cGMP production at 64 s was normalized to 1. A mono-exponential fitting curve with τ = 18 s. n=3; error bars = SD, pH=7.35.

As indicated from the slower kinetics, the BeCyclOp D283C might be more sensitive to light. So we use 532 nm green lights with different intensities to illuminate BeCyclOp D283C expressing oocytes membrane for 2 min. Then we compare the cGMP production to measure the light sensitivity of BeCyclOp D283C. As shown in Figure 3.37, BeCyclOp D283C is much more sensitive to 532 nm light with a $K_{0.5}$ = ~ 3 µW/mm^2, while the wild type BeCyclop is about 55 µW/mm^2 in comparison.

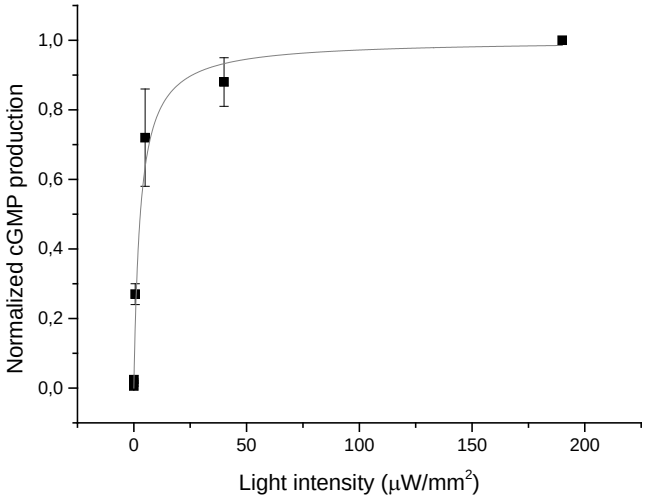

Figure 3.37 Light sensitivity of BeCyclOp D283C.

532 nm green lights with different intensities were used to illuminate BeCyclOp D283C expressing oocyte membranes for 2min. For each set of data, the cGMP production at 190 µW/mm^2 was normalized to 1.

A Michaelis-Menten curve with $K_{0.5}$ = 3 µW/mm^2 was fitted. n=3, error bars = SD, pH=7.35.

The GC BeCyclOp D283C (a time constant τ = ~ 18 s and $K_{0.5}$ at about 3 µW/mm^2) seems to be similar to the AC bPAC (a time constant τ = ~ 23 s and $K_{0.5}$ at about 4 µW/mm^2), albeit the reaction is not performed the same way and BeCyclOp D283C is in the plasma membrane and bPAC is a soluble protein.

3.3 Guanylyl Cyclase Opsins with two components system

Clues about existence of rhodopsin cyclases were first provided by Suneel Kateriya *et al.* through a search of the *Chlamydomonas* EST and genome data base[11]. All of such rhodopsin cyclases encode a rhodopsin domain, a His-Kinase and a response regulator which could form complete "Two Components Systems" and a C-terminal squence domain with clear homology to nucleotide cyclases (Figure 3.38). Such structures suggest a possible biochemical signaling cascade action of these rhoodopsin cyclases including light induction, phosphate transfer and Guanylyl Cyclase (GC) activity regulation. But none of them has been experimentally proven to be functional, until now. In 2012, Luck *et al.* expressed the opsin part of the large protein COP5 and reported a UVA-absorbing rhodopsin that is bimodally switched between a UV- and a blue light-absorbing form by illumination[80]. The regulation of the cyclase activity of this rhodopsin is however still uncertain.

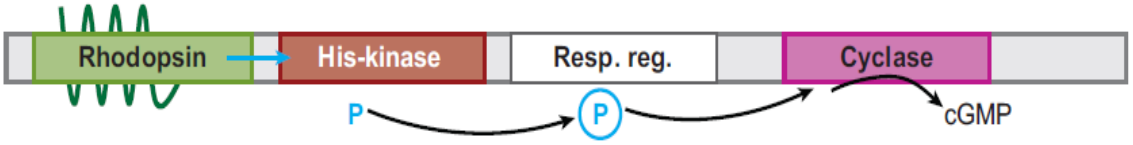

Figure 3.38 Schematic of Guanylyl Cyclase Opsins from *C. reinhardtii*.

Guanylyl Cyclase Opsins with possible phosphate transfer mechanism through two components system to regulate GC activity. Picture from [81]

3.3.1 Guanylyl Cyclase Opsins from *C. reinhardtii* and *Volvox carteri*

Here we try to clone different such large microbial rhodopsins fused to signalling chain modules and a guanylyl cyclase from *C. reinhardtii* and *V. carteri*. The cloned cyclase rhodopsin genes were then heterologous expressed in *Xenopus* Oocyte for functionality test.

Opsins	Origin	GC activity	Light regulation	Remarks
COP5	*C. reinhardtii*	No	No	
COP6a	*C. reinhardtii*	No	No	First COP6 sequence
COP6b	*C. reinhardtii*	Yes	No	COP6 variant with new C-terminus
COP6c	*C. reinhardtii*	Yes	Light inhibition	COP6 variant with new C-terminus and middle linker part sequence
COP7	*C. reinhardtii*	No	No	
COP8	*C. reinhardtii*	No	No	
VOP5 ATG2	*V. carteri*	No	No	VOP5 using the 2nd ATG as start codon
VOP6 ATG1	*V. carteri*	Yes	No	VOP6 using the 1st ATG as start codon
VOP6 ATG2	*V. carteri*	Yes	No	VOP6 using the 2nd ATG as start codon
COP6v6c	artificial	Yes	No	Old COP6 with C-terminus changed to 161aa from VOP6 after the Cyclase domain
COP56c	artificial	Yes	Light inhibition	COP5 with Cyclase domain and C-terminus changed with COP6nn

Table 3.2 Guanylyl Cyclase Opsins cloned and tested from *C. reinhardtii* and *V. carteri*

C. reinhardtii and *V. carteri* seem to be complex with several opsins beside two Channelrhodopsins [11]. 4 new opsins with GC domain are cloned from *C. reinhardtii* and 2 from *V. carteri*. Among the 4 new opsins from *C. reinhardtii*, we get 3 sequence variants for COP6. After testing in oocytes, 2 COP6

variants and VOP6 showed obvious GC activity while others had no GC activity. Only 1 variant of COP6, COP6c, showed clearly light regulation (inhibition by light) (Table 3.2).

3.3.2 COP6c is a light-inhibited Guanylyl Cyclase Opsin

Our preliminary results showed light-inhibited GC activity for COP6c from *Xenopus* oocytes in an in vivo assay (Figure 3.39a). But the in vivo system is especially difficult for the assay of light-inhibited GC activity due to the cGMP accumulation in oocytes during the expression of proteins in dark. Because of the inaccurate light intensities for illumination during oocyte incubaton, we can not compare the effect of different light from Figure 3.39a. Further experiments need to be performed by an in vitro assay system for the COP6c action spectrum.

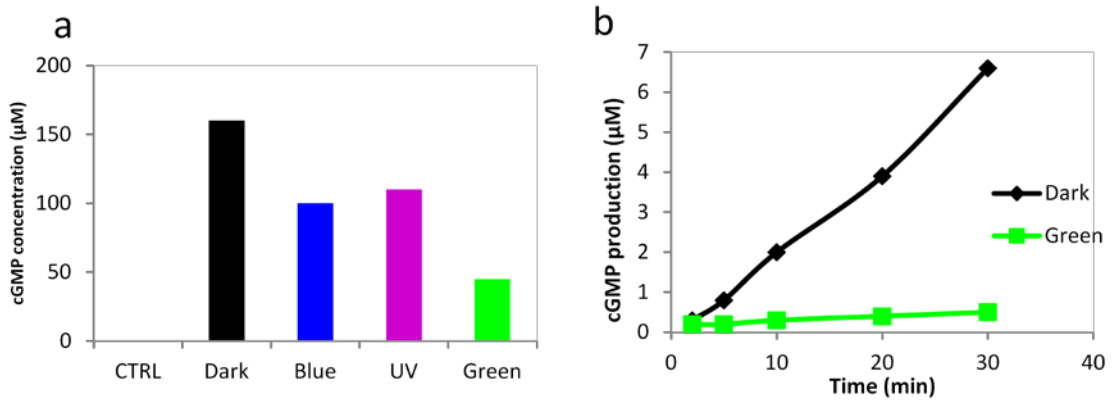

Figure 3.39 L**ight-inhibited GC activity of COP6c**

a. cGMP productions of oocytes expressing COP6c under dark and different light illumination for 1 day 2 dpi. b. cGMP production of COP6c expressing membrane under dark and green (532nm, ~0.1 mW/mm^2) light.

The in vitro assay shows clearly light-inhibited COP6c GC activity. In dark, COP6c expressing oocyte membrane has a GC activity of 0.24±0.05 µM/min, and under ~ 0.1 mW/mm^2 532 nm light illumination it was 0.02±0.01 µM/min (Figure 3.39b). The ratio from Dark to Light (D/L) is about 15±3.

3.3.3 The cyclase domain of COP6c could restore the COP5 GC activity

An alignment of GC domains of CYG12[82], COP5, COP6, bPAC (BgPAC) and Cya2[82,83] showed that COP5 has very low homology in positions with important roles in the GC function (Figure 3.40). This suggested that COP5 possibly can not function as a GC by itself and might need to form hetero-dimer to function in vivo.

```
                                #                                       @   #
CYG12           APAQEHPEATVLFSDIVGFTEIASRSSPLEVCSLLDELYQRFDAAIEEYPQLYKVETIGD 60
Cop6            FVADSHGHVVILFSDIVGFTSLSSKLPTAEVFLMLSNMFTAFDKLTDRFS-VYKVETIGD 59
Cya2            KMGGDRRPITILTSDLRGFTSTSEGLNPEEVVKVLNIYFGKMADVITHHG-GTIDEFMGD 59
BgPAC           TVEPQLVEKIIFFSDILAFSTLTEKLPVNEVVILVNRYFSICTRIISAYG-GEVTKFIGD 59
Cop5            TTLQMFESLTLLEVRLVNLGDLLASVPASDLLVALASLFHDLDTLLEQHG-CYLLEGLDE 59
                         ::   :  :          ::   :   :         .      : :.:

                                                                +
CYG12           AYMVVCNVTVPCDDHAD-----VLLEFALRMHEEASRVASSL-GEPVRIRVGMHSGPVVA 114
Cop6            AYMVAAGHDEDEDKEAKGSPLMRVLGFARAMLDVVRNITAPN-GERLRIRIGVHCGPAFA 118
Cya2            GILVLFGAPTSQQDDALR-AVACGVEMQLALREVNQQVTGLG-LQPLEMGIGINTGEVVV 117
BgPAC           CVMASFTK--EQGDAAIR----TSLDIISELKQLRHHVEATNPLHLLYTGIGLSYGHVIE 113
Cop5            SHLIVSGLDNVGDQVLHA------LGLARSLIAAADTFALGGRRSKLHLAVGVHTGPAQG 113
                  :          .          : :   :      .        :   :*:  * .

                           @      &   $
CYG12           GVVG-RKMPRFCLFGDTVNTASRMESHG--EAGQIHIS----EACYCCLRSKERFEIRER 167
Cop6            GVIG-MKCPRYCFLGDTVNTASRMESTG--FPMCIHVS----ENVFKHHPAAE-AELQEV 170
Cya2            GNIGSEKRTKYGVVGAQVNLTYRIESYT--TGGQIFISSTTLEAAGDRVHVNGNRTVQPK 175
BgPAC           GNMGSSLKMDHTLLGDAVNVAARLEALTRQLPYALAFTAGVKKCCQAQWTFINLGAHQVK 173
Cop5            VLVG-YSHPLIFFTGQLPAEVHMLQATCP--PNCVHVS----ARVLESVAHSEREHFVPA 166
                  :*        . *     .  :::        : .:

                          +
CYG12           GNIT------VKGKGTMRTYLLSPLER 188
Cop6            GERD------IKGKGHMRTGQLAPSRP 191
Cya2            GVKDPVVIWDVAGVGEPYNLSLAVEEQ 202
BgPAC           GKQEAIEVYTVNEAQKYYDTLQITQLI 200
Cop5            GVMASGATTYLMKVGGWEGGGIVAASE 193
                *     :
```

Figure 3.40 Alignment of GC domains

An alignment of GC domains of CYG12, COP5, COP6, bPAC(BgPAC) and Cya2. #: Metal Binding,@: Base recognition, +: Triphosphate positioning residue, & Ribose orienting residue, $: Transition state stabilizing residue.

We then generated a COP5 Chimera COP5/6c with changing the COP6c cyclase domain, which has been proven to be functional as homo-dimer, to COP5. The COP5/6c also showed light-inhibited GC activity in a *Xenopus* oocytes in vivo assay (Figure 3.41). But the GC activity of this artificial construct is very low, addition of 2 mM $MnCl_2$ is necessary to make the GC activity obvious. Further in vitro assays need to be performed for better characterization of this chimera together with COP6c in vitro assays.

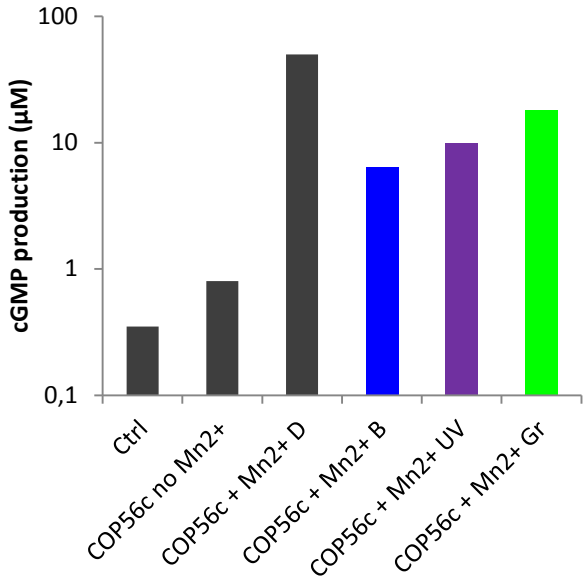

Figure 3.41 Light-inhibited GC activity of COP5/6c

After 3days under dark in normal ND96, final concentration of 2mM $MnCl_2$ was added and incubate for 1 more day under different light condition(D: dark, UV: UV LED, B: Blue LED, Gr: Green LED). Note the logrithtic scale here.

3.4 Combination of bPAC and CNG channels

Photo-activated Adenylyl Cyclases (PACs) are proteins with BLUF domains which can be activated by blue light. They can be used to regulate the cAMP production by blue light. They could also be used to activate CNG channels through the light-gated cAMP production. bPAC is now the most popular PAC due to its high efficiency and small size. Here we introduce new strategy of combining bPAC and CNG channel together with advantages for certain purpose.

3.4.1 Membrane targeting of bPAC reduces its dark activity

bPAC as a photo-activated AC has obvious dark activity. The dark activity can be reduced by certain mutations such as K197A or R278A, but such mutants are with obvious loss of light activation (Figure 3.42).

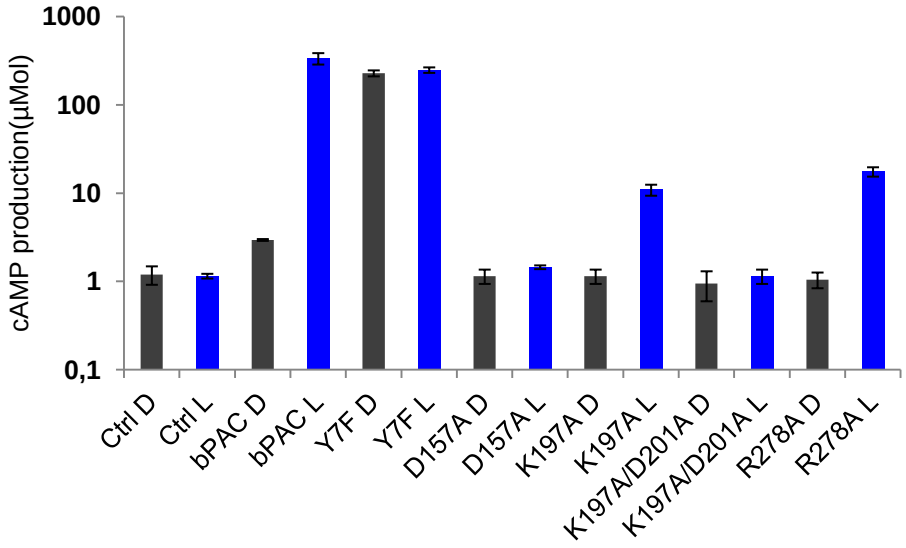

Figure 3.42 AC activity of bPAC mutants

AC activity of different bPAC mutants under dark and blue light illumination. n=2 experiments, each with 4 oocytes; error bars = SD.

In our study, we fused CNG channels (CNGA2 and OLF/T573S) with bPAC to generate a light-gated CNG channel. A YFP was put in between for such constructs. The fusion construct OLF-Y-bP showed no obvious dark activity from oocytes in vivo assay while the light activity is not greatly reduced (Figure 3.43).

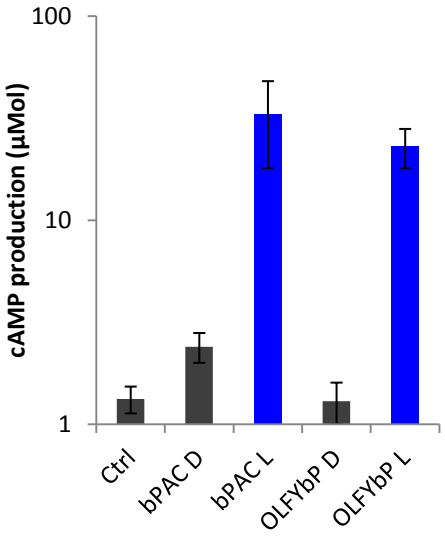

Figure 3.43 AC activities of bPAC and OLF-Y-bP

AC activities of bPAC and OLF-Y-bP in dark and blue light illumination. D, dark, L, blue LED illuminatin for 2 min. Samples are made 2 dpi. 28 ng cRNA were injected for OLF-Y-bP and 14 ng for bPAC. n=3 experiments, each with 4 oocytes; error bars = SD.

We then measured the AC activity of OLF-Y-bP by in vitro assay which is more accurate. The dark activity is very weak for OLF-Y-bP and not so obvious (Figure 3.44). Its activity in dark is 0.004 ± 0.001 pMol/(min * 2 oocytes membrane) and under blue LED (200mA) illumination is 13 ± 1.6 pMol/(min * 2 oocytes membrane. The calculated L/D ratio here is 3250 which is greatly enhanced in comparion to 300 of bPAC.

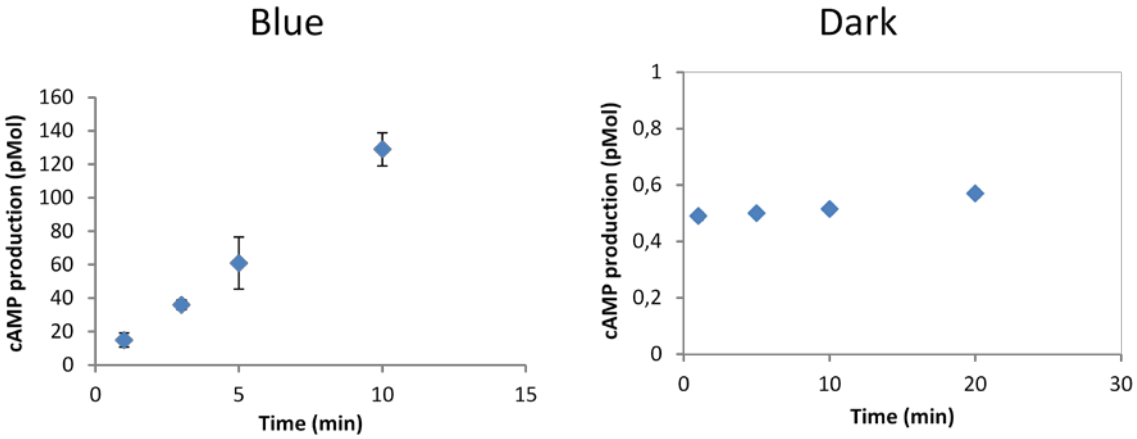

Figure 3.44 AC activity of OLF-Y-bP in dark and blue light

Blue LED (200mA) was used for illumination. 23ng cRNA were injected, membranes are extracted 3dpi. n=3; error bars = SD, pH=7.35.

3.4.2 Electrophysiological measurements of CNGA2/OLF-Y-bP in *Xenopus* oocytes

OLF-Y-bP and CNGA2-Y-bP could be expressed in oocytes while CNGA2-Y-bP is weaker expressed (Figure 3.45). Membrane potentials are recorded after 1s blue laser illumination (473 nm, 5 mW/mm^2) for oocytes expressing OLF-Y-bP and CNGA2-Y-bP. Although the CNGA2-Y-bP is weaker expressed in oocytes, its hyperpolarization effect last longer than OLF-Y-bP after 1 s illumination because it's more sensitive to cAMP[78].

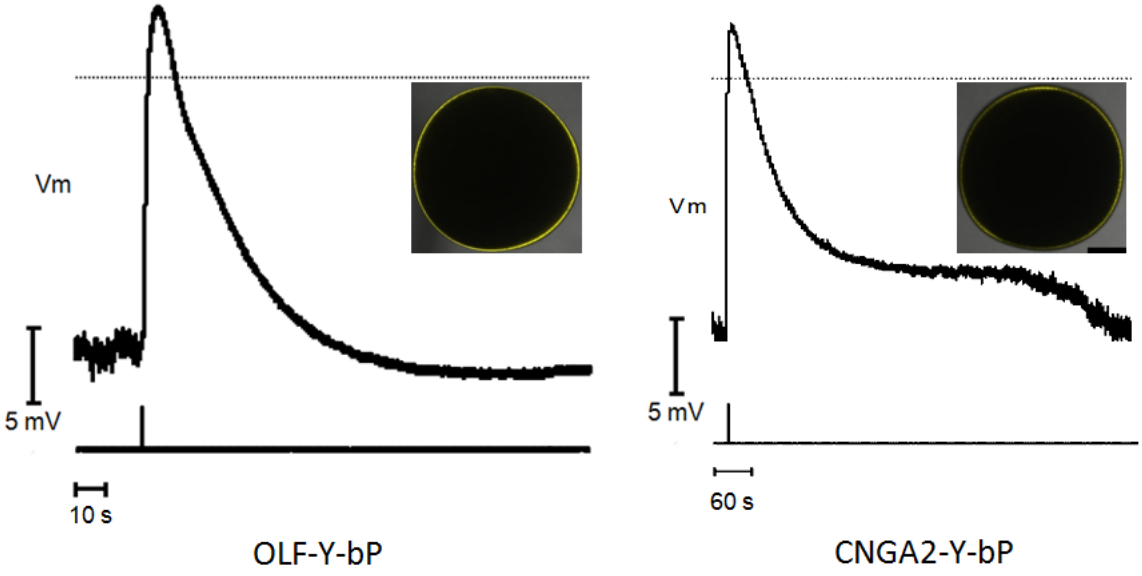

Figure 3.45 Membrane potential changes caused by blue illumination of OLF-Y-bP and CNGA2-Y-bP

Membrane potential recordings of oocytes expressing OLF-Y-bP and CNGA2-Y-bP after 1s Blue laser illumination (473 nm, 5 mW/mm^2) . Small pictures show the expression of OLF-Y-bP and CNGA2-Y-bP judged by the YFP fluorescence. 20 ng cRNA were injected for both, 3dpi.

Voltage clamp was also used to measure OLF-Y-bP and CNGA2-Y-bP. As shown in Figure 3.46, 1 s blue laser illumination could induce about 5 µA current for OLF-Y-bP. But since CNGA2-Y-bP is much more sensitive to cAMP, 1 s blue laser illumination is already too much for voltage clamp recording of CNGA2-Y-bP, for which the voltage can not be clamped due to the huge current. 0.1 s blue laser illumination was used for CNGA2-Y-bP and it could induce about more than 1 µA current.

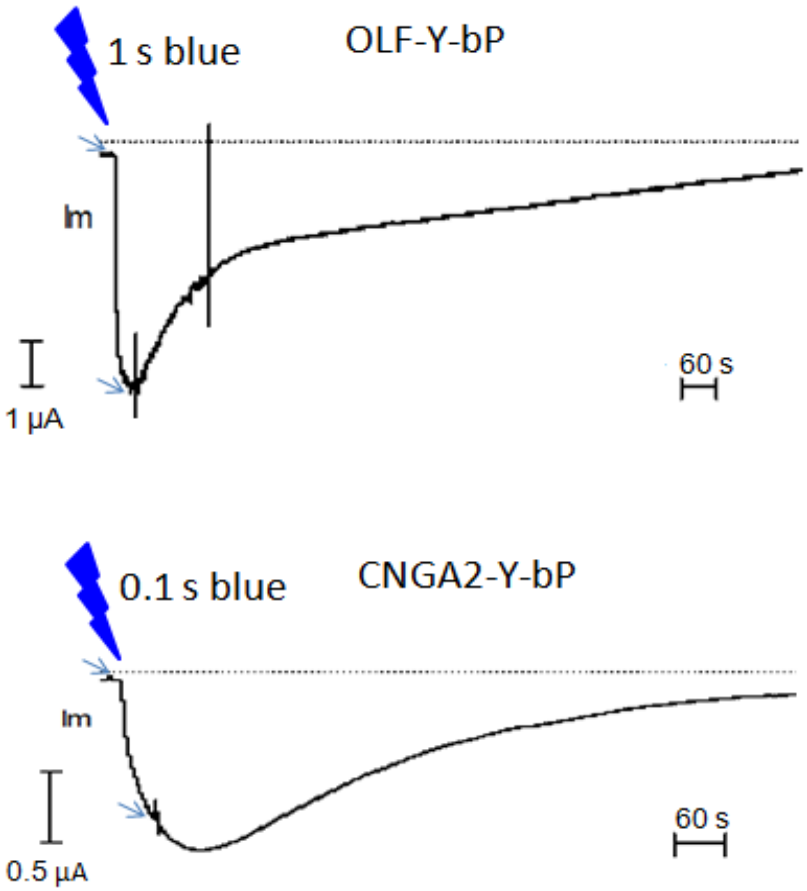

Figure 3.46 Voltage Clamp measurement of OLF-Y-bP and CNGA2-Y-bP

Voltage clamp recordings of oocytes expressing OLF-Y-bP and CNGA2-Y-bP after 1s (for OLF-Y-bP) or 0.1 s (for CNGA2-Y-bP) blue laser illumination (473 nm, 5 mW/mm^2). 20 ng cRNA were injected for both, measured 3dpi. Arrows indicated current changes caused by the defined potential changes from -60 mV to -50 mV.

Lei Jin et al. have tested OLF-Y-bP in mouse neuron cells, the OLF-Y-bP is even more powerful than ChR2 XXL mutant which is the most powerful Channelrhodopsin now to our knowledge (Personal communication with Lei Jin, Forschungszentrum Jülich).

4. Discussion

4.1 FR and chFR as possible optogenetic tools

As a strong light-gated proton pump, FR can pump the proton outside of the cell to generate more negative membrane potential (Figure 4.1). So the FR can be used to hyperpolarize the cell in principle.

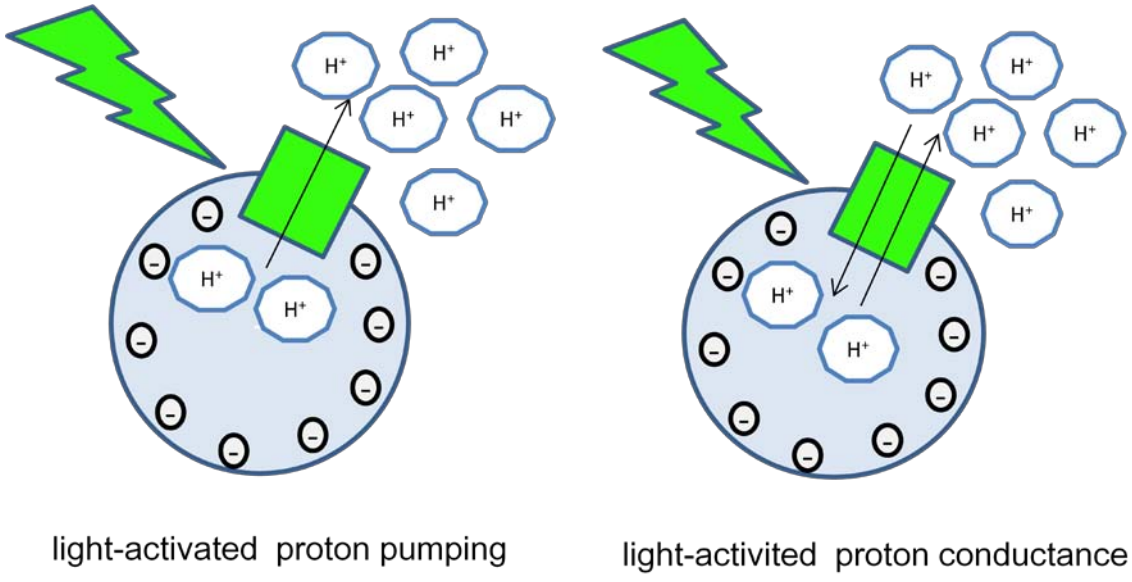

Figure 4.1 FR and chFR as possible optogenetic tools.

FR could be used to hyperpolarize the cell by pumping proton outside. chFR can be used to adjust the cellular pH according to the outside pH.

Principly the chFR can depolarize the cell, but the effect will be too weak compared to channelrhodopsins. The chFR would be ideal for changing the cellular pH since it could transport the protons into the cell or outside of the cell according to the membrane potential and proton gradient.

But for the application in new systems as an optogenetic tool, it also depends a lot on the expression and correct targeting. So the real application of FR in other systems also needs more tests with different systems. During the FR study, we developed a new strategy for improving the plasma membrane targeting of FR in *Xenopus* oocytes which also improve the plasma membrane targeting of BR and EeChR1. This strategy or similar methods might also be useful in other systems for plasma membrane targeting.

Similar mutation like chFR mutant in BR could also reverse the proton pump activity of BR. Further study with this mutant would also help to learn more about microbial rhodopsins.

4.2 FR shed light on new energy conversion mechanism in polar diatom

FR is from the polar area diatom *F. cylindrus* in sea ice and at the ice-edge zone. Metatranscriptome shows ecological importance of eukaryotic rhodopsins in iron-limited oceans (Personal communication with Jan Strauss et al., University of East Anglia, Norwich, UK). The q-PCR analysis

for both FR copies (longer FR and shorter FR) showed highly up-regulated expression under stress, especially low iron condition (Figure 4.2a). A gene specific qPCR for the longer FR (confirmed to be functional by us) showed that the longer FR can only be detected under iron-limited condition (Figure 4.2b). This is identical with our cloning result that the longer FR can only be amplified from cDNA under iron-limited condition.

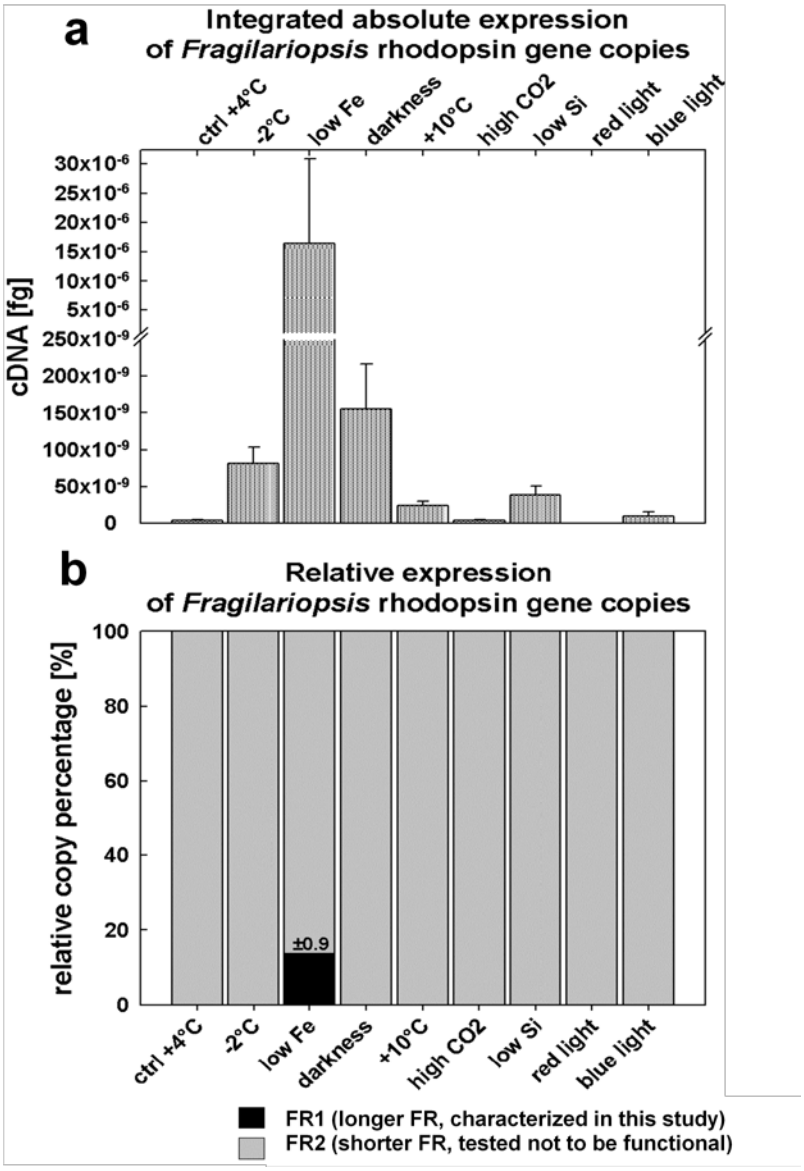

Figure 4.2 q-PCR of two FR copies under different culture condition.

a. Integrative qPCR analysis for both FR copies (longer and shorter) together under different conditions. b. Gene specific qPCR analysis to determine the expression percentage of two FR copies under different conditions. (Unpublished data from Jan Strauss et al.).

The FR is probably localized to the chloroplast of *F. cylindrus* as FR-GFP targeted to the chloroplast of *P. tricornutum* (Personal communication with Jan Strauss). And tests from Jan Strauss et al. showed

that *F. cylindrus* grows faster under green light than red light when iron is limited (Figure 4.3). The green light is around the peak of FR action spectra.

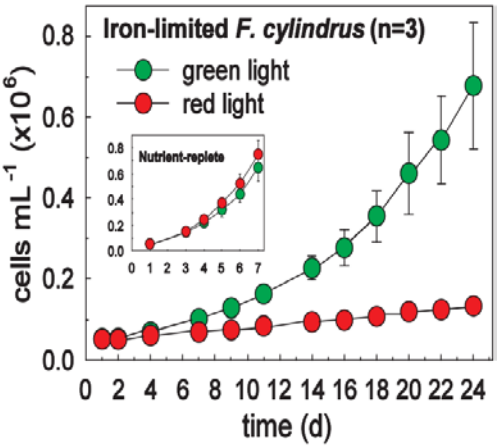

Figure 4.3 Iron limited *F. cylindrus* show increased growth under green light, likely conferred by rhodopsin. (Unpublished data from Jan Strauss et al.).

Proton pump rhodopsins were thought to be related with energy production due to the proton gradient generated [84]. Taken our data together, FR seems to be able to provide energy production under low iron condition when the photosynthesis is limited because of lack of iron-containing enzymes. Under iron limited condition, FR is highly expressed and localizaed to chloroplast. The proton gradient produced by FR pumping was then used by the ATPase to generate ATP or to fuel the metal transporters for the cell energy as shown in Figure 4.4.

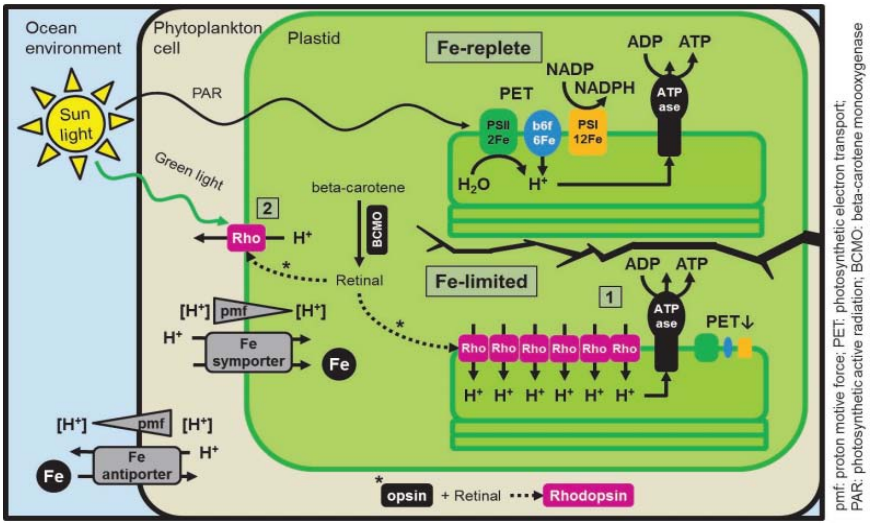

Figure 4.4 Hypothetical model of rhodopsin functions in a phytoplankton cell: Generation of (1) ATP production or (2) proton motive force to fuel metal transporters. (Picture from Jan Strauss et al.).

4.3 BeCyclOp is a new class of microbial rhodopsins

The channelrhodopsins from *Chlamydomonas* lay a real foundation to optogenetics. More and more microbial rhodopsins and also other photoreceptors are found and applied in optogenetics. Up to now,

all microbial rhodopsins are with 7 TM with highly conserved TM3 and a lysine in TM7 for Schiff-base binding of the retinal chromophore to our knowledge. Fungal CyclOps now add a novel aspect to the diversity of type I rhodopsins in that they contain an additional N-terminal TM0 with a relative long N terminus, ~ 140 aa, predicted to be cytosolic. We confirmed this by our BiFC experiment by attaching the split YFP to the N and C terminal ends.

The BiFC experiment also suggests possible interactions between N an C terminus for the regulation of GC activity. We have also generated a N-terminally shortened BeCyclOpS which showed higher dark activity and lower light-induced cGMP production, suggesting that the N-terminus is involved in tight light-regulation of the cytosolic GC activity.

The cyclase opsins (CyclOps) from several fungal species are a new class of type I opsins with novel function and structure. Among the CyclOps characterized in our study, BeCyclOp is the best for the light-regulated efficacy and specificity of GC activity. BeCyclOp is very specific for cGMP production, and no obvious cAMP generation could be detected from both in vitro and in vivo assay in *Xenopus* oocytes. And for bPAC and mPAC, low but obvious GC activity could be detected beside their high AC activity. We also determined a very high ratio of light vs. dark activity (L/D) of 5000 for BeCyclOp, which was reduced to 1100 by fusing YFP to the C-terminus; this was mainly due to a four-fold increased dark activity possibly caused by the dimerization effect of YFP. Previously the highest L/D ratio (300) was reported for bPAC from *Beggiatoa*[24].

The time constant for light-activation of the GC is expected to be faster than 1 ms if BeCyclOp is similar to other type I opsins; in fact it is too fast to be measured by our methods. In contrast to the previously described flavoproteins and adenylyl cyclases bPAC and mPAC (~20 and 10 s, respectively[24,76]), also inactivation upon light-off (~300 ms) is relatively fast for BeCyclOp, enabling good optogenetic control, provided PDEs are (intrinsically) expressed in the cells addressed.

The faster photocycle of BeCyclOp resulted in light-sensitivity lower than that of bPAC and mPAC, but more light-sensitive mutants were obtained by a point mutation which slows down the photocycle. This mutant can even be activated by far red light. The action spectrum of wild type BeCyclOp is a typically broad rhodopsin spectrum with a maximum at 530 nm. Though BeCyclOp is most sensitive to green light, it is still responsive to violet and red light, but not to far red light. To avoid pre-activation of BeCyclop, we worked under far-red light (650-720 nm).But for the mutant, it is more difficult to handle as stricter dark required this can be managed by performing reaction in black eppi tubes and very weak far-red light. This mutant would be useful for certain purpose such as deep within tissue in animals.

4.4 BeCyclOp is proven to be a good optogenetic tool in *C. elegans*

To assess the potential of BeCyclOp in animal optogenetics, Nagpal *et al.* from Alexander Gottschalk group of Goethe University expressed BeCyclOp in *C. elegans* muscles together with the TAX-2/-4

CNG channel. evoked by Photoactivation of BeCyclOp/TAX-2/-4 (with ATR) by blue light could evoke long lasting contractions and recovered to a plateau of about 3 % within ~ 30 s (off ~ 8.1 s) while the green light has stronger effect. BeCyclOp can be repetitively activated with three consecutive light pulses over three minutes evoking comparable effects with contractions of similar values. Animals raised without ATR were used as a control since the chromophore is absent in *C. elegans*. No contraction could be observed without ATR addition for BeCyclOp/TAX-2/-4.

GC function is abundantly found in sensory neurons in many animals. Nagpal *et al.* also expressed BeCyclOp in oxygen sensory BAG neurons, which intrinsically use cGMP for signaling. Photostimulation of BeCyclOp in BAG caused transient slowing responses similar as expressing ChR2 in BAG. For both optogenetic tools, stimulus protocols could be repeated, leading to similar results.

BeCyclOp is thus proven to be a good optogenetic tool for specific 2^{nd} messenger (cGMP) manipulation in *C. elegans*. But also in other systems, such as sperm swimming or animal vision where cGMP plays a role, CyclOp might become an important optogenetic tool.

4.5 In vitro assay with *Xenopus* oocyte crude membrane extracts

The *Xenopus* oocyte system is very efficient in expressing heterologous proteins for functional study. But it is not perfect for quantitative analysis due to the variability between individual oocyte, and the variability between different batches of oocytes is even bigger. During the work with BeCyclOp we developed an in vitro assay system with crude membrane extracts from oocytes for enzymatic membrane proteins.

The crude membrane extracts were obtained easily with two step centrifugation. The first low speed (~1000 g) centrifugation was used to centrifuge down the cell debris and big pellet. A second high speed (~ 20000 g) centrifugation was used to centrifuge down the membrane extracts. The preparation of CyclOp-containing membranes from oocytes allowed the biophysical characterization of CyclOp proteins without the interference of PDEs.

In addition to the in vitro assay system, we also built a computer-controlled system which allows the in vitro assay to be stopped by quenching with buffer containing 0.1 M HCl in ms range after a short laser flash. With this system we have measured the BeCyclOp closing kinetics successfully. It will also be useful to the study of other photoreceptors such as EuPAC etc.

4.6 Guanylyl Cyclase Opsins from *Chlamydomonas*

We have also characterized new rhodopsins (COPs) from *Chlamydomonas with* Guanylyl Cyclase activity. Although they have same output (Guanylyl Cyclase) as CyclOps from Fungi, the COPs from *Chlamydomonas* are much bigger proteins with a His-Kinase domain and a response regulator domain between the rhodopsin domain and the Guanylyl Cyclase domain. The regulation seems more complex through the two component system in between.

We have proven the functional Guanylyl Cyclase Opsin COP6C to be a light-inhibited Guanylyl Cyclase while the fungal CyclOps are light-activated Guanylyl Cyclases. The functions of *Chlamydomonas* Guanylyl Cyclase Opsins are obscure. And in *C. reinhardtii* there are lot of Guanylyl Cyclases and several photoreceptors including ChR1 and ChR2 which make the functional study of these Guanylyl Cyclase Opsins especially difficult.

Future work will be focused on the rhodopsin proteins to study the light regulation of GC activity by mutations in different key points. The light-inhibited GC activity somehow mimics the cGMP regulation in the visual system. It is possible to use these rhodopsins as optogentic tools in combination with light-regulated PDEs for fast decreasing cGMP level in cells.

4.7 Fusing PACs with CNG channels

Fusing PACs or even the CyclOps with CNG channels could generate new light-regulated channels through the built-in cAMP or cGMP signal transduction. These kind of new optogenetic tools have advantages according to the PACs or CNG channels used. In our study, the successful combination of bPAC and OLF/CNGA2 channels yield new tools with high conductance (property from CNG channel) and high sensitivity to blue light (property from bPAC). Compared to channelrhodopsins such as ChR2, CNG channels also have other advantages such as the Ca^{2+} conductance etc. Fusing bPAC to other CNG channels with specific ion permeability such as K^+ will also have special advantage.

In addition, cAMP assay of the membrane-bound OLF-Y-bP construct showed that OLF-Y-bP has very weak dark activity and very high L/D ratio of more than 3000 which is much higher than 300 of soluble bPAC. Although bPAC is very efficient in light-regulated cAMP production, the high dark activity is a problem for its optogenetic application. The membrane targeting bPAC fusion construct greatly reduced the dark activity. If we could mutate the OLF channel to be inactive, we could possibly get a membrane targeting bPAC with very weak dark activity.

5. References

1 Zhang, F. *et al.* The microbial opsin family of optogenetic tools. *Cell* **147**, 1446-1457, doi:10.1016/j.cell.2011.12.004 (2011).

2 Gradinaru, V. *et al.* Molecular and cellular approaches for diversifying and extending optogenetics. *Cell* **141**, 154-165, doi:10.1016/j.cell.2010.02.037 (2010).

3 Fiala, A., Suska, A. & Schluter, O. M. Optogenetic approaches in neuroscience. *Current biology : CB* **20**, R897-903, doi:10.1016/j.cub.2010.08.053 (2010).

4 Fenno, L., Yizhar, O. & Deisseroth, K. The development and application of optogenetics. *Annual review of neuroscience* **34**, 389-412, doi:10.1146/annurev-neuro-061010-113817 (2011).

5 Deisseroth, K. Optogenetics. *Nature methods* **8**, 26-29, doi:10.1038/nmeth.f.324 (2011).

6 Arrenberg, A. B., Stainier, D. Y., Baier, H. & Huisken, J. Optogenetic control of cardiac function. *Science (New York, N.Y.)* **330**, 971-974, doi:10.1126/science.1195929 (2010).

7 Nagel, G. *et al.* Channelrhodopsin-2, a directly light-gated cation-selective membrane channel. *Proceedings of the National Academy of Sciences of the United States of America* **100**, 13940-13945, doi:10.1073/pnas.1936192100 (2003).

8 Nagel, G. *et al.* Channelrhodopsin-1: a light-gated proton channel in green algae. *Science (New York, N.Y.)* **296**, 2395-2398, doi:10.1126/science.1072068 (2002).

9 Tischer, D. & Weiner, O. D. Illuminating cell signalling with optogenetic tools. *Nature reviews. Molecular cell biology* **15**, 551-558, doi:10.1038/nrm3837 (2014).

10 Merchant, S. S. *et al.* The Chlamydomonas genome reveals the evolution of key animal and plant functions. *Science (New York, N.Y.)* **318**, 245-250, doi:10.1126/science.1143609 (2007).

11 Kateriya, S., Nagel, G., Bamberg, E. & Hegemann, P. "Vision" in single-celled algae. *News in physiological sciences : an international journal of physiology produced jointly by the International Union of Physiological Sciences and the American Physiological Society* **19**, 133-137 (2004).

12 Sineshchekov, O. A., Jung, K. H. & Spudich, J. L. Two rhodopsins mediate phototaxis to low- and high-intensity light in Chlamydomonas reinhardtii. *Proceedings of the National Academy of Sciences of the United States of America* **99**, 8689-8694, doi:10.1073/pnas.122243399 (2002).

13 Berthold, P. *et al.* Channelrhodopsin-1 initiates phototaxis and photophobic responses in chlamydomonas by immediate light-induced depolarization. *The Plant cell* **20**, 1665-1677, doi:10.1105/tpc.108.057919 (2008).

14 Kato, H. E. *et al.* Crystal structure of the channelrhodopsin light-gated cation channel. *Nature* **482**, 369-374, doi:10.1038/nature10870 (2012).

15 Nagel, G. *et al.* Channelrhodopsins: directly light-gated cation channels. *Biochemical Society transactions* **33**, 863-866, doi:10.1042/bst0330863 (2005).

16 Wang, H. *et al.* Molecular determinants differentiating photocurrent properties of two channelrhodopsins from chlamydomonas. *The Journal of biological chemistry* **284**, 5685-5696, doi:10.1074/jbc.M807632200 (2009).

17 Lin, J. Y., Lin, M. Z., Steinbach, P. & Tsien, R. Y. Characterization of engineered channelrhodopsin variants with improved properties and kinetics. *Biophysical journal* **96**, 1803-1814, doi:10.1016/j.bpj.2008.11.034 (2009).

18 Boyden, E. S., Zhang, F., Bamberg, E., Nagel, G. & Deisseroth, K. Millisecond-timescale, genetically targeted optical control of neural activity. *Nature neuroscience* **8**, 1263-1268, doi:10.1038/nn1525 (2005).

19 Nagel, G. *et al.* Light activation of channelrhodopsin-2 in excitable cells of Caenorhabditis elegans triggers rapid behavioral responses. *Current biology : CB* **15**, 2279-2284, doi:10.1016/j.cub.2005.11.032 (2005).

20 Li, X. *et al.* Fast noninvasive activation and inhibition of neural and network activity by vertebrate rhodopsin and green algae channelrhodopsin. *Proceedings of the National*

Academy of Sciences of the United States of America **102**, 17816-17821, doi:10.1073/pnas.0509030102 (2005).

21 Ishizuka, T., Kakuda, M., Araki, R. & Yawo, H. Kinetic evaluation of photosensitivity in genetically engineered neurons expressing green algae light-gated channels. *Neuroscience research* **54**, 85-94, doi:10.1016/j.neures.2005.10.009 (2006).

22 Bi, A. *et al.* Ectopic expression of a microbial-type rhodopsin restores visual responses in mice with photoreceptor degeneration. *Neuron* **50**, 23-33, doi:10.1016/j.neuron.2006.02.026 (2006).

23 Zhang, F. *et al.* Multimodal fast optical interrogation of neural circuitry. *Nature* **446**, 633-639, doi:10.1038/nature05744 (2007).

24 Stierl, M. *et al.* Light modulation of cellular cAMP by a small bacterial photoactivated adenylyl cyclase, bPAC, of the soil bacterium Beggiatoa. *The Journal of biological chemistry* **286**, 1181-1188, doi:10.1074/jbc.M110.185496 (2011).

25 Schroder-Lang, S. *et al.* Fast manipulation of cellular cAMP level by light in vivo. *Nature methods* **4**, 39-42, doi:10.1038/nmeth975 (2007).

26 Ryu, M. H., Moskvin, O. V., Siltberg-Liberles, J. & Gomelsky, M. Natural and engineered photoactivated nucleotidyl cyclases for optogenetic applications. *The Journal of biological chemistry* **285**, 41501-41508, doi:10.1074/jbc.M110.177600 (2010).

27 Wang, X., Chen, X. & Yang, Y. Spatiotemporal control of gene expression by a light-switchable transgene system. *Nature methods* **9**, 266-269, doi:10.1038/nmeth.1892 (2012).

28 Motta-Mena, L. B. *et al.* An optogenetic gene expression system with rapid activation and deactivation kinetics. *Nature chemical biology* **10**, 196-202, doi:10.1038/nchembio.1430 (2014).

29 Zhang, K. & Cui, B. Optogenetic control of intracellular signaling pathways. *Trends in biotechnology*, doi:10.1016/j.tibtech.2014.11.007 (2014).

30 Weitzman, M. & Hahn, K. M. Optogenetic approaches to cell migration and beyond. *Current opinion in cell biology* **30**, 112-120, doi:10.1016/j.ceb.2014.08.004 (2014).

31 Wojtovich, A. P. & Foster, T. H. Optogenetic control of ROS production. *Redox biology* **2**, 368-376, doi:10.1016/j.redox.2014.01.019 (2014).

32 Karunarathne, W. K., O'Neill, P. R. & Gautam, N. Subcellular optogenetics - controlling signaling and single-cell behavior. *Journal of cell science* **128**, 15-25, doi:10.1242/jcs.154435 (2015).

33 Oesterhelt, D. & Stoeckenius, W. Rhodopsin-like protein from the purple membrane of Halobacterium halobium. *Nature: New biology* **233**, 149-152 (1971).

34 Takeda, K. *et al.* A novel three-dimensional crystal of bacteriorhodopsin obtained by successive fusion of the vesicular assemblies. *Journal of molecular biology* **283**, 463-474, doi:10.1006/jmbi.1998.2103 (1998).

35 Pebay-Peyroula, E., Rummel, G., Rosenbusch, J. P. & Landau, E. M. X-ray structure of bacteriorhodopsin at 2.5 angstroms from microcrystals grown in lipidic cubic phases. *Science (New York, N.Y.)* **277**, 1676-1681 (1997).

36 Mitsuoka, K. *et al.* The structure of bacteriorhodopsin at 3.0 A resolution based on electron crystallography: implication of the charge distribution. *Journal of molecular biology* **286**, 861-882, doi:10.1006/jmbi.1998.2529 (1999).

37 Luecke, H., Schobert, B., Richter, H. T., Cartailler, J. P. & Lanyi, J. K. Structure of bacteriorhodopsin at 1.55 A resolution. *Journal of molecular biology* **291**, 899-911, doi:10.1006/jmbi.1999.3027 (1999).

38 Kimura, Y. *et al.* Surface of bacteriorhodopsin revealed by high-resolution electron crystallography. *Nature* **389**, 206-211, doi:10.1038/38323 (1997).

39 Grigorieff, N., Ceska, T. A., Downing, K. H., Baldwin, J. M. & Henderson, R. Electron-crystallographic refinement of the structure of bacteriorhodopsin. *Journal of molecular biology* **259**, 393-421, doi:10.1006/jmbi.1996.0328 (1996).

40 Essen, L., Siegert, R., Lehmann, W. D. & Oesterhelt, D. Lipid patches in membrane protein oligomers: crystal structure of the bacteriorhodopsin-lipid complex.

Proceedings of the National Academy of Sciences of the United States of America **95**, 11673-11678 (1998).

41 Chow, B. Y. *et al.* High-performance genetically targetable optical neural silencing by light-driven proton pumps. *Nature* **463**, 98-102, doi:10.1038/nature08652 (2010).

42 Avelar, G. M. *et al.* A rhodopsin-guanylyl cyclase gene fusion functions in visual perception in a fungus. *Current biology : CB* **24**, 1234-1240, doi:10.1016/j.cub.2014.04.009 (2014).

43 Ruffert, K. *et al.* Glutamate residue 90 in the predicted transmembrane domain 2 is crucial for cation flux through channelrhodopsin 2. *Biochemical and biophysical research communications* **410**, 737-743, doi:10.1016/j.bbrc.2011.06.024 (2011).

44 Wietek, J. *et al.* Conversion of channelrhodopsin into a light-gated chloride channel. *Science (New York, N.Y.)* **344**, 409-412, doi:10.1126/science.1249375 (2014).

45 Gunaydin, L. A. *et al.* Ultrafast optogenetic control. *Nature neuroscience* **13**, 387-392, doi:10.1038/nn.2495 (2010).

46 Berndt, A., Yizhar, O., Gunaydin, L. A., Hegemann, P. & Deisseroth, K. Bi-stable neural state switches. *Nature neuroscience* **12**, 229-234, doi:10.1038/nn.2247 (2009).

47 Dawydow, A. *et al.* Channelrhodopsin-2-XXL, a powerful optogenetic tool for low-light applications. *Proceedings of the National Academy of Sciences of the United States of America* **111**, 13972-13977, doi:10.1073/pnas.1408269111 (2014).

48 Berndt, A. *et al.* High-efficiency channelrhodopsins for fast neuronal stimulation at low light levels. *Proceedings of the National Academy of Sciences of the United States of America* **108**, 7595-7600, doi:10.1073/pnas.1017210108 (2011).

49 Lin, J. Y., Knutsen, P. M., Muller, A., Kleinfeld, D. & Tsien, R. Y. ReaChR: a red-shifted variant of channelrhodopsin enables deep transcranial optogenetic excitation. *Nature neuroscience* **16**, 1499-1508, doi:10.1038/nn.3502 (2013).

50 Zhang, F. *et al.* Red-shifted optogenetic excitation: a tool for fast neural control derived from Volvox carteri. *Nature neuroscience* **11**, 631-633, doi:10.1038/nn.2120 (2008).

51 Klapoetke, N. C. *et al.* Independent optical excitation of distinct neural populations. *Nature methods* **11**, 338-346, doi:10.1038/nmeth.2836 (2014).

52 Kleinlogel, S. *et al.* A gene-fusion strategy for stoichiometric and co-localized expression of light-gated membrane proteins. *Nature methods* **8**, 1083-1088, doi:10.1038/nmeth.1766 (2011).

53 Chuong, A. S. *et al.* Noninvasive optical inhibition with a red-shifted microbial rhodopsin. *Nature neuroscience* **17**, 1123-1129, doi:10.1038/nn.3752 (2014).

54 Iseki, M. *et al.* A blue-light-activated adenylyl cyclase mediates photoavoidance in Euglena gracilis. *Nature* **415**, 1047-1051, doi:10.1038/4151047a (2002).

55 Gasser, C. *et al.* Engineering of a red-light-activated human cAMP/cGMP-specific phosphodiesterase. *Proceedings of the National Academy of Sciences of the United States of America* **111**, 8803-8808, doi:10.1073/pnas.1321600111 (2014).

56 Tarutina, M., Ryjenkov, D. A. & Gomelsky, M. An unorthodox bacteriophytochrome from Rhodobacter sphaeroides involved in turnover of the second messenger c-di-GMP. *The Journal of biological chemistry* **281**, 34751-34758, doi:10.1074/jbc.M604819200 (2006).

57 Ryjenkov, D. A., Simm, R., Romling, U. & Gomelsky, M. The PilZ domain is a receptor for the second messenger c-di-GMP: the PilZ domain protein YcgR controls motility in enterobacteria. *The Journal of biological chemistry* **281**, 30310-30314, doi:10.1074/jbc.C600179200 (2006).

58 Ryu, M. H. & Gomelsky, M. Near-infrared light responsive synthetic c-di-GMP module for optogenetic applications. *ACS synthetic biology* **3**, 802-810, doi:10.1021/sb400182x (2014).

59 Matsumoto, H. *et al.* Aromatic retinal analogues and their interaction with cattle opsin. *Biochemistry* **19**, 4589-4594 (1980).

60 AzimiHashemi, N. *et al.* Synthetic retinal analogues modify the spectral and kinetic characteristics of microbial rhodopsin optogenetic tools. *Nature communications* **5**, 5810, doi:10.1038/ncomms6810 (2014).

61 Gorman, D. S. & Levine, R. P. Cytochrome f and plastocyanin: their sequence in the photosynthetic electron transport chain of Chlamydomonas reinhardi. *Proceedings of the National Academy of Sciences of the United States of America* **54**, 1665-1669 (1965).

62 Thurston, C. F., Perry, C. R. & Pollard, J. W. Electrophoresis of RNA denatured with glyoxal or formaldehyde. *Methods in molecular biology (Clifton, N.J.)* **4**, 1-11, doi:10.1385/0-89603-127-6:1 (1988).

63 Cole, K. S. & Curtis, H. J. ELECTRIC IMPEDANCE OF THE SQUID GIANT AXON DURING ACTIVITY. *The Journal of general physiology* **22**, 649-670 (1939).

64 Neher, E. & Sakmann, B. Single-channel currents recorded from membrane of denervated frog muscle fibres. *Nature* **260**, 799-802 (1976).

65 Hamill, O. P., Marty, A., Neher, E., Sakmann, B. & Sigworth, F. J. Improved patch-clamp techniques for high-resolution current recording from cells and cell-free membrane patches. *Pflugers Archiv : European journal of physiology* **391**, 85-100 (1981).

66 Robida, A. M. & Kerppola, T. K. Bimolecular fluorescence complementation analysis of inducible protein interactions: effects of factors affecting protein folding on fluorescent protein fragment association. *Journal of molecular biology* **394**, 391-409, doi:10.1016/j.jmb.2009.08.069 (2009).

67 Kerppola, T. K. Bimolecular fluorescence complementation (BiFC) analysis as a probe of protein interactions in living cells. *Annual review of biophysics* **37**, 465-487, doi:10.1146/annurev.biophys.37.032807.125842 (2008).

68 Larkin, M. A. *et al.* Clustal W and Clustal X version 2.0. *Bioinformatics* **23**, 2947-2948, doi:10.1093/bioinformatics/btm404 (2007).

69 Crooks, G. E., Hon, G., Chandonia, J. M. & Brenner, S. E. WebLogo: a sequence logo generator. *Genome Res* **14**, 1188-1190, doi:10.1101/gr.849004 (2004).

70 Krogh, A., Larsson, B., von Heijne, G. & Sonnhammer, E. L. Predicting transmembrane protein topology with a hidden Markov model: application to complete genomes. *J Mol Biol* **305**, 567-580 (2001).

71 Omasits, U., Ahrens, C. H., Muller, S. & Wollscheid, B. Protter: interactive protein feature visualization and integration with experimental proteomic data. *Bioinformatics* **30**, 884-886, doi:10.1093/bioinformatics/btt607 (2014).

72 Kall, L., Krogh, A. & Sonnhammer, E. L. A combined transmembrane topology and signal peptide prediction method. *J Mol Biol* **338**, 1027-1036, doi:10.1016/j.jmb.2004.03.016 (2004).

73 Ullrich, S., Gueta, R. & Nagel, G. Degradation of channelopsin-2 in the absence of retinal and degradation resistance in certain mutants. *Biol Chem* **394**, 271-280, doi:10.1515/hsz-2012-0256 (2013).

74 Linder, J. U. Class III adenylyl cyclases: molecular mechanisms of catalysis and regulation. *Cell Mol Life Sci* **63**, 1736-1751, doi:10.1007/s00018-006-6072-0 (2006).

75 Linder, J. U. & Schultz, J. E. The class III adenylyl cyclases: multi-purpose signalling modules. *Cell Signal* **15**, 1081-1089 (2003).

76 Raffelberg, S. *et al.* A LOV-domain-mediated blue-light-activated adenylate (adenylyl) cyclase from the cyanobacterium Microcoleus chthonoplastes PCC 7420. *The Biochemical journal* **455**, 359-365, doi:10.1042/BJ20130637 (2013).

77 Hu, C. D., Chinenov, Y. & Kerppola, T. K. Visualization of interactions among bZIP and Rel family proteins in living cells using bimolecular fluorescence complementation. *Mol Cell* **9**, 789-798 (2002).

78 Altenhofen, W. *et al.* Control of ligand specificity in cyclic nucleotide-gated channels from rod photoreceptors and olfactory epithelium. *Proc Natl Acad Sci U S A* **88**, 9868-9872 (1991).

79 Schultheis, C., Liewald, J. F., Bamberg, E., Nagel, G. & Gottschalk, A. Optogenetic long-term manipulation of behavior and animal development. *PloS one* **6**, e18766, doi:10.1371/journal.pone.0018766 (2011).

80 Luck, M. *et al.* A photochromic histidine kinase rhodopsin (HKR1) that is bimodally switched by ultraviolet and blue light. *The Journal of biological chemistry* **287**, 40083-40090, doi:10.1074/jbc.M112.401604 (2012).

81 Hegemann, P. Algal sensory photoreceptors. *Annual review of plant biology* **59**, 167-189, doi:10.1146/annurev.arplant.59.032607.092847 (2008).

82 Misono, K. S. *et al.* Structure, signaling mechanism and regulation of the natriuretic peptide receptor guanylate cyclase. *The FEBS journal* **278**, 1818-1829, doi:10.1111/j.1742-4658.2011.08083.x (2011).

83 Rauch, A., Leipelt, M., Russwurm, M. & Steegborn, C. Crystal structure of the guanylyl cyclase Cya2. *Proceedings of the National Academy of Sciences of the United States of America* **105**, 15720-15725, doi:10.1073/pnas.0808473105 (2008).

84 Choi, A. R., Shi, L., Brown, L. S. & Jung, K. H. Cyanobacterial light-driven proton pump, gloeobacter rhodopsin: complementarity between rhodopsin-based energy production and photosynthesis. *PloS one* **9**, e110643, doi:10.1371/journal.pone.0110643 (2014).

6. Appendix

6.1 Supplement Table

Table S1 List of primers used in this study

name	sequence 5'- 3'	remarks
bpac D157A F	GATCATCTTCTTCAGCGCCATCCTGGCCTTCAGC	for bPAC mutation
bpac D157A R	GCTGAAGGCCAGGATGGCGCTGAAGAAGATGATC	for bPAC mutation
bpac K197A F	CTACGGCGGCGAAGTGACCGCGTTCATCGGCGACTGCGTG	for bPAC mutation
bpac K197A R	CACGCAGTCGCCGATGAACGCGGTCACTTCGCCGCCGTAG	for bPAC mutation
bpac K197A/D201A F	GCGGCGAAGTGACCGCGTTCATCGGCGCCTGCGTGATGGCCAGC	for bPAC mutation
bpac K197A/D201A R	GCTGGCCATCACGCAGGCGCCGATGAACGCGGTCACTTCGCCGC	for bPAC mutation
bpac R278A F	CGTGAACGTGGCCGCCGCGCTGGAAGCCCTGACAAG	for bPAC mutation
bpac R278A R	CTTGTCAGGGCTTCCAGCGCGGCGGCCACGTTCACG	for bPAC mutation
bpac Y7F F	GATGAAGCGGCTGGTGTTCATCAGCAAGATCAGC	for bPAC mutation
bpac Y7F R	GCTGATCTTGCTGATGAACACCAGCCGCTTCATC	for bPAC mutation
COP5 BH5	TAGGATCCATGGCACCCACCGGCAGCCT	for COP5 cloning
COP5 HD3n	GCGCAAGCTTCTACATGAACAGCGCCTGCG	for COP5 cloning
COP6 Bgl5	GGAAGATCTATGAAGCTGCGTCAGCGCACG	for COP6 cloning
COP6 HD3	GCGCAAGCTTTCAAGGCTGTAGCACGGCAG	for COP6 cloning
β linker BH5	TAGGATCCATGGCAGCCCTGCAGGAGAAGAAG	for constructs with β linker
β Linker BglXb3	TGCTCTAGAAGATCTGGAGCTGTTTTCAGAGATGTTG	for constructs with β linker
EeChR1 SalStopHd 3R	CTCCAAGCTTAGGTCGACTGCTTAACGGTGTCCTC	for EeChR1 cloning
EeChR1 BH5F	TAGGATCCGCCACCATGGATCATCCTTTGGCG	for EeChR1 cloning
EeChR1 D151C QC F	GGCTTACTCGTCTCGTGTATTGGCTGTATCGTG	for EeChR1 mutation
EeChR1 D151C QC R	CACGATACAGCCAATACACGAGACGAGTAAGCC	for EeChR1 mutation
FR start BH5	TAG GAT CC ATGCTGTGGTCAAAAACAAGG	for FR cloning
FR Xh3 stop Hd3	CTCCAAGCTTACTCGAGCAAAGGCGTTTCTTCGT	for FR cloning
BeGC1 BH5F	CGGGATCCGCCACCATGAAGGA	For cloning BeCyclOp
BeGC1 Hd3R	GCCCAAGCTTACTTTCTTCCCAGCACCCAGTA	For cloning BeCyclOp
BeGC1 Kpn5F	CGGGGTACCATGAAGGACAAGGACAACAAC	For BeCyclOp BiFC construct
YFP N155 HdR	GCCCAAGCTTAGGCCATGATATAGACGTTGT	For BeCyclOp BiFC construct
YFP C85 BHF	CGGGATCCGCCACCATGGCCGACAAGCAGAAGAACGG	For BeCyclOp BiFC construct

6.2 Supplement Figure

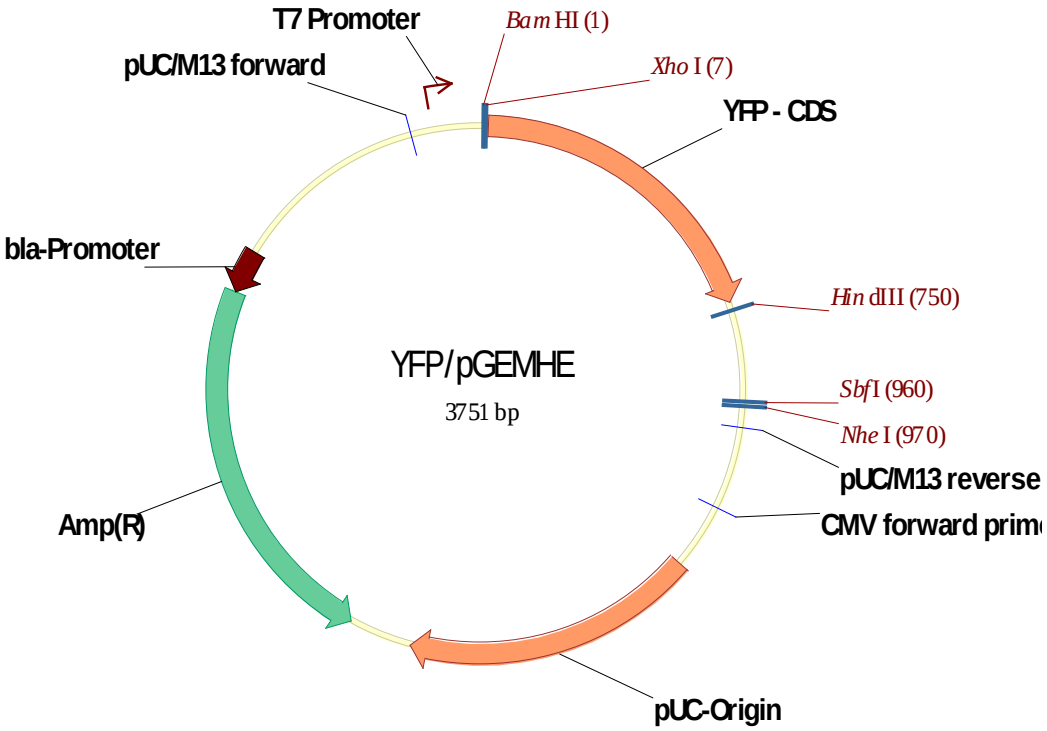

Figure S1. The map of vector pGEM-HE.

The vector pGEM-HE was used for generating cRNA after linearization with SbfI or NheI for *Xenopus* oocyte injection. The in vitro transcription starts with the T7 promoter. Constructs with YFP tag can be generated by ligation between the BamHI and XhoI sites. Constructs without YFP tag can be ligated between the BamHI and HindIII sites.

6.3 Abbreviation

A	ampere; Alanine
aa	amino acid
AC	adenylyl cyclase; Acetate
AD	activation domain
AP	action potential
ATP	adenosine 5'-triphosphate
ATR	all-trans-retinal
BiFC	Bimolecular Fluorescence Complementation
BLUF	sensors of blue-light using FAD
bp	base pair
BR	bBacteriorhodopsin
BSA	bovine serum albumin
C	Cysteine
cAMP/cGMP	Cyclic adenosine/guanosine monophosphate
C-di-GMP	cyclic dimeric guanosine monophosphate
cDNA	complementary DNA
CDS	coding sequence
Chop1	Channelopsin-1
Chop2	Channelopsin-2
ChR1	Channelrhodopsin-1
ChR2	Channelrhodopsin-2
CNG	cyclic nucleotide gated
COP	chlamy opsin
cRNA	complementary RNA
CvRh	*Chlorella vulgaris* rhodopsin
CyclOp	Cyclase Opsin
D	Dark; Aspartic acid
DEVC/TEVC	Double/Two Electrode Voltage Clamp
DMSO	Dimethyl sulfoxide
DNA	desoxyribonucleic acid
dNTP	desoxynucleoside triphosphate

dpi	day post injection
dpi	days post injection
DTT	dithiothreitol
E	Glutamic acid
EDTA	ethylenediaminetetraaceticacid
ER	Endoplasmic reticulum
EST	expressed sequence tags
F	Phenylalanine
FR	*Fragilariopsis cylindrus* rhodopsin
G	Glycine
g	gram
GC	guanylyl cyclase
GFP	green fluorescent protein
GPCR	G-protein coupled receptor
H	hour
His/H	Histidine
HR	Halorhodopsin
I	Ileucine
IVT	In vitro Transcription
K	Lysine
kb	kilobase
kD	kilodalton
L	light; Leucine; liter
LB	Lysogeny broth
LED	Light Emitting Diode
LOV	Light-Oxygen-Voltage-sensing
LSM	laser scanning microscope
M	mili
M	molar; Mega; Methionine
min	minute
mRNA	messenger RNA
N	nano; number

NLS	nuclear localization signal
NMG	N-Methyl-(D)-Glucamin
OD	optical density
ORi	Oocyte ringer solution
PAC	Photoactivated adenylyl cyclase
PCR	polymerase chain reaction
PDE	phosphodiesterase
PGC	Photoactivated guanylyl cyclase
qPCR	Quantitative PCR
qRT PCR	Quantitative real-time PCR
R	Arginine
RACE	rapid amplification of cDNA ends
Rcf	relative centrifugal force
RGPs	ROS-generating proteins
RNA	ribonucleic acid
RNase	Ribonuclease
ROS	Reactive Oxygen Species
Rpm	rounds per minute
RT	room temperature
RT-PCR	reverse transcription PCR
S	Serine
S	second
SD	standard deviation
SDS	sodium dodecyl sulfate
SDS-PAGE	SDS-polyacrylamide gel electrophoresis
SFOs	step function opsins
SOB	Super Optimal Broth
SOC	SOB with Catabolite repression
T	Threonine
TM	transmembrane
TYE	Membrane Trafficking signal-YFP-ER export signal
µ	micro

U	Unit; potential
UPM	Universal Primer A Mix
UTR	untraslated regrions
UV	Ultra violet
V	Volt; Valine
W	Watt; Tryptophan
WT	wild type
Y	Tyrosine
YFP	yellow fluorescent protein

Acknowledgements

First of all, I would like to extend my sincere gratitude to my supervisor, Prof. Dr. Georg Nagel, for all the supervision, discussion and great support in these years. He provided me great opportunities to participate in several different projects from which I benefit a lot. In addition, he also helped a lot with designing set-ups for the experiments. Thanks to Prof. Dr. Klaus Fendler from the Max Planck Institute of Biophysics as my secondary supervisor.

Thanks to our collaborators from University of East Anglia, Prof. Thomas Mock and his group member Dr. Jan Strauss, for the collaboration in FR work.

Thanks to our collaborators from Goethe University, Prof. Dr. Alexander Gottschalk and his group members Jatin Nagpal and Martin Schneider, for the collaboration in CyclOp work.

Thanks to our collaborators from University of Bielefeld, Prof. Dr. Armin Hallmann and his group members Reza Ramezannejad Ghadi and Lars Abram, for the collaboration in EeChR1 and Volvox GC rhodopsins work.

I would like to give many thanks to all of my colleagues in the department, especially in the group of Nagel, Elfriede Reisberg, Linzhu Wang, Ronnie Gueta, Sybille Ullrich, Christoph Stangl and Sabrina Förster to offer help whenever needed. Thanks to Maria Theiss and Juna Knop for help with experiments, and Elfriede Reisberg for expert technical assistance.

Thanks to all of my friends in Wuerzburg and Germany for the help in my life.

Last but not least I want to thank my family. My wife Lei Li not only support me in life but also help a lot in the tivial lab work such as PCR, plasmid extraction, gel extraction, cAMP/cGMP assay etc. Our son David is born and grows up together with my PhD study, he brings lot of fun to our life and also gives me another degree as father.

This work was funded by the Louis-Jeantet Foundation and SFB 1047, TP A3 to G.N.

Declaration of independence

I hereby declare that my thesis entitled:

Characterizing New Photoreceptors to Expand the Optogenetic Toolbox.

is the result of my own work. I did not receive any help or support from commercial consultants. All sources and / or materials applied are listed and specified in the thesis.

Furthermore, I confirm that this thesis has not yet been submitted as part of another examination process neither in identical nor in similar form.

Wuerzburg

Date:

Signature:

Shiqiang Gao

Curriculum Vitae

PERSONAL INFORMATION

Name: Shiqiang Gao

Date and place of birth: 06.10. 1982 in Shandong, China

Current address: Waltherstr. 18 97074 Wuerzburg

E-mail: gao.shiqiang@uni-wuerzburg.de gaosq1122@hotmail.com

EDUCATION AND WORKING EXPERIENCE:

06.2010 – now Ph.D. in Julius-von-Sachs-Institute of Biosciences, Botany I, Department of Molecular Plant Physiology and Biophysics, University of Wuerzburg, Germany

07.2008 – 05.2010 Assistant research officer in Temasek life sciences laboratory, National University of Singapore, Singapre

08.2007 – 06.2008 Research assistant in Institute of plant protection, Chinese academy of agricultural science, Beijing, China

09.2004 – 07.2007 Master study in Institute of plant protection, Chinese academy of agricultural science, Beijing, China

09.2003 – 07.2007 Bachelor study in School of Life Sciences, Shandong University, Jinan, China

PUBLICATIONS:

1. Gao, S.Q., Nagpal J., Schneider M., Nagel G., Gottschalk A., 2015. Optogenetic increase of cGMP levels in cells and animals using CyclOp, a tightly light-regulated guanylyl cyclase opsin. Submitted.
2. Dawydow, A., Gueta, R., Ljaschenko, D., Ullrich, S., Hermann, M., Ehmann, N., Gao, S.Q., Fiala, A., Langenhan, T., Nagel, G., Kittel, R.J., 2014. Channelrhodopsin-2-XXL, a powerful optogenetic tool for low-light applications. Proceedings of the National Academy of Sciences of the United States of America 111, 13972-13977.
3. Raffelberg, S., Wang, L., Gao, S.Q., Losi, A., Gartner, W., Nagel, G., 2013. A LOV-domain-mediated blue-light-activated adenylate (adenylyl) cyclase from the cyanobacterium Microcoleus chthonoplastes PCC 7420. The Biochemical journal 455, 359-365.
4. Qu, J., Mao, H.Z., Chen, W., Gao, S.Q., Bai, Y.N., Sun, Y.W., Geng, Y.F., Ye, J., 2012. Development of marker-free transgenic Jatropha plants with increased levels of seed oleic acid. Biotechnology for biofuels 5, 10.

5. Qu, J., Ye, J., Geng, Y.F., Sun, Y.W., Gao, S.Q., Zhang, B.P., Chen, W., Chua, N.H., 2012. Dissecting functions of KATANIN and WRINKLED1 in cotton fiber development by virus-induced gene silencing. Plant physiology 160, 738-748.
6. Gao, S.Q., Qu, J., Chua, N.H., Ye, J., 2010. A new strain of Indian cassava mosaic virus causes a mosaic disease in the biodiesel crop Jatropha curcas. Archives of virology 155, 607-612.
7. Ye, J., Chua, N.H., Qu, J., Gao, S.Q., 2012. Control of pests in plants. U.S. Patent Application US 2012/02400288A1.
8. Gao, S.Q., Zhang, X.J., Wu, M.S., He, C.Y., 2009. Differential expression of pathogenicity genes of *Xanthomonas oryzae* pv. *Oryzae* and deletion mutants △gacAxoo and △fleQxoo in vitro and in planta revealed by DNA microarray analysis. Acta Phytopathologica Sinica 39(6), 653-658.
9. Zhang, X.J., Gao, S.Q., Wu, M.S., He, C.Y., 2009. DNA Microarray Expression Analysis of *Xanthomonas oryzae* pv. *oryzae* in Rice Leaves at Early Infection Stages Using Selective Bacterial Transcript Labeling with Genome-Directed Primers. Scientia Agricultura Sinica, 42(10), 3501-3508.
10. Gao, S.Q., Zhang, X.J., Wu, M.S., He, C.Y., 2008. DNA Microarray Technology and Its Application in Transcriptional Profiling of Bacterial Pathogens. Scientia Agricultura Sinica 41(5), 1341-1346.
11. Qi, F.J., Gao, S.Q., Wu, M.S., He, C.Y., 2006. Analysis of Synergetic Induction of Hypersensitive Response by Nitric Oxide and Hydrogen Peroxide in Rice Suspension Cultured Cells. Scientia Agricultura Sinica 39(1), 61-65.
12. Qi, F.J., Gao, S.Q., Wu, M.S., He, C.Y., 2006. A Method for the Quantitative Determination of Hypersensitive Response of Rice Cells. Plant Physiology Communications 42(1), 87-90.
13. Qi, F.J., Gao, S.Q., Wu, M.S., He, C.Y., 2005. Hypersensitive response of rice cells induced by hydrogen peroxide. Acta Phytopathologica Sinica 35(6), 504-508.

RECENT AWARDS:

09.2012 The Rank Prize Funds Optoelectronics Committee Prize for Best Contributed Paper at the Symposium "Optogenetics" 10th to 13th September 2012, Windermere, Cumbria

Date:

Signature: